Development of a prevascularized bone implant

***

Entwicklung eines prävaskularisierten Knochenimplantats

Doctoral thesis for a doctoral degree

Julius-Maximilians-Universität Würzburg

submitted by

Christoph Rücker

born in Mellrichstadt

Würzburg 2018

Submitted on:

Members of the committee

Chairperson:

Primary supervisor: Prof. Dr. Heike Walles

Supervisor (second): PD Dr. Alois Palmetshofer

Date of public defense ……

Date of receipt of certificates …….

Table of contents

List of Figures

List of Tables

Abbreviations

Table 1:List of abbreviations

Abbreviation	
AMG	Arzneimittelgesetz
ATMP	Advanced Therapy Medicinal Product
AV loop	Arteriovenous loop
BioVaSc-TERM®	Biological vascularized scaffold
BMP	Bone morphogenetic protein
CAD	Computer-aided design
CHMP	Committee for Medicinal Products for Human Use
CT	Computed tomography
DAPI	4',6-diamidino-2-phenylindole
DMEM	Dulbecco's Modified Eagle's medium
DMSO	Dimethyl sulfoxide
FCS	Fetal calf serum
FDA	Food and Drug Administration
FGF	Fibroblast growth factor
DBM	Demineralized bone matrix
EC	Endothelial cell
EC	European Commission
ECFC	Endothelial colony forming cells
ECGM	Endothelial cell growth medium
ECM	Extracellular matrix
EDTA	Ethylenediaminetetraacetic acid
Em	Emission
EOC	Endothelial outgrowth cells
EPC	Endothelial progenitor cell
EtOH	Ethanol
Ex	Extinction
FGF	Fibroblast growth factor
FITC	Fluorescein isothiocyanate
g	g-force
G-CSF	Granulocyte colony stimulating factor
GMP	Good Manufacturing Practice
H&E	Haematoxylin and eosin
HA	Hydroxyapatite
hmvEC	Human microvascular endothelial cells
LDL	Low-density lipoproteins
MSC	Mesenchymal progenitor cells
MSCGM	Mesenchymal stem cell growth medium
NaCl	Sodium chloride
OEC	Outgrowth endothelial cell

Abbreviation	
PBS	Phosphate buffered saline
PEI	Paul-Ehrlich-Insitut
PFA	Paraformaldehyde
PPARγ	peroxisome proliferator-activated receptor
RANKL	Receptor activator of nuclear kappa-B ligand
SIS	small intestine mucosa
β-TCP	β- tricalcium phosphate
TGF	Transforming growth factor
TNF	Tumor necrosis factor
U	Units
VEGF	Vascular endothelial growth factor

Abstract

The skeletal system forms the mechanical structure of the body and consists of bone, which is hard connective tissue. The tasks the skeleton and bones take over are of mechanical, metabolic and synthetic nature. Lastly, bones enable the production of blood cells by housing the bone marrow. Bone has a scarless self-healing capacity to a certain degree. Injuries exceeding this capacity caused by trauma, surgical removal of infected or tumoral bone or as a result from treatment-related osteonecrosis, will not heal. Critical size bone defects that will not heal by themselves are still object of comprehensive clinical investigation. The conventional treatments often result in therapies including burdening methods as for example the harvesting of autologous bone material. The aim of this thesis was the creation of a prevascularized bone implant employing minimally invasive methods in order to minimize inconvenience for patients and surgical site morbidity. The basis for the implant was a decellularized, naturally derived vascular scaffold (BioVaSc-TERM®) providing functional vessel structures after reseeding with autologous endothelial cells. The bone compartment was built by the combination of the aforementioned scaffold with synthetic β-tricalcium phosphate. In vitro culture for tissue maturation was performed using bioreactor technology before the testing of the regenerative potential of the implant in large animal experiments in sheep. A tibia defect was treated without the anastomosis of the implant's innate vasculature to the host's circulatory system and in a second study, with anastomosis of the vessel system in a mandibular defect. While the non-anastomosed implant revealed a mostly osteoconductive effect, the implants that were anastomosed achieved formation of bony islands evenly distributed over the defect.

In order to prepare preconditions for a rapid approval of an implant making use of this vascularization strategy, the manufacturing of the BioVaSc-TERM® as vascularizing scaffold was adjusted to GMP requirements.

Zusammenfassung

Das Skelett bildet die mechanische Struktur des Körpers und besteht aus Knochen, einem harten Bindegewebe. Knochen übernehmen mechanische, metabolische und synthetische Aufgaben. Schlussendlich ermöglichen Knochen die Synthese von Blutzellen durch die Beherbergung des Knochenmarks. Wird die Heilungskapazität von Knochen durch Trauma, operative Entfernung von infiziertem oder tumorösem Knochen oder als Ergebnis behandlungsbedingter Osteonekrose, überschritten, findet keine vollständige Heilung statt. Knochendefekte, die eine kritische Größe überschreiten, sind daher immer noch Gegenstand umfangreicher, klinischer Forschung. Bei herkömmlichen Behandlungsmethoden können Eingriffe notwendig werden, die den Patienten belasten, wie bei der Gewinnung von autologem Knochenmaterial. Das Ziel der vorliegenden Arbeit war die Herstellung eines prävaskularisierten Implantats unter Verwendung minimalinvasiver Methoden, um die Belastung von Patienten und die Morbidität an der Entnahmestelle, zu verringern. Zur Herstellung eines vaskularisierten Implantats bildete ein dezellularisiertes Darmsegment (Jejunum) porcinen Ursprungs die Grundlage (BioVasc-TERM®). Diese Trägerstruktur stellte ein funktionales Blutgefäßsystem nach Wiederbesiedelung mit autologen Endothelzellen bereit. Der Knochenanteil des Implantats wurde durch die Kombination der genannten Trägerstruktur mit dem synthetischen Knochenersatzmaterial β-Tricalciumphosphat gebildet. In-vitro-Kultivierung in einem Bioreaktor führte zur Reifung des Implantats vor der Testung seines Potenzials zur Knochenregeneration in Großtierversuchen bei Schafen. Ein Tibiadefekt wurde behandelt ohne die Anastomose des implantateigenen Gefäßsystems an den Blutkreislauf und ein Mandibeldefekt wurde mit Gefäßanschluss behandelt. Das Implantat ohne Gefäßanschluss hatte einen osteokonduktiven Effekt, während das anastomosierte Implantat zur Bildung zahlreicher Knocheninseln, gleichmäßig über den Defekt verteilt, führte. Um eine zügige Zulassung eines Implantats, das diese Strategie zur Vaskularisierung von Knochen nutzt, zu ermöglichen, wurde die Herstellung der BioVaSc-TERM® an die Vorgaben der Guten Herstellungspraxis angepasst.

1 Introduction

1.1 Bone

1.1.1 Bone structure

The functions of bone include structural support of the body, the protection of internal organs, facilitation of movements, cell production and mineral storage. Bone is a very dynamic tissue in a constant process of growth, modeling and remodeling. Growth of bone can take place in two different processes. In the so-called endochondral ossification, bone is created over the intermediate step of cartilage formation. This type of bone growth contributes to longitudinal growth of long bones at the growth plates in the epiphyseal plate. During longitudinal growth, chondrocytes proliferate constantly and lay down cartilage that pushes the diaphysis outwards. Osteoblasts mineralize the cartilage in order to form new bone. The second variant of bone formation is the intramembranous ossification during which no transitional cartilage is formed. Mesenchymal progenitor cells from the embryonal connective tissue condense to form dense clusters. Those cells develop into osteoblasts laying down bone matrix and eventually becoming osteocytes. Bone modeling is the adaption in shape depending on mechanical forces. Bone can progressively adjust to the physical signals it is exposed to. During this process, bone formation and resorption are not as closely linked as it is the case in remodeling [1]. Remodeling is the mechanism of bone resorption and formation as a response to physiological requirements and as a steady process in order to eliminate micro damage. Mechanical stimulation results in improved bone structure especially if mechanical load is applied at discrete intervals instead of one long uninterrupted period, because cells need several hours for resensitization [2].

The three major components of bone are minerals, collagen type I and water. Depending on the type of bone, the relative proportions vary, especially proportions between mineral and water, while the relative amount of collagen remains the same [3].

The collagenous protein amount makes up about 90 % of the organic matrix with the remaining 10 % consisting of osteocalcin, osteonectin, osteopontin, fibronectin, bone sialoprotein and bone morphogenic proteins (BMPs) [4, 5].
The inorganic phase of bone consists of phosphate and calcium as well as bicarbonate, sodium, potassium citrate, magnesium, carbonate, fluorite, zinc, barium, and strontium [5].
The characteristic cell types of bone include osteoblasts, osteoclasts, osteocytes, osteoprogenitors and lining cells. Osteoblasts derive from mesenchymal progenitor cells; they are the bone forming cells, act as groups, and secrete the bone matrix. They are thus the main source for collagen in bone tissue and subsequently mineralizing the bone matrix. The collagenous ground substance before mineralization is the so-called osteoid. As mineralization follows, the osteoid transforms into an osteon, the primary functional unit of cortical bone [6]. The osteoid and inactive bone tissue in general are covered with quiescent osteoblasts in a flattened morphology [7]. In this mode, they are called the bone lining cells and act as a blood-bone barrier by controlling the influx and efflux into and out of the bone extracellular fluid. They can differentiate into osteoblasts again by parathyroid hormone or mechanical force [8]. Osteoblasts surrounded by mineralized matrix become osteocytes, a scattered cell type embedded in an extensive network of canaliculi that connects them to other osteocytes, the bone lining cells on the surface and osteoblasts. They make up the majority of bone cells and are responsible for important functions within the bone [9, 10]. The canaliculi network allows for cell-cell communication between osteocytes and provide a mechanosensory capacity which is a prerequisite for the adaption to mechanical forces [11, 12]. It was suggested that, appropriate to the stimuli they register, osteocytes regulate the activity of osteoblasts and osteoclasts. This way, they are a main control unit of remodeling [13, 14]. Mechanical stress for example results in the production of different growth factors by osteocytes which lead to bone production [5, 15]. On the contrary, physical unloading elicits the expression of various proteins reducing bone formation by inhibiting the Wnt signaling pathway [16]. Apoptosis of osteocytes functions as chemotactic signal for osteoclast attraction [17]. MSCs, osteocytes and osteoblasts contribute to

osteoclast formation which enables bone resorption [18]. Osteoclasts acidify their surrounding and dissolve bone minerals while the protease cathepsin K catabolizes collagens, elastin and gelatin and thus effectively breaks down the proteinaceous aspect of bone [19]. The range of influence of the acidic environment is confined by the so-called sealing zone. It seals the resorbing compartment, namely the extracellular space in which bone resorption takes place [20].

All these components make up the bone as a discrete system that allows de novo bone formation, growth, remodeling and adaption to requirements arising from the outside environment as well as healing and its functions as structural supportive organ.

1.1.2 Bone healing and blood supply

In case of injury, two modes of healing exist, primary and secondary bone healing. Primary bone healing can only take place in areas of functional periosteum and when the fracture ends are in direct contact to each other [21]. Depending on the size of the gap, osteoblasts of the endosteum are activated and new bone is generated in the gap until the osteons of both fracture ends fuse. This mode of healing occurs in gaps smaller than 0.01 mm and is a rare natural process of fracture healing [22]. The second mode of primary bone healing occurs in gaps up to 1 mm [23]. In this case, the gap is bridged with perpendicularly oriented lamellar bone, which is then, in a second step, reorganized by cutting cones corresponding to the process described before. Only after the reorganization, the bone regains its biomechanical properties [22, 24].

Secondary bone healing is more frequent and consists of endochondral and membranous bone formation. In contrast to primary bone healing, gentle movement and weight bearing support it. Blood entering the fracture gap builds a hematoma and an inflammatory response is initiated. Granulation tissue and connective tissue formation connect fracture ends flexibly and limit movements during the endochondral ossification. At the same time, intramembranous ossification occurs beneath the periosteum close to the fracture ends and results

in a hard bony callus surrounding the soft fibrocartilaginous callus, gradually mineralized by activated osteoblasts [25].

In bone, as in other tissues, the formation of new vascular networks is vital for the regenerative potential. The entry of blood vessels into the avascular cartilage during endochondral ossification is essential for further bone formation. The blood flow within bone is closely connected to its metabolic activity and is a common limiting factor in regeneration [26]. The creation of blood vessels in embryogenesis is achieved by vasculogenesis, the de novo formation of blood vessels. During this process, mesodermal cells differentiate into hemangioblasts and migrate to sites of simple blood vessel formation [27]. The second mode of blood vessel formation is angiogenesis, a mechanism responsible for the vast majority of vascular networks. The term describes the extension of existing vasculature by branching and sprouting. This mechanism is characterized by endothelial cells, which grow toward an angiogenic stimulus such as VEGF, PDGF or FGF [28, 29]. Although angiogenesis is following the same principles in all tissues, it is discussed that blood vessels become specialized depending on the hosting tissue [27, 30]. The hierarchal topography and organization of the vasculature in bone is similar to other organs: an artery provides a delicate vessel network with blood flow, which is directed away by a vein.

The necessity of endochondral angiogenesis for endochondral ossification reflects the close connection of bone regeneration to blood supply. Blood vessels invade hypertrophic cartilage and only then, a progression of bone formation is taking place [31]. The release of growth factors by maturing chondrocytes ensures further expansion of the vasculature in the growth plate [32].

Comprehensively, different sources provide for the profuse blood supply and thus healing capacity of bone. In long bones, the nutrient artery enters the medullary cavity and supplies the bone marrow and feeds into the endosteum [33]. Additionally, the artery anastomoses with metaphyseal and epiphyseal vessels. The metaphyseal capillary network derives from system blood vessels that directly drive into the metaphysis and support the blood flow provided by the nutrient artery [34]. The epiphyseal arteries enter the epiphysis through discrete openings in the bone. They supply the ossification centers and while the growth

plate itself is avascular, it receives nutrients from the metaphyseal and epiphyseal vessels [35].

The blood supply of the outer surface of bone is achieved by the periosteum, a tissue consisting two layers, the outer fibrous and the inner cambium layer. The vascular structures of the periosteum cover the entire length of bone shafts. They supply the outer third of compact bone by entering the Volkmann's channels and the Haversian system [36]. In bone regeneration, the periosteum is – apart from its role in blood supply – of exceptional importance as source of osteoprogenitor cells and growth factors [37]. The periosteum's influence on bone healing was demonstrated in numerous studies.

1.1.3 Bone defects

Despite bone's high regenerative capacity of scarless healing, there are numerous scenarios that necessitate clinical support for bone healing. Trauma, healing disorders, malignant tumor removal as well as infection, osteomyelitis or radiation/medication-related osteonecrosis are causes for impaired healing or so-called critical size defects. The accurate definition of a critical size defect describes the smallest possible defect that does not heal during the lifetime of an organism [38]. Traumatic bone defects are usually result of high force impacts or stress caused by falls, road traffic or ski accidents [39]. In this case, the bone itself is healthy and is damaged by external factors. A pathological fracture in contrast is a bony defect resulting from diseases that weaken the structure of the bone with a resulting injury from common loads during everyday life.

1.2 Tissue engineering and bioreactor technology

Today's view on tissue engineering (TE) affiliates this field of study with the development of biological substitutes that have the ability the replace degenerated or diseased tissues or defective organs in order to restore their designated function as for example in bone, when critical size defects do not heal naturally [40]. Classically, cellular components, undergoing application-specific

treatment e.g. genetic modification or physical and chemical stimulation in vitro, are combined with supportive biomaterials. This illustrates the interdisciplinary nature of tissue engineering, which integrates cell biological science, medicinal findings and material science, as well as bioreactor engineering. The understanding of cellular behavior towards materials and surfaces, cells are in contact with, gives guidance to material scientists to develop materials or surface modifications that either provide an environment for cell-specific niches or help directing cell fate into a desired linage [41]. In the narrow sense, tissue engineering starts exactly at the point when conventional 2D culture conditions turn to 3D conditions during tissue generation; this is when suitable cells, usually stem cells or differentiated primary cell types, get seeded on a 3D matrix that already fosters basic tissue development processes [42]. With progressing tissue generation, increasing volumes necessitate techniques that allow for optimal supply of nutrients and oxygen. Thus, the development of bioreactors closely interconnects with the progress in tissue engineering. Bioreactors provide the possibility of influencing cells by the exertion of physical regulatory signals encouraging cells to maintain their phenotype or to differentiate [43]. In vascularized bone tissue engineering, perfusion of scaffolds can help upregulating osteogenic markers, while shear stress in vascular structures caused by continuous medium flow contributes to vascular patency and endothelial cell health [44]. The general aim is creating conditions in vitro that are as close as possible to the in vivo condition. This objective naturally leads to the opportunity to derive findings from in vitro models and compare them to the in vivo situation. For example, well-characterized cell types in specific environments allow the prediction of the effects of pharmaceuticals and investigation of natural biological processes or pathologic conditions without the necessity of in vivo experimentation [45].

Another aspect is the transportation of completed complex tissue engineered implants from the site of manufacture to the clinical site. For the preservation of the integrity of vital grafts, it is necessary to provide optimal conditions in a mobile bioreactor system. The control of temperature and gas composition (among

others like pressure regime, perfusion) can be relevant parameters depending on the tissue to be transported.

1.3 Relevant cell types for bone tissue engineering

The following chapter will address the cell types relevant for the tissue engineering of a prevascularized bone graft as realized in this thesis. The cell types were chosen for their unique properties while other approaches might successfully use other cell types.

1.3.1 Mesenchymal stem cells

Mesenchymal progenitor cells (MSCs) were first discovered 1976 in bone marrow and described as fibroblasts with the ability to commit to the osteogenic linage. Today, further sources for mesenchymal stem cells are muscles, fat, blood, periosteum, dental pulps, lung and bones [46]. Bone marrow and fat derived mesenchymal stem cells are frequently used for scientific purposes due to their accessibility [47]. They possess high potential for proliferation, self-renewal and the ability to differentiate into various cell types. Adipocytes, chondrocytes and osteoblasts are possible target differentiations as well as myoblasts, stromal cells and fibroblasts [48]. The antigen profile of mesenchymal progenitor cells has been under extensive investigation in order to characterize them on a molecular biological level. The results showed a general expression of the following markers: CD9, CD10, CD13, CD29, CD34, CD44, CD49d, CD49e, CD54, CD55, CD59, CD105, CD146, CD166. While they are negative for the markers: CD3, CD4, CD11c, CD14, CD15, CD16, CD19, CD31, CD34, CD38, CD45, CD56, CD61, CD62P, CD104, CD144 [49]. It was revealed that the expression profiles differ dependent on the origin of the cells. For example, progenitor cells from fat are positive for CD49d and negative for STRO-1 and CD106 while bone marrow-derived MSC show the opposite expression of those markers. MSC are a heterogeneous population of cells that display different amounts of differentiation potential and plasticity. Due to the complex expression profiles of antigens for the

verification of MSC the International Society for Cellular Therapy (ISCT) proposed the following characterization: 95 % of cells have to express the factors CD73, CD90 and CD105, while 98 % of cells have to be negative for CD14, CD35, CD45, CD79α and HLA-DR. According to the definition, the cells additionally have the ability to adhere to plastic surfaces under standard culture conditions and can differentiate into adipocytes, chondrocytes and osteoblasts [50].
MSC exhibit a number of attributes that make them attractive for the application in tissue engineering. They can secrete bioactive molecules that inhibit apoptosis of surrounding cells, reduce scar formation and fibrosis in damaged tissue, induce angiogenesis and thus establish blood supply [51]. They are also capable of stimulating proliferation of tissue-specific progenitor cells [52].

1.3.2 Microvascular endothelial cells

The inside of blood vessels is lined with endothelial cells (ECs) which regulate the exchange between bloodstream and the surrounding tissue. They possess and keep the ability to proliferate for their lifetime and to adjust their number and alignment according to the requirements of the surrounding [53]. Virtually all tissues are dependent on blood supply guided by vessels made up by endothelial cells. They are capable of extending vascular networks and thus facilitate growth or healing of tissues [54].
Arteries and veins possess a wall of connective tissue und smooth muscles whose diameter is dependent on the vessel size. Small diameter vessels like capillaries and sinusoids lack the muscle and connective tissue layer and possess only an incomplete endothelium in order to allow for the exchange of big molecules between bloodstream and tissue as for example in the liver. [55].
Endothelial cells conserve their ability for cell division and migration as requirement for the formation of vessels by angiogenesis. New vessels develop by sprouting from existing vessels. Vessel formation sets in as answer to specific signals that induce endothelial cells to form extensions that guide the developing sprouting while growing into surrounding tissue. First, cells form a dense sprout that converts into a tube like structure by the fusion of the cells' vacuoles. The

result is the canal of a capillary. Angiogenesis is strongly dependent on the surrounding extracellular matrix of adjacent cells. Endothelial cells for example produce laminin that facilitates the establishment of capillaries [56].
Cells suffering from hypoxia release angiogenesis promoting growth factors in order to induce an extension of the blood vessel system. A four-stage process is initiated by such growth factors. Proteases breach the basal lamina, cells migrate towards the source of the signal while proliferating and eventually forming a channel for the intake of the bloodstream. These steps can be triggered individually or simultaneously for example by the growth factor vascular endothelial growth factor (VEGF) that specifically affects endothelial cells [55].
The complexity of the vascular endothelium lies in the number of biological functions it fulfills. It guides the blood circulation without provoking platelet aggregation or leucocyte adhesion while inhibiting smooth muscle cell proliferation [57, 58]. Vasoconstrictive and vasodilatory mechanisms, i.e. recognition of hormones, physiological chemical signals, orchestrate the vascular tone and provide suitable blood fluidity in all conditions, so that the blood circulation can fulfill its function as interface between blood, organs and tissues. The endothelium selectively distributes macromolecules to their place of consumption, releases waste products into the bloodstream and regulates the recruitment of blood circulating cells into extravascular tissues [59]. This plays a crucial role for example in angiogenesis, vasculogenesis and during wound healing, as control of inflammation is another of its function. Environmental cues, mechanical forces and inflammatory and angiogenic stimuli regulate the endothelium [59].

1.3.3 Endothelial progenitor cells

In general, the term endothelial progenitor cells (EPCs) describes cells capable of decisively influencing angiogenesis and vasculogenesis. Angiogenesis is the process of vessel formation by sprouting from an existing vessel while vasculogenesis addresses the formation of vessels without former precursor (de novo) [60].

There are numerous methods to isolate EPCs and many different marker profiles defining different subpopulations of EPCs that have different functions and contributions to vessel formation. The term ‘true EPC’ is discussed controversially [61]. Hematopoietic cells are known to participate in angiogenesis and are found at the site of injured vessels, but studies also suggest, that they do not directly form functional endothelium but secrete factors aiding the angiogenic actions of resident endothelial cells [62, 63]. The nonhematopoietic EPCs in contrast are more apt to actual de novo vessel formation [64].

Therefore, the two major classifications of EPCs are hematopoietic and nonhematopoietic EPCs. They differ in origin as well as methods of isolation. Their contributions to angiogenesis or vasculogenesis base on different modes of action [64].

Asahara et al. first isolated endothelial progenitor cells (EPCs) in 1997. The discovery concerns a hematopoietic cell population in adult blood capable of inducing de novo vessel formation. There is no unique marker identifying this type of cell. Animal models showed the capability of ischemic rescue and peripheral limb ischemia in such $CD34^+$ hematopoietic EPCs [65]. In human trials, CD133+ cells showed potential for treatment of myocardial and peripheral ischemia [66]. Thus, circulating hematopoietic EPC can be targeted by CD34 and/or CD133 positive cell characterization. Due to their role in enhancing angiogenesis rather than directly forming vessels, they are also referred to as circulating angiogenic cells. Since the regenerative and proliferative capacity in mature endothelial cells is limited, there was consensus about the existence of a circulating cell type [67]. Nonetheless, it has been shown that in response to injury a endothelial cell population is capable of extensive proliferation [68]. This cell population is residual in the tunica intima - the innermost layer in a blood vessel - and it was recently identified as CD117 expressing EPC [69]. The nomenclature for nonhematopoietic EPCs derives from their characteristic to grow out from endothelium and are thus called “outgrowth endothelial cells / endothelial outgrowth cells” (OECs or EOCs). An additional term is “endothelial colony forming cells“ (ECFCs) describing their tendency to form colonies after isolation from mononuclear blood derived cells [70]. They usually do not express CD41

[71]. Still, this classification is not complete. Bou Khazam et al. describe different morphologies and functions for EOCs (in this case: early outgrowth cells) and ECFCs [72]. The proliferation of EOCs is very limited as is their ability to form tube-like structures; they probably do not actively integrate into vasculature and act via paracrine factors, which makes them more similar to hematopoietic EPCs. ECFCs in contrast have been shown to become part of newly formed blood vessels [73]. The application of EPC in the context of bone regeneration led to interesting results. In a sheep model, a 3.2 cm defect in the tibia was created and treated with EPC transplantation with good results regarding bone volume regeneration [74]. A similar approach was applied in clinical practice in a case report [75]. A patient with tibial fracture received an open reduction and internal fixation. The treatment resulted in a nonunion and was hereinafter successfully treated with granulocyte colony stimulating factor (G-CSF) mobilized CD34+. G-CSF lead to detachment of some of the cells of the hematopoietic linage from their bone marrow surrounding. The cells entered the peripheral bloodstream and were collected by apheresis. A subsequent FACS sorting resulted in the isolation CD34+ hematopoietic EPCs. An absorbable collagen scaffold was used to immobilize the cells at the site of the defect additionally to bone grafting using autologous cancellous bone from iliac crest.

1.3.4 Synergies in MSC and EPC

MSCs and EPCs each for themselves exhibit attributes that make them suitable for the use in bone tissue engineering. The combined use of the cell types can result in synergies due to the employment of different pathways towards bone formation that further improve the possibilities in their application [76].
A calvarium defect in rats filled with ß-TCP as control and ß-TCP seeded with a coculture of MSCs and EPCs as testing sample showed and increased amount of bone found in the testing samples were double the bone area was formed as compared to controls after 12 weeks [77]. In a similar fashion, significantly increased bone density was detected in a rabbit segmental bone defect. However, bone area and height were similar in this case [78]. Apart from promoting bone formation by providing enhanced conditions for angiogenesis

and the prevention of the central necrosis in regeneration bone, it is discussed that EPC also participate in actual bone formation by differentiating into osteogenic cells themselves [74, 79]. The findings are supported by other in vitro and in vivo experiments investigating the bone regenerative potential of CD34 positive EPCs [80, 81]. Yet, these discoveries are not undisputed: a series of other studies could not illustrate an increased bone formation associated with the activity of EPCs alone [82, 83]. The difficulty of identification of subpopulations of EPCs is suspected to be the reason for the contradicting results as they might act differently from each other.

1.4 Strategies for bone regeneration

In Europe, the number of patients undergoing bone reconstruction surgeries is greater than one million per year [84]. The complexity and variety of different bone defect settings gave rise to a multitude of approaches aiming at the restoration of lost or injured bone. The following chapters give an overview on strategies for bone regeneration that are similar or otherwise connected to the methods in this thesis.

1.4.1 Synthetic biomaterials

As no biomaterial to date can replace bone regarding its mechanical properties, the biodegradability is an important aspect for implanted material. Bone defects are stabilized by metal plates and filled with bone substitute material, so that their mechanical properties are secondary. Therefore it is important to control the degradation rate of a biomaterial in order to allow for rapid replacement of the material by natural bone [85]. General requirements to bone substitute materials include interconnected porous structures with 90 % porosity. The pore diameter should range from 100 – 500 µm in order to allow for cell seeding and the ingrowth of bone tissue, including blood vessels and the exchange of nutrients and waste products [86]. Porosity in the range of 2 – 10 µm is crucial for the initial adhesion of proteins and cells, as well as migration [87].

Biodegradable ceramics were the first synthetic biomaterials used in bone regeneration [88]. Ceramics in the form of calcium sulfate have osteoconductive attributes; the osteoinductivity of calcium sulfate was suggested by the reduced pH during calcium sulfate dissolution. The local pH reduction results in local bone demineralization leading to a release of osteoinductive proteins [89, 90]. It has been used in numerous studies proving its biocompatibility and rapid biodegradability [85]. Following calcium sulfates, calcium phosphates gained scientific interest, due to their similarity to the inorganic phase of natural bone. Calcium phosphates are considered biocompatible and osteoconductive with osteoinductive potential [91]. Their chemical and morphological attributes are well controllable via manufacturing conditions. It is possible to adjust surface area and porosity, which have an influence on the biological responses in bone regeneration [88, 92]. The most common forms of calcium phosphate used in bone regeneration are hydroxyapatite and β-tricalcium phosphate (β-TCP). Both materials share similar biological characteristics but differ significantly in degradation rate. Hydroxyapatites have a very slow degradation rate that can lead to remnants of the material in a defect site for years, making the area vulnerable to fatigue fractures [88, 93]. In β-TCP, the degradation rate is much higher, making it possible to control degradation rate by combining hydroxyapatite with β-TCP in a biphasic ceramic.

Similar to the aforementioned materials, bioactive glass is both osteoconductive and osteoinductive [94]. Bioactive glass was the first artificial material able to chemically bond to bone [87]. Contact of the material to physiological fluids results in the local formation of hydroxyapatite to which bone can bond and bone growth is promoted by the release of physiological concentrations silica and calcium ions [95, 96].

Different materials share certain properties and differ in other aspects. In the case of hydroxyapatite and calcium phosphate, it can be beneficial to combine different materials in composites. There is a magnitude of material combinations available, examples are polymers, chitosan composites, bioactive glass and ceramic combinations.

1.4.2 Bone graft prefabrication following the in vivo bioreactor principle

A tissue engineering strategy for bone regeneration similar to the approach in this thesis is the technique of the in vivo bioreactor principle. Instead of in vitro maturation and vascularization this method uses the patients' own bodies as place of bone graft generation. Thus, the term "in vivo bone graft bioreactor principle" emerged [97].

The muscular flap is an obvious option for the in vivo bioreactor principle due to muscles' high degree of vascularization and good accessibility. Additionally, muscles are a source of progenitor cells for bone healing [98]. It was suggested that muscle satellite cells contribute to bone regeneration in case of damaged or absent periosteum [99]. Satellite cells provide a source of growth factors as BMPs, IGF-1 and FGF-2 [100]. First in 1991, a muscle flap was inserted into mold of a rat femur cast using inert silicone. BMP-3 was injected into the flap and after 10 days in vivo, the muscle inside the mold transformed into newly formed, mainly cancellous bone [101]. In another study, a collagen I carrier mixed with BMP-2 was wrapped around the tip of a latissimus dorsi muscle flap in rats. After 3 weeks, the flap – depending on the used dosage of BMP-2 (2 – 50 µg) – resulted in ectopic trabecular bone formation. Whereas in the control without BMP, there was no bone formation detectable [102]. This indicates muscle flaps provide a suitable environment for vascularization and bone formation if strong osteogenic promoters (e.g. BMPs) are supplementally present.

A variation of the muscular is the periosteal flap technique. In fact, its availability is limited but the periosteum can be a major factor regarding bone regeneration. Thus, it can be used successfully whenever periosteum is available. The fibrous outer layer is responsible for the stability of the periosteum. Blood vessels that supply the bone itself and adjacent skeletal muscle traverse it. The inner cambium contains mainly mesenchymal progenitor cells, differentiated osteogenic cells as well as osteoblasts and fibroblasts [103, 104]. Within its niche in the bone environment, it participates in the membranous and endochondral ossification. Thus, it is reasonable to use its potential to investigate the suitability of the periosteal flap as a bone forming aspect. Typically, the flap is used to cover

a tissue engineered construct that contains progenitor cells and/or osteogenic signals in order to trigger a bone healing reaction exploiting the favorable preconditions of the periosteum [97]. Apart from the periosteum's ability to secrete growth factors as BMPs, TGF-ß1 and IGF-1 [97, 105], the provision of a dense vascular network is an major advantage of the tissue.

More broadly applicable is the arteriovenous loop that was first described by Erol and Spira in 1979. This technique was further developed and is still under investigation today. The AV loop is an in vivo model of axial vascularization and was successfully applied in small as well as large animals [106–108].

The AV loop can be used to vascularize various tissues and materials by placing them in close vicinity to a prominent vessel of adequate size in a so called isolation chamber in uninjured areas of the host's body. The chamber creates some degree of autonomy of the created biovascularized neotissue graft [109].

Historically, the use of the AV loop in the context of bone regeneration focused on osteogenesis while the aspect of vascularization within bone was investigated subsequently. In a large animal study the successful employment of the methods of AV loop graft generation in sheep is presented [106]. It is demonstrated that the natural diffusion range could be increased in bone substitute materials such as TCP or hydroxyapatite in granular form as well as in solid form of relevant dimensions [110]. An increase in perfusion density was observed for 12 weeks by MRI before the endpoint analyses. Vascularization increased by sprouting from the main vessel of the AV loop. Limitations lie in the formation of new bone material, which could not be confirmed by histological means in this configuration. Additionally, the feasibility of the procedure was demonstrated in standard surgical context. The method got refined further by investigating the effect of the combination of intrinsic and extrinsic vascularization within the vascularization chamber [107]. The difference in both setups is the isolation chamber which was accessible by the surrounding tissue through perforation of the titanium chamber, so that vascularization was possible along the AV loop utilized (intrinsic vascularization) as well as through the surrounding area. The exclusively intrinsic vascularization was achieved by a Teflon chamber that allowed no external access except for the arteriovenous vessel that was intruded into the chamber.

The joint mechanisms of intrinsic and extrinsic vascularization proved to be superior to their single capacities [107]. An early clinical attempt of vascularizing a bone graft in human host tissue was the implantation of a mandibular bone graft for the restoration of the lower jaw. For in vivo vascularization, the graft consisting of bovine derived bone mineral was mixed with recombinant human BMP-7 and bone marrow aspirate. This method avoided creating a second site bone damage but caused donor-site morbidity in the latissimus dorsi muscle that served as a basis for graft vascularization [111]. Further clinical applications of the AV loop technique were described for a tibial defect and a large bone defect in the wrist due to carcinoma removal and it could contribute to the healing of those defects that previously did not heal without further intervention. The technique was modified in a way that the AV loop was created directly in the defect site, rendering a donor site redundant and thus, eliminating a major issue at least for specific cases since not all areas are eligible for this procedure [112].

1.4.3 Naturally derived decellularized scaffolds

Native bone as it is used in autologous bone transplants is the golden standard for the treatment of large defects. The critical disadvantages of this approach can be controlled by the use of allogenic or xenogenic bone that has been decellularized. Among others, an important factor for the osteoconductive effect of materials used for bone regeneration is the micro- and macrostructure, e.g. the pore shape and size, the geometry as well as micropores and roughness of the surface [113]. All of these aspects can be utilized by decellularizing bone harvested from allogenic or xenogenic sources and thus overcoming the disadvantage of limited availability. During the essential removal of all cellular components, the bone extracellular matrix also loses many of its biologically active signals [114] while it still remains a potent biomaterial. A reintroduction of cues facilitating bone regeneration is possible via seeding decellularized bone with autologous cells or the addition of growth factors and thus, restoring a great deal of regenerative potential.

Decellularized vascular structures are a promising component of the tissue engineering approach at supporting cells and tissues of a regenerative implant

that exceeds the dimensions that can be supported by diffusion alone with adequate amounts of nutrition and oxygen. Decellularized tissues are composed of a biocompatible extracellular matrix that naturally possesses mechanical properties suitable for the application of the intended purpose. The extracellular matrix itself can have a critical role in the regeneration of different tissues and additionally, it can be reseeded with human primary cells of endothelial linage to restore functionality of a vessel system that is capable of providing nutrition for other cell types in coculture. An example is the reintroduction of microvascular endothelial cells into the vascular structures of decellularized porcine jejunum of the small intestine as the so-called “biological vascularized scaffold” (BioVaSc-TERM®) that is also one component of this thesis [115]. The repopulation of the vessel system of such a scaffold with endothelial cells reduces the probability of thrombus formation and the calcification of vessels [116]. The reseeded vascular structures can be dynamically perfused in specifically designed bioreactor systems in order to preserve the characteristics of differentiated endothelial cells or to initiate the differentiation of endothelial progenitor cells by applying shear stress [117]. It was shown that such a vascular graft could support survival of three-dimensional tissue of considerable size. A prevascularized scaffold of this type was filled with hepatocytes in the former lumen and a complex, structured liver-like tissue was formed. It was supported by capillaries sprouted from existing small vessels of the wall of the jejunum into the lumen [118].

In orthopedic surgery, decellularized matrices in the shape of demineralized bone matrices (DBM) are a commonly used bone substitute material for filling defects. Donors of the bone are usually of bovine origin. During preparation of the demineralized matrix, soft tissue, blood, lipids are removed before acid demineralization. The result is a mixture of collagen type I, IV and X together with non-collagenous proteins, including BMP [119, 120]. The application of the matrix often takes place cell free but there are also experiments with previous cell seeding [120].

1.5 Growth factors and the special role of BMP

Bone morphogenetic proteins (BMPs) hold a prominent position in bone regeneration for their very efficient induction of bone formation. The following chapter addresses the BMPs' attributes, their capabilities in bone regeneration and clinical limitations that explain why they are not a cure-all despite their excellent qualities. BMPs are members of the transforming growth factor TGF-beta superfamily and are capable of differentiating mesenchymal stem cells into osteoblasts and thus form bone in targeted area. They influence and control differentiation, proliferation, state of maturation of a number of cells and they interact with other regulatory factors [121]. When BMPs interact with the surface receptor of a mesenchymal a complex cascade, which results in signals to the cell nucleus that induces the upregulation of gene expression that results in the production of molecules responsible for cartilage or bone formation. BMPs exerting a significant osteogenic activity are BMP-2, 4, 5, 6, 7, and 9 [122, 123]. BMP-2 and 7 have been studied intensively and are under investigation in human clinical trial especially targeting fracture healing and spinal fusions [124]. In the course of a number of successful applications of BMP-2 in clinical settings and with a magnitude of supporting research, it was rapidly becoming a frequent element of spinal surgeries in the USA since 2002 [125]. The success of recombinant human BMP-2 led to the approval for the use in human surgery by the FDA [126]. While the approval referred to the specific use of BMP in combination with a carrier matrix in a specific setting, the approval also inspired an extensive off-label use in clinical application. This means the application of pharmaceutical drugs for an indication different from the approved one or in unapproved dosages, age groups or routes of administration [127]. To date, there is no approval for a BMP-7 application for the use in human surgery.

While the main attribution of BMPs is the formation of bone, its effects are not limited to that. It is able to trigger fat formation as well as adipogenesis in different environments [128, 129]. Additionally, it affects the expression of inflammatory cytokines and tumor necrosis factor TNF-α as well as receptor activator of nuclear kappa-B ligand (RANKL) that can elicit osteoclast activity. The sheer range of

effects that BMP-2 can have immediately suggest that clinically relevant reactions, apart from the desired bone formation, can be the result.

An obvious side effect of BMP-2 as potent factor for bone induction is ectopic bone formation. BMPs can differentiate a range of cell types and thus a leakage of BMP during surgery leads to bone formation also in an environment of fibroblasts[130], myoblasts, adipocytes or chondrocytes [130–133]. The rate for ectopic bone formation in surgeries with BMP application was 70.1 % while the respective rate without BMP was 12.9 % [134]. Ectopic bone formation can be asymptomatic while in other settings can be a risk in the immediate vicinity of the spinal canal [135].

It is well-known that BMP-2 can induce osteoclast activity especially in cancellous bone [136]. A study that aimed at highlighting previously unreported incidents occurring alongside the use of BMP in clinical application during spine fusion reported a 69 % incidence rate for bone resorption. The study was based on the evaluation of CT images and states a patient selection bias due to the fact that CT scan are usually only performed on patients who experience complications postoperatively [137]. The results were confirmed in another study [138] and while the final results of the operative procedures indicate good fusion rates, it is demonstrated that especially during the early phase of resorption, osteolytic defects can occur due to the use of BMPs and should be subject to consideration during bone grafting.

While local and systemic infections are generally a possible side effect of invasive procedures, the incident rate for delayed wound infections increased 3-fold in lumbar fusion surgeries [129] and 5-fold in anterior/posterior surgeries when BMP was applied [139]. Similarly, the general wound complication rate increased from 18 % to 31 % in the BMP treatment group as compared to the control group [140].

Altogether, the use of BMP holds significant advantages in treatment of bone defects. Yet, its versatile nature and many modes of effect require thoughtful use and a clearly defined application profile in order to prevent any of the possible side effects. Therefore emerges the urgent necessity of approval of BMP use for very specific clinical settings by the cognizant authorities.

1.6 Animal models

In bone, a critical size defect is defined as the smallest defect size that does not heal during the lifetime of an organism. In many scenarios the term critical size defect is accepted whether or not it is known if the defect is of the smallest size because the end of an experiment is most of the time determined by the endpoint rather than the natural lifespan of an organism [141]. The development of an effective bone regeneration implant is dependent on a relevant animal model that is able to expose the capabilities and limitations of the designated implant. Within the wide range of available animal models, the choice should be made for those with the general attributes of allowing for reproducibility, low morbidity and mortality until the end of the experiment. More specifically in the bone regeneration investigation the size should be comparable with human defects as well as the expected strain in order to gain information and to be able to assess the suitability and practicability if the procedures were projected onto human patients/comparability with the human clinical setting.

1.7 Translation of research into clinical application

The ultimate goal of research in the field of regenerative medicine is the approval for human use in order to treat diseases and functional dysfunctions of the human body. Comprehensive regulations apply in order to ensure patient safety for the permission to manufacture Advanced Therapy Medicinal Products (ATMPs) intended for human use. ATMPs include gene therapy, cell therapy and tissue engineered products as well as combinations of ATMPs and medicinal devices [142].

In Europe, the regulation of ATMPs is centralized and ensures a comparable assessment of quality, harmlessness and efficacy of pharmaceuticals. ATMPs are controlled by the regulation 1394/2007, which introduces additional provisions to those laid down in Directive 2001/83/EC. Those are technical requirements, in particular the type and amount of quality, preclinical and clinical data necessary to demonstrate the quality, safety and efficacy of the product.

Due to the highly specific requirements, those aspects need to be established specifically for tissue engineered products in regulation 1394/2007. Centralized ATMP approvals are coordinated by the European Medicines Agency involving an expert committee, the Committee for Advanced Therapies (CAT), which was installed as official counselor responsible for judging the quality, safety and efficacy of each ATMP. Its recommendations are passed on to the Committee for Medicinal Products for Human Use (CHMP). Finally, the European Commission (EC) decides on the issuance of the permission for a manufacturing authorization based on the CHMP's advice [142, 143].

For the approval of ATMPs, there is an exception regulation that allows national approvals. The prerequisites are non-routinely production following specific quality standards in a specialized institution for patient care in the member state. The liability of the treatment is accepted by a physician on individual prescription. According to the German drug law (AMG) § 4b par. 3, ATMPS are object to approval by the Paul-Ehrlich-Institut (PEI), which ensures the demonstration quality, efficacy and harmlessness during the authorization process.

The quality standards that apply to nationally approved ATMPs are the same as on European level. In order to conform with the required quality standards the so-called good manufacturing practices (GMP) have to apply [142].

The GMP guidelines postulate a quality management system including standard operating procedures, qualified personnel, GMP-compliant facilities and equipment. Quality control, handling of complaints and self-audits are additional aspects. These are installed with the aim of avoiding contaminations during the production and ensuring continuous and reproducible quality and complete traceability [144].

1.8 Aim of the thesis

This thesis addressed the following clinically relevant aspects of bone grafting:
The production of a bone graft using minimally invasive methods, prevascularization based on the BioVaSc-TERM® in order to allow for an implant covering critical size defects and testing the regenerative potential thereof in an appropriate animal model. Additionally, the development of a mobile incubator system approached the transportation of the complex implant from the manufacturing site to the clinical site over a long distance. The whole developmental procedure considered GMP-conformity aspects for the option of rapid translation into clinical application.
The identification of suitable cell sources is crucial for the aim of a minimally invasive concept of implant construction. Mesenchymal progenitor cells as well as endothelial progenitor cells both fulfill the requirements of being readily accessible, circumventing the problematic nature of donor site morbidity, and a functionally suitable choice of cells. Their high proliferation capacity and their ability to facilitate angiogenesis, bone formation in a synergistic fashion predestinates their employment in bone tissue engineering.
The BioVaSc-TERM®, a naturally derived scaffold with vascular structures reseeded with endothelial progenitor cells, provides the basis for the vascularization of the implant, while ß-tricalcium phosphates seeded with mesenchymal progenitor cells are the mineral and cellular foundation for bone formation.
The resulting construct is a complex implant that requires specialized equipment for transportation from the manufacturing site to the clinical site. An issue that is dealt with by the design of a mobile incubator and bioreactor that provides a controlled environment and physiological stimuli for the implant.
The hypothesis that the manufactured implant is capable of inducing bone formation by providing effective cell delivery and survival due to vascularization was tested in vivo in sheep animal models.

2 Material

Table 2: Laboratory equipment

Equipment or device	Manufacturer
Accu-jet® pro pipettor	Brand, Wertheim (GER)
Analytical balance	Kern, Balingen-Frommern (GER) Sartorius, Göttingen (GER)
Aspiration device	Integra Biosciences, Fernwald (GER)
Autoclaves: Tecnoclav Table-top autoclave Varioclav	 Biomedis, Giessen (GER) Systec, Wettenberg (GER) H+P, Hackermoos (GER)
Bioreactor	Weckert Labortechnik, Kitzingen (GER)
Blocking station: EG1150H	Leica, Wetzlar (GER)
Cassette printer: VCP5001	Vogel Medizintechnik, Gießen (GER)
Cell incubator Haraeus: BBD6220 37 °C, 5 % CO_2	Thermo Fisher Scientific, Dreieich (GER)
Centrifuges: Multifuge X3R Centrifuge 5417R Centrifuge 5424	 Thermo Fisher Scientific, Dreieich (GER) Eppendorf, Hamburg (GER) Eppendorf, Hamburg (GER)
Cold-storage room, 4 °C	Genheimer, Höchberg (GER)
Cryostat: CM 1850 UV	Leica, Wezlar (GER)
Digital camera	Canon, Krefeld (GER)
Dish washer	Miele, Gütersloh (GER)
Drying oven	Memmert, Schwabach (GER)
Electrospinning apparatus	Department of Functional Materials, Würzburg (GER)
Embedding station: Microm STP 120	Thermo Fisher Scientific, Dreieich (GER)
Freezer: -80 °C -20 °C	 Kendro, München (GER) Liebherr, Biberach a.d. Riss (GER)
Freezing container “Mr. Frosty”	VWR, Darmstadt (GER)
Fume hood	Prutscher Laboratory Systems, Neudörfl (AUT)
Hot air sterilizer	Memmert, Schwabach (GER)
Ice machine: AF-80	Scotsman, Milan (I)
Imaging station: FluorChem Q	Biozym Scientific GmbH, Hessisch Oldendorf (GER)
Immersion thermostat for water bath	Lauda, Lauda-Königshofen (GER)

Equipment or device	Manufacturer
Laminar air flow cabinet: Safe 2020	Thermo Fisher Scientific, Dreieich (GER)
Liquid nitrogen storage tank: MVE 815 P-190	German-cryo, Jüchen (GER)
Magnetic stirrer: 720-HPS	VWR, Darmstadt (GER)
Micro-plate reader: Tecan Infinite M200	Tecan, Crailsheim (GER)
Microscopes: Axiovert 40C Biorevo BZ-9000 Evos AMG Scanning electron microscope Zeiss DSM 940A	Zeiss, Oberkochen (GER) KEYENCE, Neu-Isenburg (GER) Life technologies, Darmstadt (GER) Zeiss, Oberkochen (GER)
Multi-Channel Pipette Plus	Eppendorf, Hamburg (GER)
Multistep pipette: Multipipette M4	Brand, Wertheim (GER)
Neubauer cell counting chamber	Hartenstein, Würzburg (GER)
Orbital shaker	NeoLab, Heidelberg (GER)
Paraffinized tissue floating bath 1052	Medax, Kiel (GER)
pH meter	Mettler Toledo, Giessen (GER)
Pipette tamping machine	BellCo Glass Dunn, Asbach (GER)
Pipettes: 0.5–10 µl, 10–100 µl, 100–1000 µl	Eppendorf, Hamburg (GER)
Power supplies: EV202, EV243	PeqLab Biotechnology, Erlangen (GER)
Rocking platform shaker	NeoLab, Heidelberg (GER)
Roller mixer	Hartenstein, Würzburg (GER)
Safety cabinet: Safe 2020	Thermo Fisher Scientific, Dreieich (GER)
Slide printer: VSP 5001	Vogel Medizintechnik, Gießen (GER)
Sliding microtome: SM 2010R	Leica, Wetzlar (GER)
Rotary Microtome RM 2255	Leica, Wetzlar (GER)
Steamer “Multi Gourmet”	Braun, Kronberg (GER)
Thermomixer comfort	Eppendorf, Hamburg (GER)
Vortex Genie 2	Scientific Industries, INc., NY (USA)
Water bath	Memmert, Schwabach (GER)
Water purification system	Millipore, Schwalbach (GER)

Table 3: Disposables

Disposable material	Manufacturer
Aluminum Foil	Carl Roth GmBH, Karlsruhe (GER)
Catheter Introcan W 14 G, 18 G, 20 G,	B. Braun Melsungen AG, Melsungen (GER)
Cell Culture Flasks: 25 cm², 75 cm², 150 cm²	TPP, Trasadingen (GER)
Cell Culture Multiwell Plates: 6 well, 12 well, 24 well, 96 well	TPP, Trasadingen (GER)
Cell culture plates 145 x 20 mm, 94 x 15 mm, 60 x 15 mm, 35 x 10 mm	TPP, Trasadingen (GER)
Centrifuge Tubes: 15 ml, 50 ml	Greiner Bio-One, Frickenhausen (GER)
Chamberslides: 8 well, Glass	Nunc, Wiesbaden (GER)
Combitips Plus: 0.5 ml, 1 ml, 2.5 ml, 5 ml	Eppendorf, Hamburg (GER)
Cover Slips for Object Slides: 24 x 60 mm	Menzel-Glaser, Braunschweig (GER)
Cryo Tubes: 1.8 ml	Nunc, Wiesbaden (GER)
Dako Pen	Dako, Hamburg (GER)
Disposal Bags	Hartenstein, Wuerzburg (GER)
Disposable microtome blades, type A35	pfm medical, Cologne (GER)
Easyflex+ empty bag sterile	Macopharma, Tourcoing (FR)
Gloves: Latex Nitrile	 Cardinal Health, Kleve (GER) Shield scientific, BENNEKOM (NL)
Grease Pencil	Dako, Hamburg (GER)
Monovette blood collection tubes	Sarstedt, Nümbrecht (GER)
Object slides	Menzel, Braunschweig (GER)
Parafilm R, M	Carl Roth, Karlsruhe (GER)
Pasteur Pipettes	Brand, Wertheim (GER)
PCR Tubes	Biozym Scientific, Oldendorf (GER)
Petri dishes: 145 x 20 mm, 94 x 15 mm, 60 x 15 mm, 35 x 10 mm	Greiner Bio-One, Frickenhausen (GER)

Disposable material	Manufacturer
Pipette Tips: 0.5 – 10 µL, 10 – 100 µL, 100 - 1000 µL	Eppendorf, Hamburg (GER)
Pump tubing	Ismatec, Wertheim-Mondfeld (GER)
Reaction Tubes: 1.5 mL, 2.0 mL	Sarstedt, Nümbrecht (GER)
Scalpel Blades, rounded	Bayha, Tuttlingen (GER)
Septophag Disposable Bags	Porod, Frauenhofen (AUT)
Diameter 50 mm, Pore Size 0.2 µm	Sartorius Stedium Biotech, Goettingen (GER)
Sewing Thread Silkan 4/0 10x45	B. Braun, Melsungen (GER)
Syringes: 5 ml, 10 ml, 20 ml, 50 ml	BD Biosciences, Heidelberg (GER)
Tygon™ Sanitary Silicone Tubing Formula 3350	Saint-Gobain, Courbevoie (FR)
Weighing Dish	Hartenstein, Wuerzburg (GER)

Table 4: Laboratory material

Laboratory material	Manufacturer
Beakers: 1 L, 500 mL, 250 mL	Schott, Mainz (GER)
Centrifuge Tubes Rack	NeoLab, Heidelberg (GER)
Cold Protection Gloves	VWR, Darmstadt (GER)
Cover slips	Menzel-Gläser, Braunschweig
Female Luer Lug Style to 200 Series Barb, 1/8" (3.2 mm)	Norson Medical, Fort Collins (USA))
Female Luer Lug Style Tee	Norson Medical, Fort Collins (USA)
Female Luer Thread Style with 5/16" Hex to 1/4-28 UNF Thread	Norson Medical, Fort Collins (USA)
Funnel	Hartenstein, Würzburg (GER)
Glass cannula	Weckert, Kitzingen (GER)
Glass Cuvette with Lid: 110 x 90 x 80 mm	Mercateo, Munich (GER)
Glas lid, 10 cm diameter	Gaßner Glastechnik, Munich (GER)
Glass Pipettes: 5 ml, 10 ml, 25 ml, 50 ml	Brand, Wertheim (GER)
Laboratory Bottle:	

Laboratory material	Manufacturer
1 L, 250 ml, 100 ml, 50 ml	Schott, Mainz (GER)
Laboratory glass bottle (Schott, GER) provided with custom glass tube connection	Weckert, Kitzingen (GER)
Male Luer Integral Lock Ring to 200 Series Barb, 1/8" (3.2 mm)	Norson Medical, Fort Collins (USA)
Male Luer Integral Lock Ring Plug, Closed at Grip	Norson Medical, Fort Collins (USA)
Magnetic Stirring Bar Retriever	Hartenstein, Würzburg (GER)
Needlefree Swabable Valve Female Luer to Male Luer Lock	Norson Medical, Fort Collins (USA)
Object Slide Racks: Glass, Stainless Steel	Mercateo, Munich (GER)
Protective Goggles	NeoLab, Heidelberg (GER)
Reaction Tubes Rack	NeoLab, Heidelberg (GER)
Surgical Knife	Bayha, Tuttlingen (GER)
Spatula	VWR, Darmstadt (GER)
Spoon Spatula	Hartenstein, Würzburg (GER)
Spray Flask (Ethanol, 70 %)	Hartenstein, Würzburg (GER)
Stainless Steel Casting Moulds for Embedding Tissue: 24 x37 x9 mm	Labonord, Moenchenglattbach (GER)
Straight Through Tube Fitting with Classic Series Barbs, 1/8" (3.2 mm)	Norson Medical, Fort Collins (USA)
Sterile Filter (Attachement for Laboratory Bottles)	Hartenstein, Würzburg (GER)
Tweezers	Assistent, Sondheim (GER)
Volumetric Flasks with Plug: 1 L, 2 L	Schott, Mainz (GER)
Y Tube Fitting with 200 Series Barbs, 1/8"	Norson Medical, Fort Collins (USA)

Table 5: Chemicals

Chemical	Manufacturer	Order number
2-Propanol	Carl Roth, Karlsruhe (GER)	9866.6
3-[(3-Cholamidopropyl) dimethylammonio]-1-Propanesulfonate (CHAPS)	Merck, Darmstadt (GER)	220201-1KG
Acetic acid (100 %)	Carl Roth, Karlsruhe (GER)	6755.2
Acetone (≥ 99,5 %)	Carl Roth, Karlsruhe (GER)	5025.5
Acetylated low density lipoprotein	Thermo Fisher Scientific, Dreieich (GER)	L3484
Acrylamide (30 %)	Carl Roth, Karlsruhe (GER)	A124.2
Agarose	AppliChem, Darmstadt (GER)	A2114/CA50
Albumine Fraction V (BSA)	Carl Roth, Karlsruhe (GER)	T844.2
Alcian blue	Sigma-Aldrich, Munich (GER)	A3157-10G/DAL1100
Amphotericin B	Gibco, Darmstadt (GER)	15290-026
Antibody diluent	Dako, Hamburg (GER)	S302283
Calcium Chloride (CaCl2)	VWR, Darmstadt (GER)	1.02391.1000
Citric Acid	VWR, Darmstadt (GER)	1.00244.1000
Collagenase	Roche, Mannheim (GER)	11213865001
Collagenase I	Worthington biochemical, USA	LS004196
Collagenase II		LS004176
DAPI Fluoromout-GTM	SouthernBiotech, Birmingham (USA)	SBA-0100-20

Chemical	Manufacturer	Order number
Deionized Water	University Hospital, Wuerzburg (GER)	
Descosept	Seidel medipool, Reichertshofen (GER)	506125
Dimethyl sulfoxide (DMSO)	Sigma-Aldrich, Schnelldorf (GER)	D2438-50ML
Donkey Serum	Sigma-Aldrich, Schnelldorf (GER)	D9663-10ML
DNase I, from bovine pancreas	Roche, Mannheim (GER)	10104159001
Dulbecco's Modified Eagle Medium (DMEM)	PAA, Colbe (GER)	G0001,3010
Eosin	Sigma-Aldrich, Seelze (GER)	861006-25G
Eosin	Morphisto, Frankfurt Main (GER)	10231
Ethanol, absolut	Carl Roth, Karlsruhe (GER)	9065.2
Ethanol, denatured (96 %)	Carl Roth, Karlsruhe (GER)	T171.2
Ethylenediaminetetraacetic acid (EDTA – Na2 *2 H2O)	Sigma-Aldrich, Seelze (GER)	E5134-1KG
Fetal Calf Serum	Lonza, Cologne (GER)	Lot No.8SBO16
Feulgen staining kit	VWR, Darmstadt (GER)	1.07907.0001
Fuchsin S, acid fuchsin	Chroma, Muenster (GER)	1B-525
Gelatine	Sigma-Aldrich, Seelze (GER)	48720-100G-F
Gentamycin (10 mg /mL)	PAA, Colbe (GER)	P11-004
Glycerol (86 %)	Carl Roth, Karlsruhe (GER)	4043.1
Glycine	AppliChem, Darmstadt (GER)	A1067,1000
H_2O_2, 30 %	Carl Roth, Karlsruhe (GER)	8070.2
Hematoxylin	Carl Roth, Karlsruhe (GER)	3861.1

Chemical	Manufacturer	Order number
Hematoxylin	Morphisto, Frankfurt Main (GER)	10231
Hydrochloric acid (HCl; 37 %, 1M)	VWR, Darmstadt (GER)	1.09057.1000
Isoflurane	Cp pharma, Burgdorf (GER)	
Isopropyl	Carl Roth, Karlsruhe (GER)	2316.5
Iron hematoxyline, Solution A	Chroma, Muenster (GER)	2E-032
Iron hematoxyline, Solution B	Chroma, Muenster (GER)	2E-052
Magnesium Chlorite Hexahydrate (MgCl2 *6 H2O)	Carl Roth, Karlsruhe (GER)	HN03.3
Mounting Medium: Entellan	Merck, Darmstadt (GER)	1079600500
Mounting Medium: Mowiol	Carl Roth, Karlsruhe (GER)	0713
Nuclear Fast Red	Merck, Darmstadt (GER)	1.15939.0025
Paraffin	Carl Roth, Karlsruhe (GER)	6642.6
Paraformaldehyde (PFA)	AppliChem, Darmstadt (GER)	A3813,1000
Penicillin / Streptomycin (100x concentrated)	PAA, Colbe (GER)	P11-010
Phosphate Buffered Saline (PBS) with calcium and magnesium	Sigma-Aldrich, Munich (GER)	D8537-6x500ml
Phosphate Buffered Saline (PBS) without calcium and magnesium	Sigma-Aldrich, Munich (GER)	D8662-6x500ml
phosphotungstic acid, 5 %	Merck, Darmstadt (GER)	1005830100
Potassium Chloride (KCl)	Merck, Darmstadt (GER)	1049361000
RBC Lysis Buffer	Biolegend	420301

Chemical	Manufacturer	Order number
Roti-Histofix 4 %	Carl Roth, Karlsruhe (GER)	P087.1
Roticlear®	Carl Roth, Karlsruhe (GER)	A538.5
Saffron	Sigma-Aldrich, Munich (GER)	S8381-5G
Sodium Chloride (NaCl)	Carl Roth, Karlsruhe (GER)	HN00.3
Sodium Deoxycholic Acid	Carl Roth, Karlsruhe (GER)	3484.7
Sodium dodecyl sulfate (SDS; 10 %)	BioRad, Munich (GER)	161-0416
Sodium Hydrogen Carbonate (NaHCO3)	Carl Roth, Karlsruhe (GER)	HN01.2
Sodium Hydroxyde (NaOH) Pellets	Carl Roth, Karlsruhe (GER)	6771.3
Sodium Pyruvate (100 mM)	Invitrogen, Darmstadt (GER)	11360-039
TGF-β1	Cell Signaling Danvers (USA)	8915
Tris	Carl Roth, Karlsruhe (GER)	4855.1
Triton-X 100	Carl Roth, Karlsruhe (GER)	3051.2
Trizma Hydrochloride	Sigma-Aldrich, Schnelldorf (GER)	T5941-1KG
Trypan Blue, 0.4 %	Sigma-Aldrich, Schnelldorf (GER)	T8154-100ML
Trypsin (0,5 % (10x) with EDTA, 4 Na)	Invitrogen, Darmstadt (GER)	18912-014
Tween-20	VWR, Darmstadt (GER)	8.22184.0500
Ultrapure Water	Millipore, Schwalbach (GER)	
Xylenes	Carl Roth, Karlsruhe (GER)	9713.3

Table 6: Cell culture media

Medium	Composition	
MSCGM	500 ml	Lonza MSCGM Basal Medium
EGM-2	500 ml	Lonza EGM-2 Basal Medium
	25 ml	FCS
	2 ml	ECGS/H-2
	5,0 µg	hEGF-5
	500 µg	Hydrocortisone-500
Vasculife	500 ml	Vasculife Basal Medium
	5 ng/ml	rh FGF basic
	50 µg/ml	Ascorbic Acid
	1 µg/ml	Hydrocortisone
	2 %	FBS
	10 mM	L-Glutamine
	15 ng/ml	rh IGF-1
	5 ng/ml	rh EGF
	5 ng/ml	rh VEGF
	0.75 U/ml	Heparin sulfate

Table 7: Buffers and solutions for cell culture

Buffer/Solution	Composition	
0.05 % Trypsin/EDTA working solution	10 % (v/v)	Trypsin/EDTA stock solution in PBS^-/EDTA solution
$CaCl_2$-solution (300 mM)	22.1 g	$CaCl_2$
	500 ml	Ultrapure water
		sterile-filtered before use
		stored at 4 °C
Collagenase (500 U/ml)	1.0 g	Collagenase
	436 ml	DMEM
		sterile-filtered before use
		stored at -20 °C
Chondroitin-6-sulfate solution	25 mg	Chondroitin-6-sulfate
	5 ml	PBS^+
		sterile-filtered before use
		stored at 4 °C
DAPI staining solution	0.1 µg/ml	DAPI in PBS^-

Buffer/Solution	Composition	
		prepared immediately before use
Dispase (2 U/ml)	400 mg 100 ml	Dispase PBS^- sterile-filtered before use stored at -20 °C
Fluorescein diacetate (FDA) solution	5 mg/ml	FDA in acetone stored at -20 °C
Fibronectin stock solution	0.5 mg/ml	Fibronectin lyophilisate in ultrapure water sterile-filtered
Fibronectin working solution (50 µg/ml)	10 % (v/v)	Fibronectin stock solution in PBS^+
Gel neutralization solution (GNL)	7.5 ml 2.5 ml 7.5 ml 232.5 ml	3 M HEPES Chondroitin-6-sulfat-solution FCS 2 x DMEM sterile-filtered stored at 4 °C
3M HEPES solution	7.15 g 10 ml	HEPES PBS^-, sterile-filtered
MTT reagent	3 mg/ml	MTT in PBS^+ sterile-filtered Stored at -20 °C
MTT solution	1 mg/ml	MTT reagent in PBS^+ Prepared immediately before use
PBS^-/EDTA solution	0.5 ml 500 ml	EDTA PBS^-
Propidiumiodid (PI) solution	2 mg/ml 1 ml	PI in PBS^+ Stored at -20 °C
PI/FDA solution	1 µl 9 µl 990 µl	FDA solution PI solution PBS^+
Red Blood Cell Lysis Buffer	10 % (v/v)	RBC Lysis Buffer stock solution in purified water
WST solution	1 mg/ml	WST reagent in PBS^+ Prepared immediately before use

Table 8: Chemicals and Solutions for Histology and Immunohistochemistry

Chemical/Solution	Composition	
Acetic acid, 3 %	3 % (v/v)	100 % acetic acid in deionized water Stored at RT
Acetic acid, 0.5 %	0.5 % (v/v)	100 % acetic acid in deionized water Stored at RT
Alkaline alcohol	10 mL 90 mL	Ammonium hydroxide 96 % Ethanol Stored at RT
Alcian blue, 1 %	10 g / L	Alcianblau 8GX In deionized water Stored at RT
Alcian blue (used for Pentachrome staining)	1 g 1 mL	Alcianblau 8GX 100 % acetic acid In deionized water Stored at RT
Alizarin Red S working solution	 1 %	Alizarin Red S Ammonia
Brilliant crocein- acid fuchsin, solution A	0,1 g 0,5 mL 99,5 mL	Brilliant Crocein R 100 % acetic acid Deionized water
Brilliant crocein- acid fuchsin, solution B	0,1g 0,5 mL 99,5 mL	Acid Fuchsin 100 % acetic acid Deionized water
Brilliant crocein- acid fuchsin, working solution	80 % (v/v) 20 % (v/v)	Solution A Solution B Stored at RT
Citrate buffer stock solution (10 x concentrated)	42 g / L 17.6 g / L	Citric acid NaOH pellets in deionized water pH 6.0 Stored at 4 °C
Citrate buffer working solution	10 % (v/v)	Citrate buffer stock solution in deionized water Stored at 4 °C.
H_2O_2, 3 %	10 % (v/v)	H_2O_2 solution (10 %) in deionized water Prepared immediately before use
HCl /EtOH (used for H&E Staining)	6.85 % (v/v)	HCl, 1M in Ethanol (50% v/v) Stored at RT
Iron hematoxylin, solution A	1g 100 mL	Hematoxylin 96 % Ethanol Stored at RT

Chemical/Solution	Composition	
Iron hematoxylin, solution B	2,48 g	Iron(III)chloride hexahydrate (FeCl3 x 6 H2O)
	1 mL	Concentrated HCl
		Add 100 ml deionized water
		Stored at RT
Iron hematoxylin, working solution	50 %	Iron hematoxylin, solution A
	50 %	Iron hematoxylin, solution B
Nuclear Fast Red	5 g	Aluminum sulfate in 100 ml deionized water
	0.1 g	Nuclear fast red added
		Stored at RT.
Oil Red O, working solution	0.5 g	Oil Red O in 100 ml isopropyl alcohol mixed with purified water 6:4 prior to use
PFA 4 %	40 g / L	Paraformaldehyde in PBS- solution (solved at 60°C)
		pH 7.4
		Stored at RT.
Pikrofuchsin	15 mL	1 % Fuchsin S, acid fuchsin
	100 mL	Saturated aqueous Pikrin acid
Resochin-Fuchsin Solution A	0.5 g	Fuchsin
	1 g	Resorchin
		In deionized water
Resochin-Fuchsin Solution B	2 g	Iron chloride
	10 mL	Deionized water
Rescohin-Fuchsin working solution	5 % (v/v)	Solution A
	5 % (v/v)	Solution B
	90 % (v/v)	HCl-Ethanol
Saffron du Gatinais	6 g	Saffron du Gatinais
	100 mL	96 % Ethanol
		Stored in the dark at RT
PBST, 0.05 M	100 mL	PBS stock 10x
	5 mL	Tween-20 (0.5 % v/v)
	900 mL	Deionized Water
		Stored at RT.

Chemical/Solution	Composition	
Phosphate buffered solution (PBS) stock, 0.5 M, 10x concentrated	191.00 g	PBS powder ad 2 L ultrapure water pH 7.2 Stored at RT.
Triton-X Permeabilizing Solution	0.2 % (v/v) in 0.05 M	Triton-X 100 TBS Buffer Stored at RT.

Table 9: Research animals

Animal	Origin
Deutsche Landschwein Rasse pigs	Niedermayer, Dettelbach (GER)
Tiroler Bergschaf	Lehr- und Forschungsgut - Veterinary Medical University Vienna
Merino sheep	Medical Engineering Research Facility (MERF), Brisbane

3 Methods

3.1 Cell culture methods

Sterile work was conducted in class II laminar flow benches. All solutions were sterile filtered before use if necessary. All material, except single-use items, were autoclaved or hot-air sterilized before use. If not otherwise stated, all cell culture media and solutions were warmed up to 37 °C in a waterbath before use. Culture of cells was performed in incubators with a relative humidity of 95 %, 5 % CO2 and a temperature of 37 °C.

3.1.1 Isolation of primary human cells

3.1.1.1 Mesenchymal progenitor cells

Primary human mesenchymal stem cells were isolated from spongy bone. 50 ml conical tubes were filled half with spongy bone and 20 ml of prewarmed PBS^+ were added. The tube was closed and manually shaken thoroughly in order to liberate cells from the spongy bone. After 5 minutes of sedimentation, the supernatant was collected in a separate tube. The procedure was repeated until the spongy bone, that previously appeared red, became almost white in color. This was usually the case after 5 washing steps. The collected cell suspension was centrifuged for 5 minutes at 270 g and the supernatant was aspirated. The cell pellet was resuspeded in 25 ml of MSCGM and cells were counted by mixing 50 µl of the cell suspension with 1 x lysis buffer 1:2 before the standard counting procedure. The buffer lysed the vast amount of red blood cells and allowed for the counting of the mononuclear cells isolated. Cell seeding took place in T150 flasks at a cell density of 3 x 10^3 cells per cm^2 and medium change took place twice a week.

3.1.1.2 Microvascular endothelial cells

Human microvascular endothelial cells were isolated from adult skin biopsies or from foreskin. Skin biopsies were placed in a Petri dish and rinsed with PBS^+ three times before fat and connective tissue were removed with a scalpel. After surface estimation of the biopsies and cutting them into stripes of 2 – 3 mm, they were transferred into another Petri dish containing 10 ml of dispase. Wrapping the dish with parafilm® it was incubated at 4°C for 16 – 18 h overnight. The next day, the dermis was separated from the epidermal layer using tweezers. The dermis was collected in a Petri dish filled with 20 ml of PBS^+. The PBS^+ was then aspirated and replaced by Versene and samples were gently swayed. Following the removal of the Versene an incubation with 10 ml of 0.05 % trypsin/EDTA per every 6 cm^2 of sample for 40 minutes achieved loosening of the tissue. The enzymatic reaction stopped after the addition of 1 % of FCS and the transfer of the dermal pieces into another Petri dish filled with prewarmed Vasculife medium followed. The actual liberation of cells from the tissue took place by squeezing the dermal stripes lengthways using tweezers and a scalpel. The procedure was repeated eight times from all sides. The resulting cell suspension was put through a strainer and collected in a 50 ml conical tube before centrifugation at 270 g for 5 minutes. Subsequent to the resuspension of the cells in Vasculife they were seeded into T25 or T75 cell culture flasks at their specific seeding density (foreskin: 1.2 x 10^4 cells/cm^2; adult skin: 4 – 5 x 10^4 cells/cm^2). Medium change took place every 2 – 3 days. Cell morphology was observed during culture of endothelial cells. In case of a contamination with fibroblasts, the medium was aspirated and cells washed with PBS^-. Versene was added for 5 – 10 min (0.15 ml/cm^2) while observation under the microscope. As soon as fibroblasts began to round up, tapping of the flasks detached the fibroblasts from the surface. After aspiration of the Versene, washing of cells followed before adding fresh Vasculife.

3.1.2 Isolation of primary ovine cells

3.1.2.1 Mesenchymal progenitor cells

Ovine mesenchymal progenitor cells were isolated from bone-marrow aspirate. Bone marrow aspirate was mixed 1:2 with PBS^- and 20 ml carefully layered over 15 ml density gradient centrifugation medium prepared in a 50 ml conical tube. Subsequently, centrifugation at 800 g at room temperature followed for 20 minutes. The centrifuge ran at low acceleration and without break. The resulting opaque layer containing the cells was transferred into a separate conical tube using a 5 ml pipette. Cells were washed with 35 ml of PBS^-/EDTA and centrifuged at 800 g for 10 minutes. The supernatant was aspirated and the washing step repeated. The resulting pellet was resuspended in 10 ml of MSCGM and transferred into a T75 cell culture flask. The next day, after attachment of the cells, they were gently washed with PBS^+ in order to remove residual erythrocytes and cell debris from the culture. Medium change took place twice a week.

3.1.2.2 Endothelial progenitor cells

Isolation of ovine endothelial progenitor cells was performed by density gradient centrifugation of peripheral whole blood using Histopaque®-1077 medium (Sigma-Aldrich Chemie GmbH, Schnelldorf, Germany). Cells were centrifuged at 400 g for 30 min. After two washing steps, the resulting cell fraction was seeded on standard cell culture surfaces with ECGM-2 medium (Promocell, Heidelberg, Germany). Surfaces were coated with 1 % fibronectin before. Medium change was performed twice a week.

3.1.3 Cell culture conditions

3.1.4 Passaging of cells

Cell expansion took place in cell culture flasks, passaged when confluence reached 80 – 90 %. To this end, the medium was aspirated and cells were washed with PBS^-. Microvascular endothelial cells were then incubated with prewarmed PBS-/EDTA for approximately 10 minutes, the solution was aspirated when cells began to round up. The incubation with 0.05 % trypsin/EDTA was performed for 3 – 5 min followed by the addition of 1 % FCS to stop the enzymatic reaction. After a microscopic check, the cells were transferred into a 50 ml conical tube and centrifuged for 5 minutes at 270 g. Following the aspiration of the supernatant, the cell pellet was resuspended in appropriate cell culture medium and their number was determined.

3.1.5 Cell counting and cell viability determination

The Neubauer counting chamber and staining with trypan blue were used to count cells and determine viability. In the presence of trypan blue, viable cells appear colorless, while dead cells are blue. After detachment, an aliquot of cells was mixed 1:2 with 0.4 % trypan blue and the resulting solution was applied to the counting chamber. The number of viable and dead cells in all four quadrants of the chamber were counted.
Viable cell number was calculated as follows:

$$VCC = M_{VCC} \times 10000 \times DF_{TB} \times V_{susp}$$

Total cell number was calculated as follows:

$$CC_{tot} = (M_{VCC} + M_{CCd}) \times 10000 \times VF_{TB} \times V_{susp}$$

Viability was calculated as follows:

$$V\ [\%] = \frac{VCC}{CC_{tot}} \times 100\ \%$$

CC	cell count	*VCC*	viable cell count
CC_{tot}	total cell count	M_{VCC}	mean viable cell count
M_{CCd}	mean dead cell count	DF_{TB}	dilution factor trypan blue
V_{susp}	volume of cell suspension	*V*	vitality [%]

3.1.6 Freezing of cells

Cells were frozen at a cell density of 1 x 10^6 cells/ml in their respective medium supplemented with 10 % FCS and 10 % DMSO. 1 ml of cells in their freezing medium was applied to cryo tubes before prompt placement into Mr Frosty freezing containers and storage at -80 °C for at least 24 h. Longtime storage took place at -180 °C in a liquid nitrogen tank.

3.1.7 Thawing of cells

Cryo conserved cells thawed at 37 °C in a waterbath before the transfer into a 15 ml conical tube and resuspension in 9 ml prewarmed cell specific medium. After centrifugation for 5 minutes at 270 g, the supernatant was aspirated and the cell pellet was resuspended in fresh cell specific medium and cells were seeded into cell culture flasks. Medium aspiration 24 h later ensured removal of debris of dead cells and new medium was added.

3.1.8 Differentiation of human and ovine mesenchymal stem cells

In order to confirm the pluripotent nature of the MSC of human and ovine origin, their ability to differentiate was checked by the differentiation into the adipogenic, chondrogenic and osteogenic linage.

3.1.8.1 Adipogenic differentiation

Differentiation of human mesenchymal stem cells into adipocytes was achieved by culture of the cells in adipogenic differentiation medium. For this, 100,000 cells were seeded into each well of a permanox 4-well chamberslide. Cells were cultured in MSCGM containing 2 % FCS until a confluent monolayer was established. Then, the culture continued in adipogenic differentiation medium.

Table 10: Composition of adipogenic differentiation medium

Component	Concentration
DMEM	
FCS	10 %
Dexamethasone	1 µM
IBMX	500 µM
Insulin	1 µg/ml
Indomethacin	100 µM

One chamber per chamberslide served as control and was cultured in MSGCM with 2 % FCS. Medium change took place three times a week over a duration of 14 days.

3.1.8.2 Chondrogenic differentiation

For the chondrogenic differentiation, MSC were culture in pellets by seeding 2.5 x 10^6 cells into a 15 ml conical tube with subsequent centrifugation at 270 g for 5 minutes.

Table 11: Composition of chondrogenic differentiation medium

Component	Concentration
DMEM	
FCS	10 %
Ascobart-2-phosphate	50 µg/ml
Dexamethasone	1 µM
Pyruvate	100 µg/ml
L-Proline	40 µg/ml
ITS+1	1 5
TGF-ß3	10 ng/ml

TGF-ß3 was added right after the addition of medium. Cell pellets in the differentiation medium without TGF-ß3 served as control. Medium was changed twice a week for 21 days in total.

3.1.8.3 Osteogenic differentiation

Osteogenic differentiation was achieved by culture of MSCs in osteogenic differentiation medium. Initially, 100.000 MSCs were seeded into each well of 4-well chamberslides in MSGCM with 2 %FCS. Upon the formation of a confluent monolayer, the medium was exchanged with osteogenic differentiation medium.

Table 12: Composition of osteogenic differentiation medium

Component	Concentration
DMEM	
FCS	10 %
Ascobart-2-phosphate	50 µg/ml
Dexamethasone	1 µM
ß-Glycerophosphate	10 mM

The MSCs of one chamber were continually cultured in MSGM with 2 % FCS as a control. Medium change took place three times a week for a total duration of 28 days.

3.2 Generation of the cell-free biological vascularized scaffold BioVaSc-TERM®

The biological vascularized scaffold (BioVaSc-TERM®) was generated from resected porcine jejunal segments including the associated supporting vessel system. Tissue harvesting from 2-year-old piglets (10 – 15 kg) was performed in compliance with the Guide for Care and Use of Laboratory Animals and approved by the local animal protection board. On explantation, the arterial and venous pedicles were cannulated and immediately perfused with 0.9 % NaCl solution in order to check venous return and to clean it from residual blood. Remnants were removed from the jejunal lumen and tissue was transferred into a pressure controlled bioreactor system for decellularization. The vascular structures and lumen were perfused with 500 ml 3.4 % sodium deoxycholate monohydrate at a pressure of 80 mmHg. Cell remnants were removed by perfusion with 1 liter 0.9 % NaCl solution. The scaffold was subsequently incubated with 250 ml 3.4 % sodium deoxycholate monohydrate overnight at 4 °C. The next day, vessel integrity of the scaffold was checked by perfusion with 2 ml of 0.1 % phenol red. In the following washing steps the BioVaSc-TERM® was perfused with 2 l of NaCl under constant pressure monitoring. DNA digestion was achieved by incubation overnight in 250 ml DNase solution. After the final washing steps of four times incubation in 250 ml 0.9 % NaCl, gamma irradiation was performed with a 25 kGy dose (BBF Sterilisationsservice GmbH, Rommelshausen, Germany). During the decellularization process samples of the solutions were taken in order to perform bile acid assay and measurement of endotoxin levels. After gamma irradiation, a small peripheral part of the BioVaSc-TERM® was taken for quality control (histology, DNA content measurement). Manufacturing protocols documented the process.

3.3 Generation of prevacularized bone implants

For the seeding of the BioVaSc-TERM® with microvascular endothelial cells or endothelial progenitor cells and bioreactor system was employed. The reactor system consisted of a sealable glass bowl with two insertions that allowed the connection to silicone tubes that established connections to a reservoir bottle and a pressure bottle. The circuit contained pumping tubes that enabled the perfusion of the system with medium via peristaltic pumps.

3.3.1 Seeding of BioVaSc-TERM® with microvascular endothelial cells

The BioVaSc-TERM® was placed in 20 ml Vasculife medium at 37°C during detachment of mvECs and 5.0 x 10^6 cells were taken up in 5 ml Vasculife medium in a syringe that then was attached to the arterial pedicle and cells were slowly inserted. The scaffold was incubated for 3 h and seeded a second time with 5.0 x 10^6 mvECs. After another 3 h of incubation the BioVaSc-TERM® was placed into the bioreactor system a perfused at 5 rpm (~ 5 ml/min) overnight. The next day, dynamic pressure conditions were established dynamically at 80 – 120 mmHg, 1 Hz, using the bioreactor and incubator system. The culture continued for two weeks with two partial media changes per week (50 ml). At the end of the culture period, perfusion with 2 ml of 0.1 % phenol red demonstrated vessel integrity of the scaffold.

3.3.2 Seeding of MSCs onto ß-TCP granules

5 ml of ß-TCP granules were filled into each well of a 6-well plate. MSCs were detached and 2.5 x 10^6 cells were seeded onto the granules in 600 µl MSCGM per well. After 20 minutes of incubation at 37 °C the medium volume was increased to 4 ml so that the granules were covered. The culture period was 3 days before the granules were combined with the BioVaSc-TERM®.

3.3.3 Combination of reseeded BioVaSc-TERM® and seeded ß-TCP

If not stated otherwise, after 3 days of culture of the MSCs on TCP and 7 days of culture of the reseeded BioVaSc-TERM® both components were combined. One end of the BioVaSc-TERM®'s lumen was clamped while from the other end, the lumen was filled with cell-seeded granules using a spatula. Approximately 10 ml of granules filled the BioVaSc-TERM® before the combined culture continued for 7 days.

3.3.4 Prevascularized bone implantation in the ovine tibia

The BoneVaSc-TERM® was brought into a critical-size tibia defect in sheep and sutured to the adjacent periosteum of the bony ends left and right from the defect. The defect was an excision of 3 cm of the tibia that was then stabilized with reconstruction plates. The plates were anchored with four screws proximally and three screws distally. The implantation was prepared as described:
Propofol (15 cm^3 at 1.0 mg/cm^3) initiated anesthesia. Flunixin-Meglumin (50 mg/ml, 2.2 mg/kg bodyweight) and Buprenorphine (0.01 ml/kg bodyweight) maintained premedication and analgesia. Pre-emptive administration of the drugs ensures multimodal pain therapy to control pain over 24 h after the surgery. Postoperative pain assessment every 8 – 10 h after surgery decided over Buprenorphine injections for up to 48 h. Antibiotics were administered approximately 8 h before surgery (Cefazolin 10 mg/kg). Additional doses followed at the time of the surgery, each day after surgery for 3 days.
During surgery, animals were intubated with a 9 – 10 mm cuffed endotracheal tube while Propofol maintained anesthesia. Heart rate, oxygen saturation and end-tidal carbon dioxide levels were monitored continuously.

3.3.5 Prevascularized bone implantation in the mandibular angle

Before surgery, 1 mg Atropine and 0.01 mg/kg Detomidin were administered as premedication before anesthesia. Anesthesia itself was initiated by 5 mg/kg of

2 % Propofol and 0.1 Fentanyl. After endotracheal intubation, anesthesia was maintained by Fentanyl 0.2 ml/kg/h, Tracrium 0.03 ml/kg/h and 2 % Propofol 0.5 ml/kg/h. Antibiotic treatment was conducted with 2.0 g of Cefazolin.

Postoperative analgesia included the administration of Buprenorphin (5 – 10 µg/kg bodyweight) intravenously every six hours and Flunixin (2 mg/kg bodyweight) subcutaneously every 24 h. The second day after the surgery a Fentanyl containing patch was applied (100 µg/h) for 72 h.

The surgical procedure was performed as follows: The skin of the sheep was shaved and disinfected in the operational area. Subsequently, the mandible was accessed by a submandibular approach. To this end, the skin was incised and the layers of subcutaneous tissue were dissected. The facial nerve and the submandibular vein were identified and conserved while elevating the periosteum exposed the inferior border of the mandible. The continuity defect was defined using a mold outlining the designated defect geometry in order to ensure the same defect in all animals. Before the creation of the defect, reconstruction plates were placed over the designated defect area and fixed with two screws on each side while they were bent to fit the individual geometry of the mandible. Following the adaption of the plates, the defect was created according to the performed definition using a piezo saw. Partial attachment of the plates together with a titan mesh followed the removal of the bone. The mesh protected the defect area and prevented prolapse of soft tissue around the defect. The BoneVaSc-TERM® was placed between the ends of the created defect and anastomosed to the facial artery and the corresponding vein using 7– 0 and 8 – 0 sutures. Visual inspection confirmed capillary patency of the vessel system before closure of the wound by repositioning and suturing muscles and skin.

3.4 Characterization

3.4.1 Histology

3.4.1.1 Fixation

Before fixation, the medium of cells on cell culture surfaces was aspirated. Following, the cells or tissues were washed with PBS^- and then fixed with 4 % PFA for 10 minutes at room temperature. Due to their thickness, tissues and collagen gels were fixed for at least 2 h to allow thorough infiltration of the tissue and proper fixation in the inner compartments.

3.4.1.2 Paraffin embedding

In order to create thin sections of tissues for further analyses, samples were embedded in paraffin. The BioVaSc-TERM® was dissected into smaller parts before paraffinization depending on the region of interest.

Samples were put on embedding paper and transferred into labeled embedding cassettes. 1 – 2 h incubation in tap water ensured removal of residual PFA before placing samples into the embedding machine that automatically carried them through the following steps:

Table 13: Paraffin embedding

Time [h]	Solution	Function
Over night	50 % EtOH	
1	70 %	
1	90 %	Dehydration
1	96 %	
1	Isopropyl alcohol I	
1	Isopropyl alcohol II	
1	Isopropyl alcohol/Xylene	
1	Xylene I	Alcohol removal

Time [h]	Solution	Function
1	Xylene II	Paraffin infiltration
1.5	Paraffin I	
1.5	Paraffin II	

Upon the finished process, tissue samples were cut into smaller pieces and placed into casting molds in a horizontal orientation to allow for longitudinal cutting later on. The molds were filled with molten paraffin in an embedding station and allowed to cool down until the paraffin completely solidified. Before the preparation of tissue sections of 5 µm, molds stayed on a cooling plate for at least 20 minutes to allow for more consistent sectioning using a sliding or a rotary microtome. Sections were placed on polysine adhesion microscope slides and straightened in a water bath at 37 °C. Sections were allowed to dry for at least 2 h and directly processes or stored at 4 – 8 °C.

In order to allow access of dyes to the prepared sections, the paraffin had to be removed and rehydrated by the process of deparaffinization. The following steps were performed manually by moving the object slides through cuvettes filled with the following solutions:

Table 14: Deparaffinization

Time [min]	Solution	Function
10	Xylene I	Deparaffinization
10	Xylene I	
Dip 3 times	96 % EtOH	Rehydration
Dip 3 times	96 % EtOH	
Dip 3 times	70 % EtOH	
Dip 3 times	50 % EtOH	
Sway until turbulence clears	Purified water	Washing

3.4.1.3 Technovit® 9100 embedding

Technovit is a plastic embedding system based on methyl methacrylate and suitable for embedding hard tissues.

Table 15: Technovit embedding

Time [h]	Solution	Function
2	4 % Formalin	Fixation
2	Purified water	Hydration
2	70 % EtOH	Dehydration
2	80 % EtOH	
2	96 % EtOH	
At least 2	Isopropyl alcohol I	
At least 2	Isopropyl alcohol II	
At least 2	Xylene	
At least 2	Xylene	
Overnight	Xylene+Technovit	
Overnight	Technovit+Hardener 1	Pre-infiltration
Overnight at 4 °C	Technovit+Hardener 1	
Overnight at 4 °C	Technovit+Hardener 1+PMMA	Infiltration
Overnight at 4 °C	Technovit+Hardener 1+ Hardener 2+PMMA+ Polymerization regulator	Embedding

During the protocol, samples were handled in 50 ml conical tubes. For the last step, samples were placed in polyethylene embedding molds. After desiccation, the molds were sealed and stored at 4 °C overnight. Semi-thin sections of 30 – 50 µm thickness were created and placed on object slides. Sections were stretched with 50 % EtOH and a PVC film was applied. Slides were placed in a section press and stored under pressure at 50 °C overnight. In order to make

plasticized sections accessible for dyes, the following deplasticizing protocol was performed:

Table 16: Deplasticizing

Time [min]	Solution	Function
2 x 20	Xylene	Deplasticizing
20	2-methoxyethyl acetate	
2 x 5	Acetone I	
2 x 5	Acetone II	
	Purified water	Washing

Samples were mounted with Mowiol®.

3.4.1.4 Hematoxylin and eosin stain

Hematoxylin and Eosin (H&E) staining is suitable method for assessing tissue morphology. It results in blue colors in acidic or basophilic structures as for example in the cell nucleus. Eosin in contrast results in red colorization in acidophilic structures of tissues or cells as for example plasma membrane proteins or collagens. Following deparaffinization and rehydration, the subsequent protocol was executed:

Table 17: H&E staining

Time [min]	Solution	Function
6	Hematoxylin (Mayer)	Staining of basophilic structures (e.g. cell nuclei)
Sway until turbulence clears	Purified water	Washing
5	Tap water	Blueing

Time [min]	Solution	Function
6	Eosin	Staining of acidophilic structures (e.g. cytoplasm)
Sway until turbulence clears	Purified water	Washing
Dip 2 times	EtOH 70 %	
2	EtOH 96 %	
5	Isopropyl alcohol I	
5	Isopropyl alcohol II	Dehydration
5	Xylene I	
5	Xylene II	

Samples were mounted with Mowiol®.

3.4.1.5 Alcian blue

Alcian blue was used to stain negatively charged sulfated proteoglycans in the chondrogenic matrix of the cell pellets created during the chondrogenic differentiation assay.
Subsequent to deparaffinization, this staining protocol followed:

Table 18: Alcian blue staining

Time [min]	Solution	Function
3	Acetic acid	
30	Alcian blue	Staining of negatively charged glycosamino- and proteoglycans
Sway until turbulence clears	Purified water	Washing
5	Nuclear fast red	Staining of nuclei
Sway until turbulence clears	Purified water	Washing

Time [min]	Solution	Function
Dip 2 times	70 % EtOH	Dehydration
2	96 % EtOH	
5	Isopropyl alcohol I	
5	Isopropyl alcohol II	
5	Xylene I	
5	Xylene II	

Samples were mounted with Mowiol®.

3.4.1.6 Alizarin Red S

The osteogenic differentiated cells were analyzed with Alizarin Red S, a dye that stains dicalcium phosphates as they are present in the extracellular matrix of osteoblasts. The staining protocol is listed below:

Table 19: Alizarin Red S staining

Time [min]	Solution	Function
Dip once	PBS^-	Washing
10	methyl alcohol, ice-cold	Fixation
Sway until turbulence clears	Purified water	Washing
2	Alizarin Red S working solution	Staining of dicalcium phosphates
0.5	Hemalaun	Staining of nuclei
1	Tap water	Blueing

Samples were mounted with Mowiol®.

3.4.1.7 Oil Red-O

The Oil Red-O staining verified the formation of lipid droplets in the adipogenic differentiation of MSCs. The azo dye is liposoluble and stains triglycerides produced by adipocytes.

Table 20: Oil Red-O staining

Time [min]	Solution	Function
Dip once	PBS^-	Washing
10	4 % PFA	Fixation
Sway until turbulence clears	Purified water	Washing
5	60 % isopropyl alcohol	
10	Oil Red-O working solution	Staining of lipid droplets
Sway until turbulence clears	Purified water	Washing
0.5	Haematoxylin	Staining of nuclei
1	Tap water	Blueing

3.4.1.8 Feulgen staining

The Feulgen staining is a suitable method for investigating the degree of decellularization. This method results in red-purple stains for DNA and thus, gives information on DNA content in a tissue. It allows the detection of residual cells, fragments of cell nuclei or DNA in decellularized tissue. For a standardized decellularized matrix, it is important to show the absence of DNA in order to exclude any effects on cells seeded on the scaffold later on.

3.4.1.9 Movat's pentachrome staining

Movat's pentachrome is a staining method for the detection of connective tissue components. This method depicts cell nuclei as blue-black, glycosaminoglycans as blue, muscle tissue as red, elastic fibers and osteoid as red, collagen yellow, cartilage red and bone as yellow-orange staining.

Table 21: Movat's pentachrome staining

Time [min]	Solution	Function
10	Alcian blue	Staining of negatively charged glycosamino- and proteoglycans
5	Purified water	Washing
60	10 % alkaline alcohol	Fixation
5	Purified water	Washing
10	Hematoxylin	Staining of basophilic structures (e.g. cell nuclei)
1	Purified water	Washing
15	Tap water	Blueing
30	Brilliant crocein	Staining of elastic fibers and cytoplasm
Sway until turbulence clears	0.5 % Acetic acid	Washing
	15.5 % Phosphotungstic acid	Differentiation
5	0.5 % Acetic acid	Washing
5	EtOH 96 %	Rinsing
5	EtOH 96 %	
60	Safron du gatinias	Staining of mineralized bone and cartilage tissue
4	EtOH 96 %	Dehydration
4	EtOH 96 %	
5	Xylene	Clearing

3.4.2 Immunohistochemistry

Immunohistochemistry is the analysis of tissue or cells with immunochemical methods as staining of cell or tissue structures with dyes linked with antibodies. There is direct staining with primary antibodies linked directly to marker.
Additionally, there are indirect methods that direct a secondary antibody against the so-called fragment crystallizable region (Fc region) of the primary antibody. The secondary antibody carries a marker that can be a chromogenic substrate or fluorescent dye. In the second case, the method is called immunofluorescence.
The principle of the method is based on the affinity of antibodies to specific epitopes of antigens on the surface or the inside of tissues or cells. Antibody and antigen stably bond while for the indirect method a secondary antibody additionally detects the primary antibody. The secondary antibody is conjugated with horseradish peroxidase (HRP) which can be made visible with substrates that are oxidized by the HRP. In case of 3,3'-diaminobenzidine (DAB) as a substrate, the result is a brown staining indicating the exact location of the targeted antigen.
This method was applied to tissue sections and cells seeded on cell culture surfaces as for example well plates or chamberslides. Cells were fixed with 4 % PFA for 10 minutes at room temperature. Tissue was prepared as described above. Antigen-retrieval was performed heat-induced in a steamer. Citrate buffer at a pH of 6 was heated up to 100 °C in the steamer, slides were then incubated for 20 minutes. The following incubation steps were carried out in a humidity chamber at room temperature:

Table 22: Immunohistochemistry

Time [min]	Solution	Function
10	3 % H_2O_2	Blocking endogenous peroxidase
3 x 5	PBS-Tween	Washing

Time [min]	Solution	Function
60	Primary antibody solution	Primary antibody
3 x 5	PBS-Tween	Washing
10	Secondary antibody solution	Secondary antibody
3 x 5	PBS-Tween	Washing
2	DAB solution	detection
3 x 5	PBS-Tween	Washing
0.5	Hematoxylin	Nucleus staining
1.5	Tap water	Blueing

In order to confirm the proper binding of the primary antibody and the exclusion of false-positive signals, for every immunohistochemical analysis a control was performed. For this, IgG is used instead of a primary antibody by otherwise unaltered protocol to evaluate nonspecific staining.

3.4.3 MTT assay

The MTT 3-(4,5-dimethylthiazol-2-yl)-2,5-diphenyltetrazolium bromide assay is a colorimetric assay that allows for the detection of the metabolic activity of cells. The assay can be used to assess general viability of cells or provide a quantitative statement on the number of viable cells when performed under standardized conditions. The assay is based on the reduction of the orange MTT dye into purple formazan salt. The amount of produced formazan can be correlated with the number of viable cells [145].

The assay was used qualitatively to confirm the presence of viable cells in the vascular structures of the BioVaSc-TERM® as well as in collagen I hydrogels or on β-TCP granules or cylinders. The medium of the respective samples was aspirated and samples were washed with PBS^+. Then they were transferred into a 50 ml conical tube and incubated with 9 ml MTT solution at a concentration of

1 mg/ml for 1 h at 37 °C in the incubator. Samples were washed with PBS+ and photographed with a digital camera or under the microscope.
In contrast to soluble assays, the MTT allows the exact localization of viable cells due to the formation of the initially insoluble formazan inside the cells.

3.4.4 Fluorescent staining

DiI (1,1'-dioctadecyl-3,3,3',3'-tetramethylindocarbocyanine perchlorate) and DiO (3,3'-dioctadecyloxacarbocyanine, perchlorate) are fluorescent dyes that are capable of inserting hydrocarbon chains into lipid bilayers of cells. This does not affect cell viability or basic physiological properties [146, 147]. The dye diffuse laterally in the cell membrane and thus stain the whole cell.
In order to label cells 50 mg DiI were resolved in 54 ml of 100 % EtOH, while 50 mg of DiO were resolved in 56.7 ml of 100 % EtOH. Cells were detached and resuspended in cell-specific, serum-free medium. Per 1 ml of cell suspension, 5 µl of dye were added and an incubation at 37 °C for 20 minutes was performed. Cells were then centrifuged at 270 g for 5 minutes, the supernatant was aspirated and cells were washed with 10 ml medium. Cells were centrifuged and the washing step was repeated. Eventually, cells were seeded on ß-TCP granules at a density of 5.0 x 10^5 cells/ml.

3.4.5 Acetylated low-density lipoprotein assay

Low-density lipoproteins (LDL) serve as vehicle for lipophilic substances that are insoluble in blood plasma as for example cholesterol, fatty acids or certain vitamins. LDL can be transferred into cells by LDL receptors, which is not the case with Acetylated-LDL (Ac-LDL). In its acetylated form LDL is not recognized by the receptors anymore and only macrophages and endothelial cells can take it up via the so-called scavenger pathway that works independent of this recognition [148]. The uptake of Ac-LDL can thus be a hint on cell identity. EPCs isolated as described in 3.1.2.2 were examined regarding the uptake of Ac-LDL. EPCs were seeded into the wells of 4-well chamberslides at a cell density of

3.0 x 10^4 cells/cm^2 in EGM-2 medium. After 3 days of culture the medium was aspirated and cells were incubated with EGM-2 medium without serum for 24 h. Subsequently, the medium was aspirated and 10 µl of Ac-LDL were added to each well. 4 h of incubation followed before each well was washed three times with PBS^+. Fixation took place by 10 minutes of incubation in 4 % PFA.
Following this, the samples were immediately analyzed under a fluorescence microscope. The used Ac-LDL is conjugated with the fluorescent dye Alexa Fluor® (Ex/Em 495/519 nm). During the experiments, all labeled Ac-LDL solutions were kept away from direct light in order to prevent bleaching of the fluorescent dye

4 Results

4.1 Mobile Incubator

A complex implant, produced at a manufacturing sitemight be far away from the clinical site where it is implanted. In this study, manufacturing and clinical site were 600 km apart. The transportation of the implants necessitated the development of mobile equipment that allowed providing a suitable environment for the live implants. The option of perfusing the vessel system was necessary as well as a constant temperature of 37 °C.

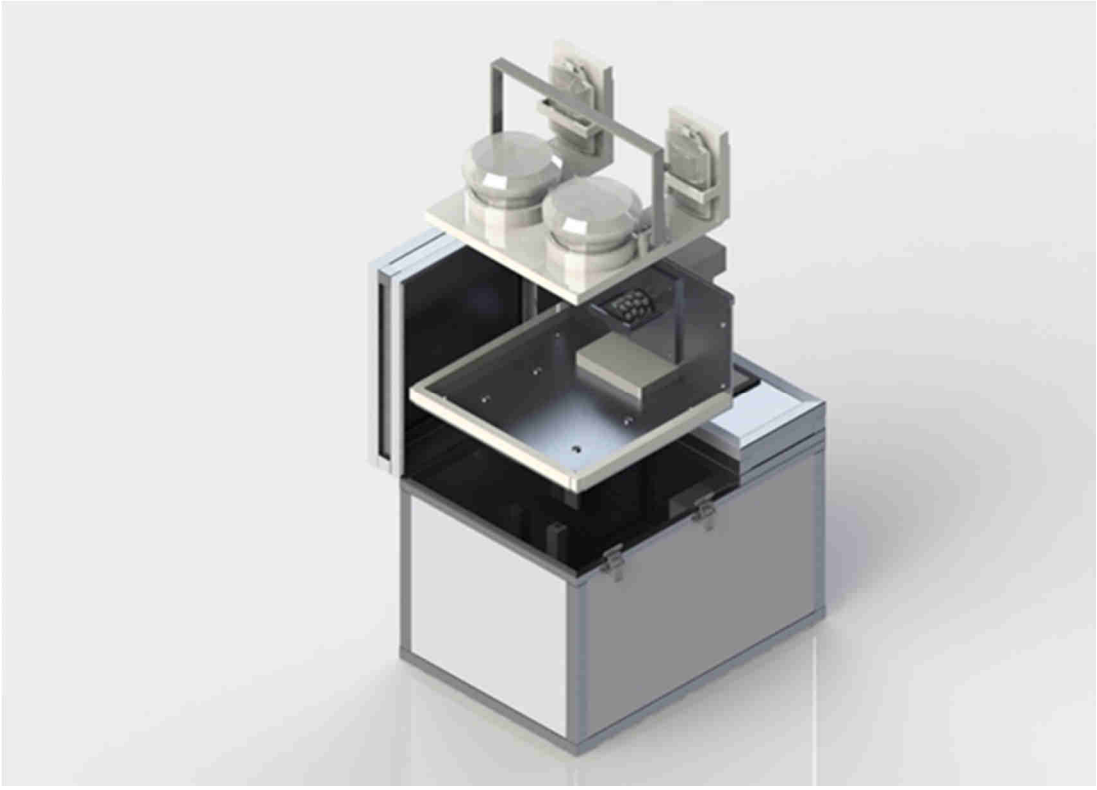

Figure 1: CAD model of the mobile incubator.

The design of the mobile incubator was executed using the 3D CAD Program SolidWorks by Dassault Systèmes (Figure 1). The housing was implemented with Adam Hall frame profiles with aluminium spacing. The incubation room was equipped with a 4-channel peristaltic pump and heating foils. The peristaltic pump featured 4 fittings for pumping tubes which allowed the perfusion of 4 implants in bioreactors at the same time. The bioreactor setup is depicted in Figure 2.

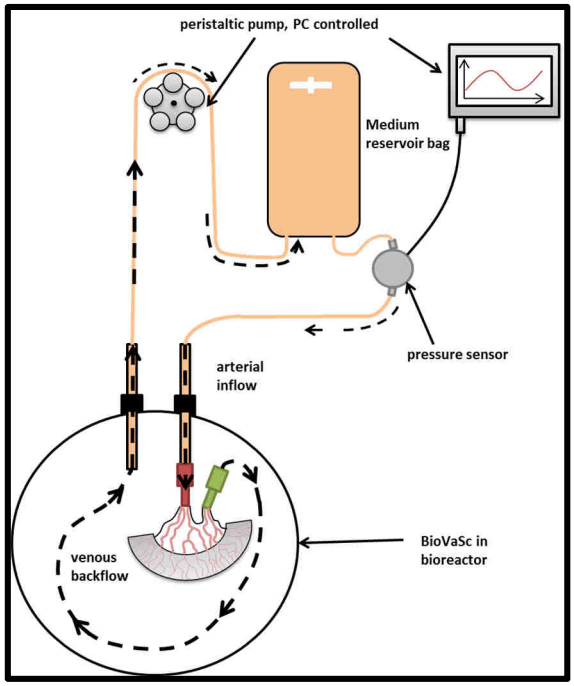

Figure 2: Schematic illustration of the bioreactor setup.
The setup allows the perfusion of the bone graft in the mobile incubator: The peristaltic pump perfuses the vascular structures of the implant in the bioreactor while ensuring pressure conditions do not exceed 120 mmHg.

Siemens SIMATIC ET 200S control unit regulated the pump and heating. For both units a desired value was predefined (temperature of 37 °C, pressure of 120 mmHg). The control unit detected the actual values via temperature sensor and MEMSCAP SP844 physiological pressure sensor and compared the actual values to the desired values. Accordingly, it in- or decreased temperature as well as in- or decreased the rotational speed of the pump in order to maintain pressure conditions of 120 mmHg.

The mobile incubator had to be operational using a standard power plug for stationary operation and via 12 V connector for transportational operation in a car. Due to the limited energy supply in a car, the components were assembled with their energy consumption in mind (Table 23).

Table 23: Calculation of electrical load.

Rotational pump	24 V	1,25 A	30 W
Heating foil 30 W	24 V	1,25 A	30 W
Heating foil 20 W	24 V	0,833 A	20 W
User interface	24 V	0,342 A	8 W
Measurement amplifier	24 V	0,1 A	2,4 W
Total		4,275 A	90,4 W

Starting from 27 °C, the combined heat output of both heating foils heated the incubation room to 37 °C within 30 minutes (Figure 3). After 34 minutes, the temperature dropped due to turning off the device.

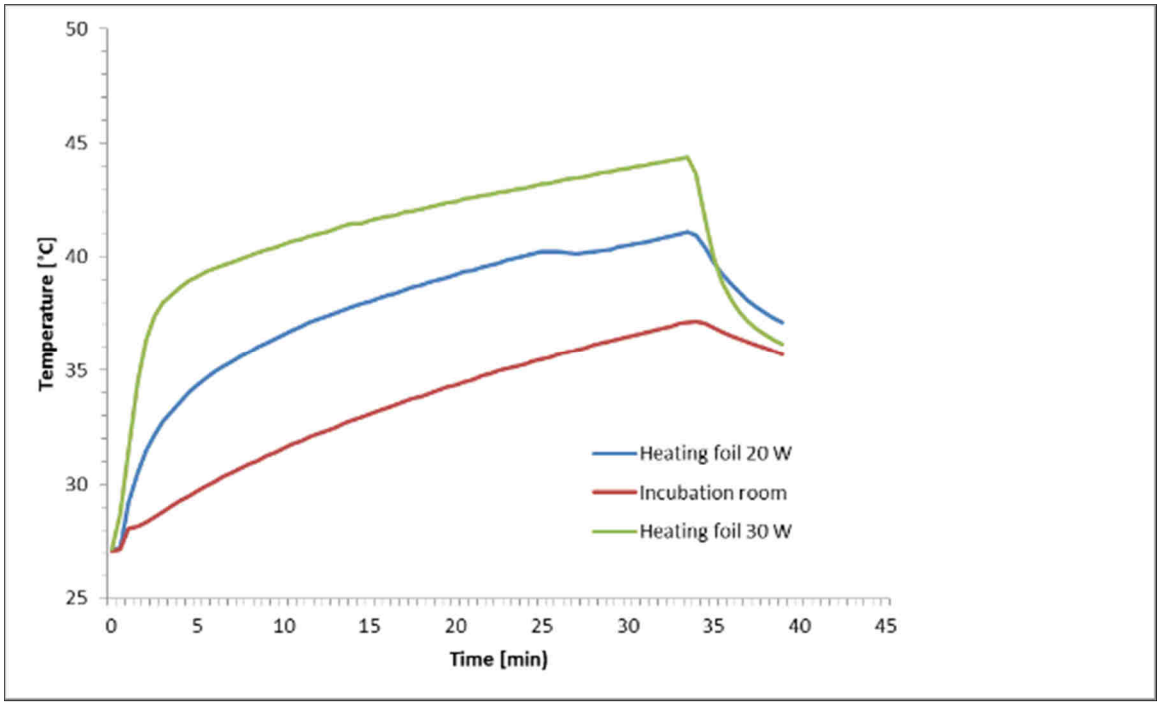

Figure 3: Heating of the incubation room of mobile incubator.

4.2 Endothelial progenitor cells

Endothelial progenitor cells are a heterogeneous cell population. An extraordinary advantage of EPCs is, as soon as isolated, their expansion potential is very high and their easy accessibility. They can be isolated from easily harvested peripheral blood. This means a simple blood donation is sufficient to

gain access to this cell type. In contrast, the isolation of microvascular endothelial cells usually requires the removal of a piece of healthy skin from the patient.
EPC were isolated from a volume of freshly taken blood from sheep and the mononuclear fraction was separated via density gradient centrifugation.

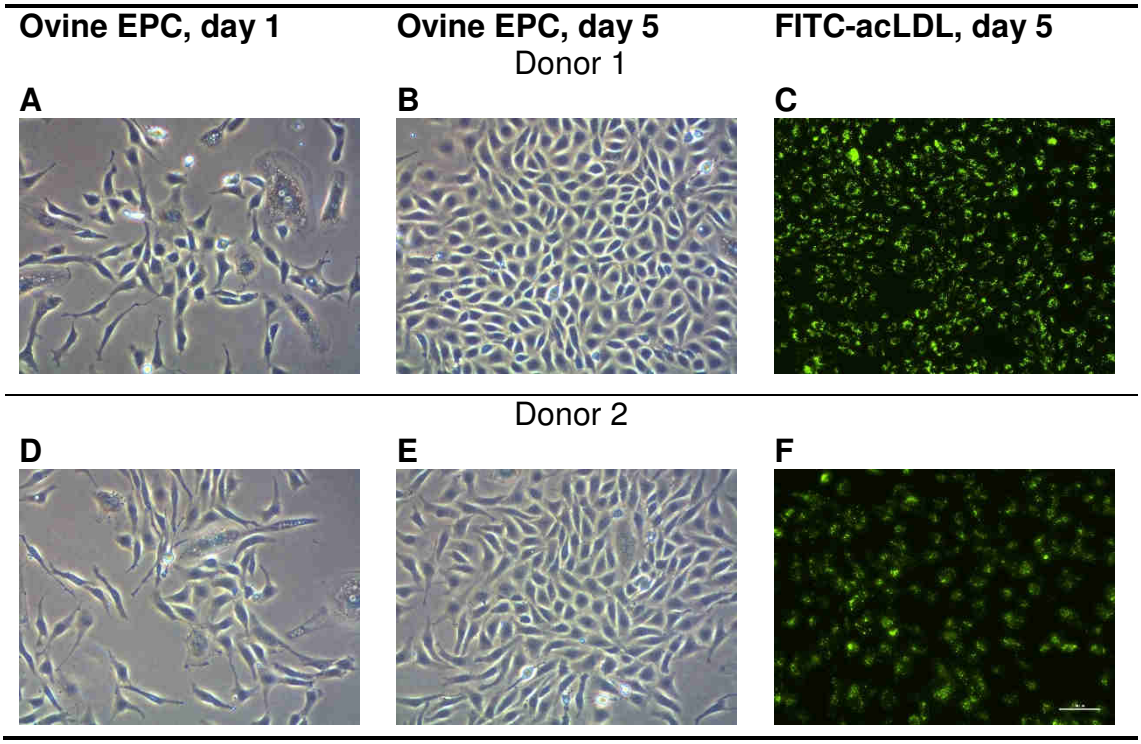

Figure 4: EPC isolated from peripheral blood.
Light microscopic images of isolated ovine EPC at passage 1, 1 (A,D) or 5 days after seeding (B,E). Fluorescent images of FITC-acLDL labelled EPC 5 days after sedding (C, D).

4.3 Differentiation of human and ovine mesenchymal stem cells

The differentiation of ovine MSCs into the 3 lineages adipogenic (Figure 5), chondrogenic (Figure 6) and osteogenic (Figure 7) was successful. The Oil red O staining revealed accumulation of fat droplets in the human and ovine cell bodies after incubation in adipogenic differentiation medium.

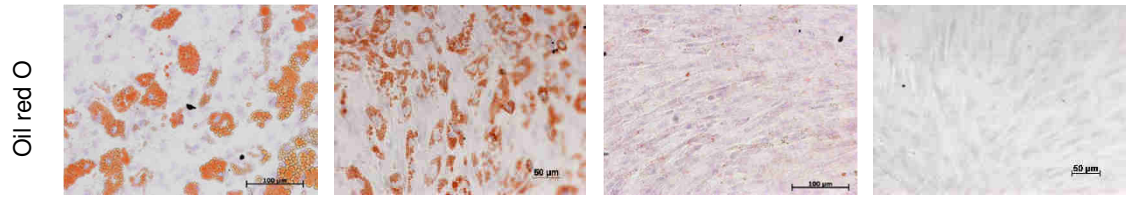

Figure 5: Histological analysis of human and ovine MSC differentiation.
Oil red O staining indicating the formation of red stained oil droplets in human and ovine MSCs after treatment with adipogenic differentiation medium. No visible oil droplets in the controls treated with MSCGM. Scale bar: 100 µm.

The chondrogenic differentiation potential of human and ovine MSCs was confirmed alcian blue and immunohistochemical staining for collagen II. The deposition of chondrogenic extracellular matrix and the expression of collagen II indicated a successful differentiation of MSC from both sources into chondrocytes.

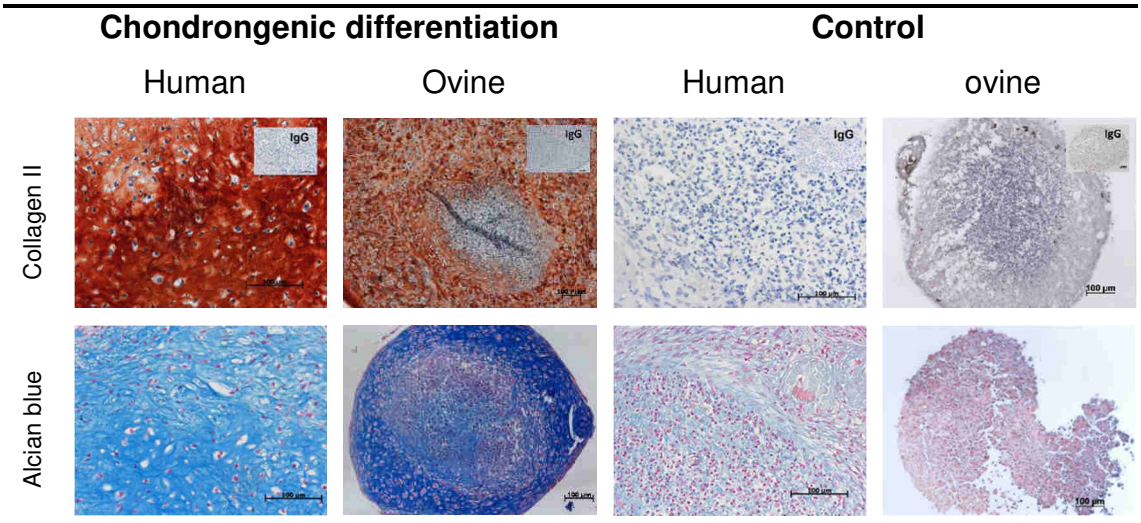

Figure 6: Histological and immunohistochemical analysis of human and ovine MSC differentiation.
The immunohistochemical staining of collagen II shows the expression of the corresponding antigen in human and ovine MSC after treatment with chondrogenic differentiation medium. The alcian blue staining resulted in strong staining in the differentiated cells of human and ovine origin. No signal was detected in collagen II staining while the alcian blue staining was weak after the culture of the cells with MSCGM. Scale bar: 100 µm.

Osteogenic culture of human and ovine MSC drove the cells into the osteogenic linage confirmed by alizarin red staining that stained the formed calcium phosphates red.

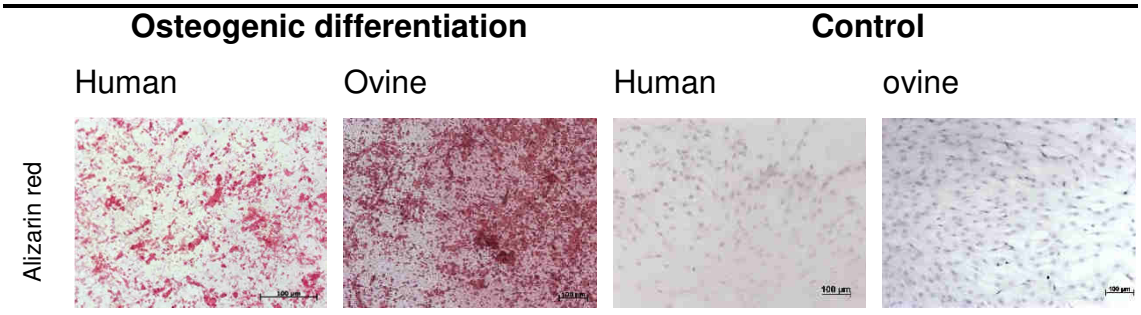

Figure 7: Histological analysis of human and ovine MSC differentiation.
Alizarin red stained human and ovine MSC after culture in osteogenic differentiation medium for 28 days. The staining highlights the formation of calcium phosphate deposits. Controls show no sign of calcium phosphate production. Scale bar: 100 µm.

4.4 BioVaSc-TERM® decellularization

The BioVaSc-TERM® was the basis for the vascularization of the bone implant. After decellularization of the jejunum of a porcine small intestine, the BioVaSc-

TERM® is a nonimmunogenic collagen I/III scaffold with preserved vascular structures.

In order to confirm that the scaffold is cell free and that there is no residual DNA that could cause immunogenic reactions or otherwise compromise the functionality of the scaffold, H&E and Feulgen stainings were performed.

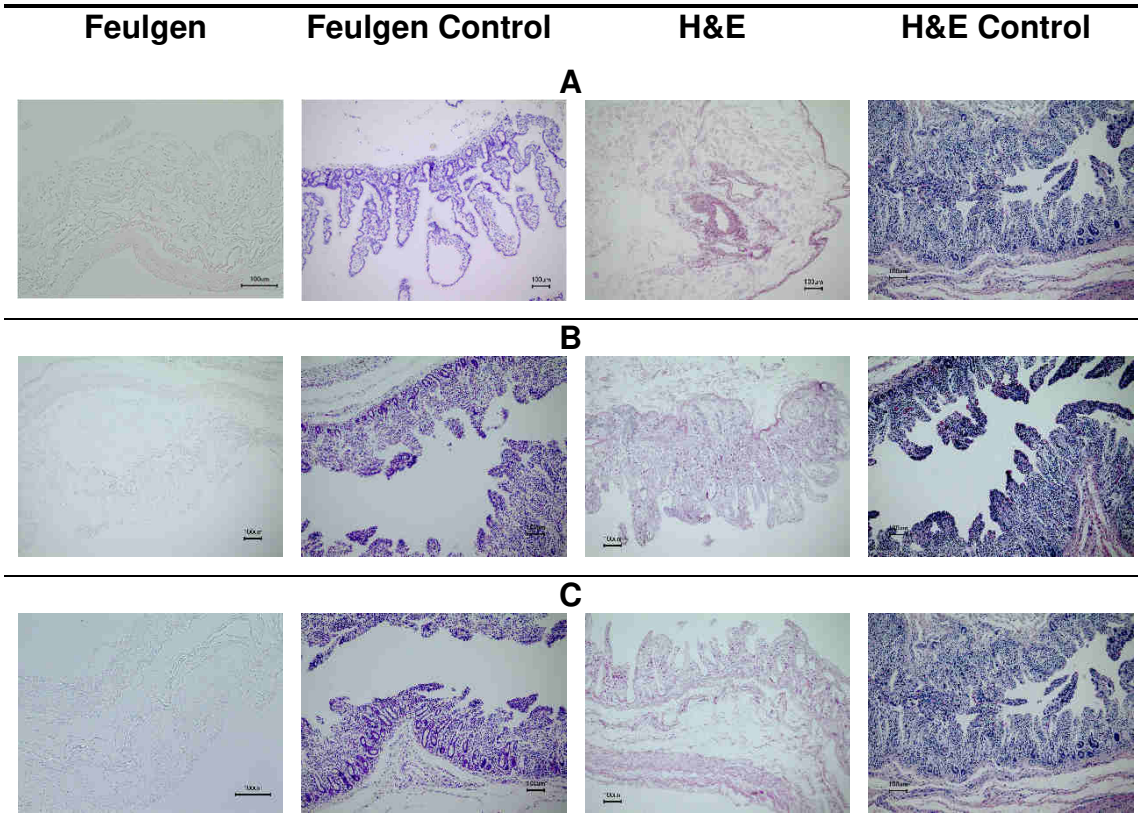

Figure 8: Staining of ECM of deceullularized porcine small intestine segments (BioVaSc-TERM®).
DNA contend of decellularized scaffolds as compared to native intestinal samples. Scale bar: 100 µm.

The Feulgen staining of 3 samples (Figure 8) indicates the successful removal of DNA during the decullularization process. In comparison to the positive control samples, there is no accumulation of blue dye detectable and thus no DNA in the samples. H&E staining confirmed the results, no nuclei were detected (blue color) and additionally the desired preservation of collagenous structures in pink color was indicated.

At the end of the decellularization process, the vessel integrity was checked by perfusing the scaffold via the arterial inlet with 2 ml of 0.5 % phenol red. This procedure gave information on the physical integrity of the vascular structures of the scaffold, which is one of the prerequisites for the functional application of the BioVaSc-TERM®. A successful decellularization process resulted in an even perfusion of all vascular pedicles and their subsequent branching (Figure 9: A, B). At the same time, the dye should not leak from any holes or damaged vessels. Accordingly, the produced scaffolds were graded from 1 to 6, with 1 being best and 6 the worst. Scaffolds that were only partly perfused due to blockades, that were punctured and leaked, were discarded (Figure 9, C; grade 6). Only scaffolds with perfectly preserved vascular structures were used for the production of implants (Figure 9, A, grade 1).

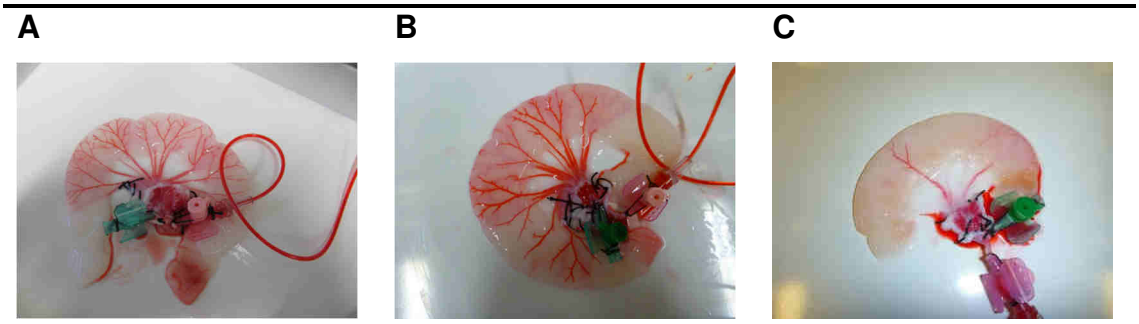

Figure 9: Quality assessment of decellularized porcine jejunum (BioVaSc-TERM®). Vascular structures of the BioVaSc-TERM® perfused with 0.1 % phenol red to check vessel integrity.

4.5 GMP conform documentation system

A standard operating procedure (SOP) for the manufacturing of the BioVaSc-TERM® ensured the consistent quality of produced matrices with a structure as follows:

Table 24: Structure of SOP for the production of the BioVaSc-TERM®.

1. Abbreviations
2. Function of the instruction
3. Responsibility
4. Applicability
5. Supply and equipment
   5.1. Reagents
   5.2. Consumables
   5.3. Devices
6. Description of the individual process steps
7. Documentation
8. Applicable documents
9. Revision tracking

The SOP defines its purpose and scope before indicating the responsible person for the document and the area of application. All necessary materials, chemicals and devices used are listed. The manufacturing section represents every process step in detail as described in the methods section of this thesis. The SOP concludes with a reference to the corresponding manufacturing protocol and an indication of applicable documents and revision tracking.

Manufacturing protocols (MP) accompanying the SOP are the specific documentation of executed working steps. The document is preformulated and only requires ticking of every step performed in a printed document. Critical steps (e.g. preparation of the decellularization solution) demand the principle of dual control that has to be confirmed by signature in the document.

The documents are supervised, checked and by the head of production, regarding manufacturing, while the head of quality control is responsible for documentation regarding quality control as required from the GMP principles.

As part of quality control, reagents, consumables and devices are defined in specification sheets and supplemented with a “Certificate of Analysis” for every batch ordered.

Table 25 summarizes the results of the quality control of the produced BioVaSc-TERM®s regarding vessel integrity by phenolred evaluation (grading 1 to 6), total bile assay evaluation (threshold <50 µM/l), endotoxin content (threshold <1 EU/ml), Feulgen evaluation (+, o, -) and H&E evaluation (+, o, -).

Table 25: Quality control overview of decellularized BioVaSc-TERM®s.

BioVaSc-TERM® No.	Phenolred evaluation 1-6	Total Bile Acid Assay evaluation <50µM/l	Endotoxin <EU/ml	Feulgen evaluation +,o,-	H&E evaluation +,o,-
B24.2	/	√	/	-	o
B25.2	/	√	/	+	+
B25.3	/	√	/	o	o
B25.5	/	√	/	o	-
B26.1	/	√	/	+	o
B26.2	/	√	/	o	o
B27.1	2	√	/	o	o
B27.3	2	√	/	-	-
B28.1	2	√	/	o	o
B28.2	1	√	/	+	+
B28.3	2	√	/	+	o
B28.5	2	√	/	+	+
GMP B25	1	X	X	-	-
GMP B35	1	√	/	-	o
GMP B49	1	√	√	+	o

BioVaSc-TERM® No.	Phenolred evaluation 1-6	Total Bile Acid Assay evaluation <50µM/l	Endotoxin <EU/ml	Feulgen evaluation +,o,-	H&E evaluation +,o,-
GMP B51	1	√	√	+	o
GMP B54	1	√	/		-
B29.3	1	√	/	o	o
B29.4	1	√	/	-	-
B29.5	1	√	/	-	+
B30.1	1	√	/	-	o
B30.2	1	√	/	o	o
B31.2	1	√	/	o	o
B32.1	1	√	/	+	+
B32.4	1	√	/	o	o
B33.2	1	√	/	o	o
B33.3	1	√	/	o	o
B33.4	1	X	/	-	-
B34.2	1	√	/	o	o
B34.3	1	√	/	+	o
B35.1	1	√	/	o	o
B35.2	1	√	/	o	o
B35.3	2	√	/	o	o
B36.1	5	√	/	-	o
B36.2	5	√	/	o	o
B36.3	3	√	/	+	+
GMP B53	3	√	√	+	+
GMP B55	1	√	√	+	o

BioVaSc-TERM® No.	Phenolred evaluation 1-6	Total Bile Acid Assay evaluation <50µM/l	Endotoxin <EU/ml	Feulgen evaluation +,o,-	H&E evaluation +,o,-
GMP B56	1	√	√	+	+
GMP B57	1	√	√	+	+
GMP B58	1	√	√	-	+
GMP B59	1	√	√	+	+
B38.1	6	√	/	+	+
B38.4	3	√	/	o	o
B39.1	2	√	/	o	-
B39.2	5	√	/	-	-
B39.3	4	√	/	-	-
B39.4	3	√	/	o	-
B39.5	4	√	/	-	o
B40.1	1	√	/	o	o
B40.2	2	√	/	-	-
B40.3	3	√	/	-	-
B40.4	4	√	/	o	-
B41.1	2	√	/	o	+
B41.2	1	√	/	-	-
B41.5	1	√	/	o	o
B42.1	2	√	/	+	o
B43.1	1	√	/	-	-
B43.3	6	√	/	+	o
B44.2	2	√	/	+	o
B44.3	2-3	√	/	+	o

BioVaSc-TERM® No.	Phenolred evaluation 1-6	Total Bile Acid Assay evaluation <50µM/l	Endotoxin <EU/ml	Feulgen evaluation +,o,-	H&E evaluation +,o,-
B45.1	1	√	/	+	+
B45.2	2	√	/	o	o
B45.3	2	√	/	+	+
B45.4	4	√	/	+	o
B46.1	2	√	/	+	+
B47.1	4	√	/	+	+
B47.3	3	√	/	+	+
B47.4	3	X	/	+	+
B48.3	3	√	/	o	o
B48.4	2-3	√	/	+	+
B49.1	1	√	/	+	+
B49.2	1	√	/	+	+
B49.3	3	√	/	+	+
B50.1	3	√	/	+	+
B50.2	1	√	/	+	+
B50.3	2	√	/	+	+
B50.4	3	√	/	-	o
B51.1	1	√	/	o	o
B51.2	1	√	/	+	+
B51.3	2	√	/	o	+
B51.4	6	√	/	+	+
B51.5	1	√	/	o	o
B53.1	2	√	/	+	o
B55.1	1	√	/	+	+
B55.3	1	√	/	o	+
B56.1	1	√	/	+	+

BioVaSc-TERM® No.	Phenolred evaluation 1-6	Total Bile Acid Assay evaluation <50µM/l	Endotoxin <EU/ml	Feulgen evaluation +,o,-	H&E evaluation +,o,-
B56.2	3	√	/	-	o
B56.3	2	√	/	+	o
B57.1	5	√	/	+	+
B57.2	1	√	/	o	-
B58.1	1	√	/	o	o
B58.2	5*	√	/	o	+
B58.3	1	√	/	o	+
B59.1	6	√	/	o	+
B59.2	1	√	/	+	+
B59.3	2	√	/	o	+
B59.4	6	√	/	o	+
B60.1	3	√	/	o	o
B60.2	1	√	/	+	o
B61.1	1	√	/	+	+
B61.2	5	√	/	+	+
B61.3	1	√	/	+	+
B62.1	1	√	/	+	+
B62.2	1	√	/	o	o
B62.3	1	√	/	+	+
B62.4	1	√	/	+	o
B62.5	1	√	/	+	o

When initially total bile or endotoxin values were not met, additional washing steps could be introduced for a sufficient reduction of the respective value. Personnel experienced with histological assessment conducted the evaluation of H&E and Feulgen staining with positive and negative samples as reference in order to achieve objective results.

4.6 Seeding of TCP granules

The bone mineral aspect of the implants consisted of ß-TCP granules that were augmented by the seeding with MSCs. The successful seeding was confirmed by florescent DAPI staining. After seeding and 3 days of incubation under standard cell culture conditions, granules were plastic embedded and sectioned.

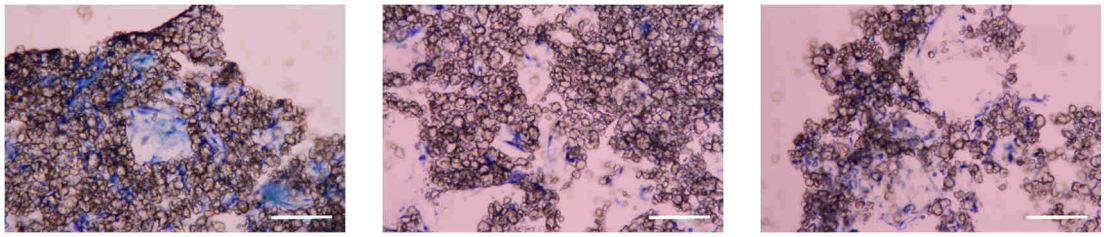

Figure 10: ß-TCP granules seeded with MSC.
DAPI staining of MSCs seeded on ß-TCP granules in a peripheral region (A) and central areas (B, C). Scale bar 50 µm.

4.7 BioVaSc-TERM® reseeding

The functionality of the BioVaSc-TERM® as a scaffold providing vascular support could only be ensured when it was successfully reseeded with endothelial cells. The scaffold was seeded with ovine endothelial progenitor cells. The MTT assay with results in the conversion of the orange MTT dye into purple formazan.

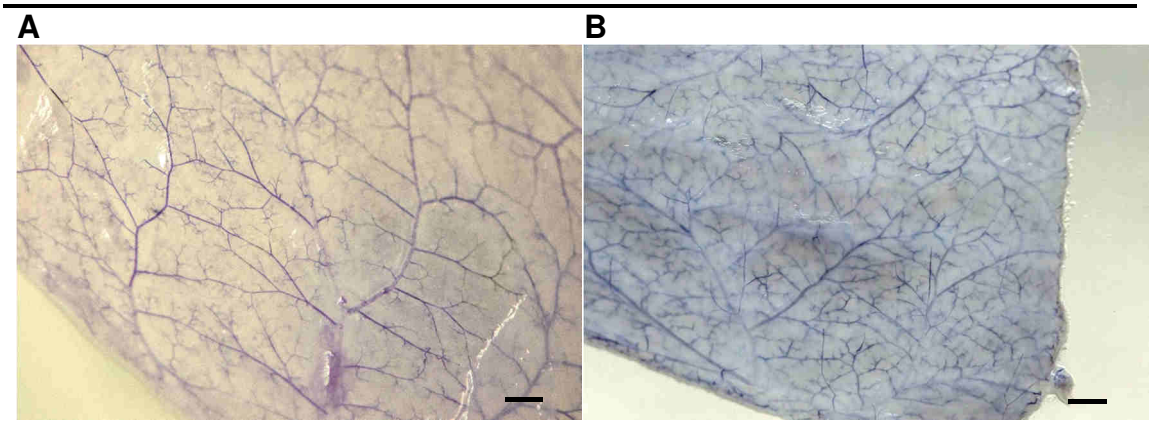

Figure 11: BioVaSc-TERM® after resseding with EPCs.
MTT staining of EPCs seeded in the vascular structures of the BioVaSc-TERM®after 1 (A) and 2 (B) weeks. Purple color indicates live cells. Scale bar 1 mm.

Figure 11 illustrates the successful population of vascular structures in a BioVaSc-TERM® with EPCs. The vessels and capillaries were evenly stained by the converted MTT indicating the presence of metabolically active cells. The MTT assay makes no statement on the identity of the cells that convert the salt. An immunochemical staining for CD31, an endothelial marker, confirmed the presence of antigens typically found in endothelial cells (Figure 12). The staining reveals the brown colored location of the CD31 antigen in vascular structures in the luminal areas (Figure 12: A, B) of the BioVaSc-TERM® as well as in the vascular pedicles Figure 12: C, D magnification of C).

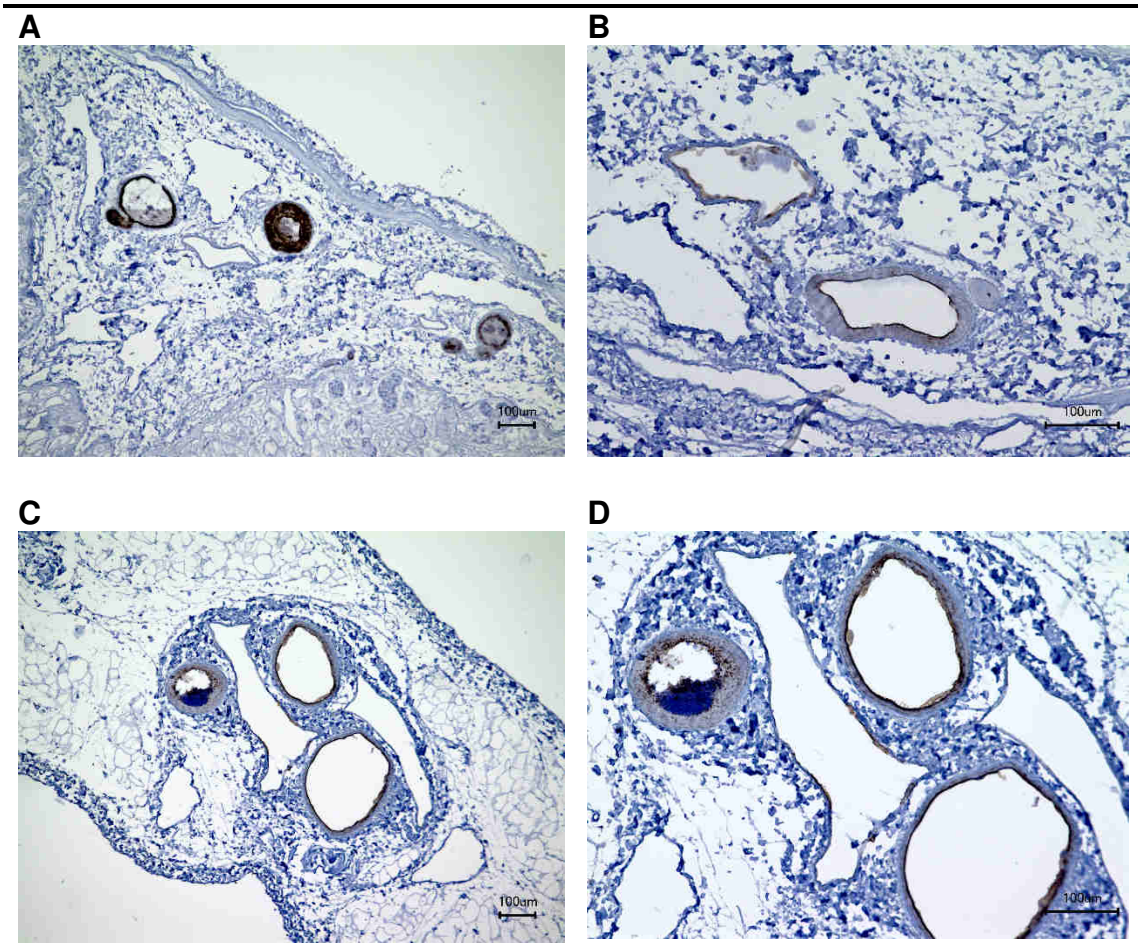

Figure 12: Immunohistological staining of section of reseeded BioVaSc-TERM®. CD31 staining of sections of the lumen (A, B) and den pedicle (C, D) of the BioVaSc-TERM®. Scale bar: 100 µm.

4.8 Animal experiment: Tibia defect in sheep

In order to test the generated implants they were implanted into a 3 cm tibial defect in sheep. To this end, a part of the tibia was excised and the periosteum at the proximal and distal bony ends was further removed for one additional centimeter in order to test the regeneration potential of the implant and not the native periosteum (Figure 13, A). However, the BioVaSc-TERM® was brought into the defect together with the ß-TCP filling in a way that it should mimic the function of the periosteum. In this case, the arterial and venous pedicles were not anastomosed to the sheeps' circulatory system but the scaffold was only pulled

over the bony ends with the ß-TCP filling the empty area of the defect. Sutures brought the scaffold and the native periosteum into close contact with each other (Figure 13, C).

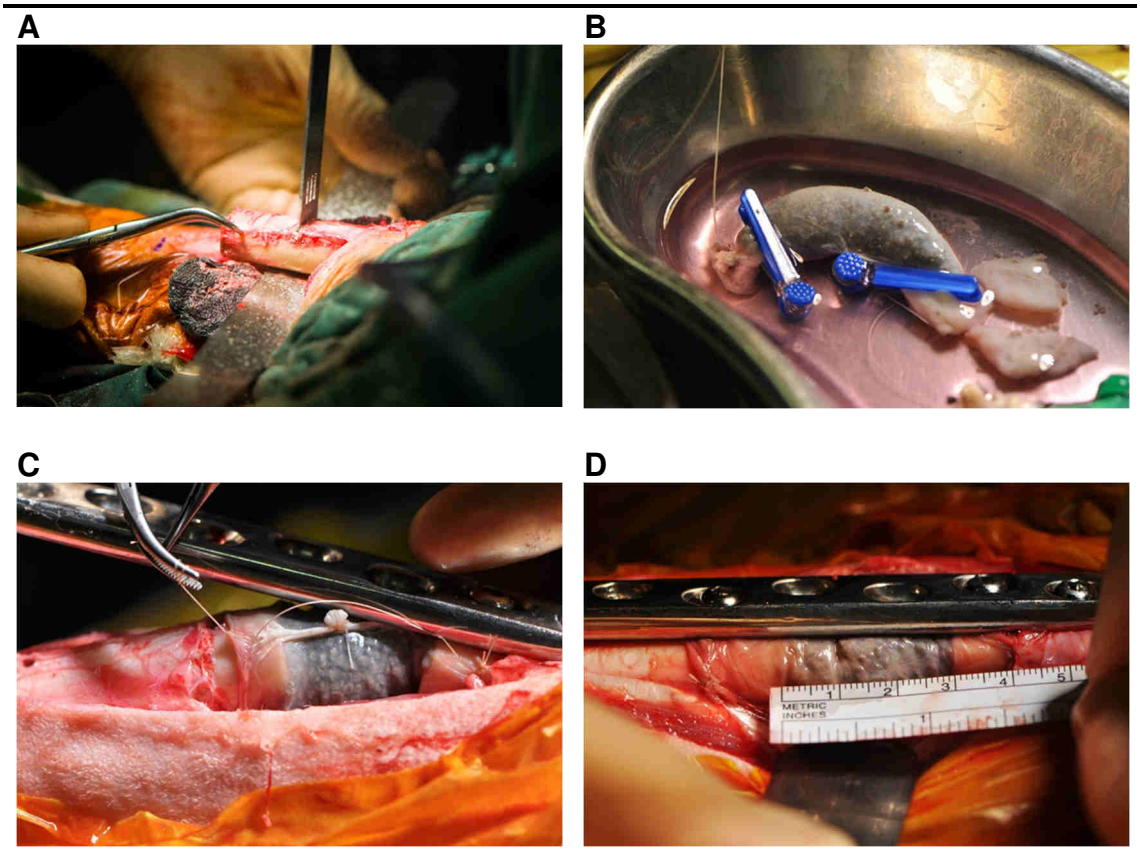

Figure 13: Tibial defect creation and bone graft implantation.
The tibia was exposed and a 3 cm defect created (A). The bone implant (B) was put over the proximal and distal ends of the bony defect and the BioVaSc-TERM® was sutured to the native periosteum (C). The defect was fixed with reconstruction plates (D) and the wound was closed.

One reconstruction plate with four screws proximally and three screws distally stabilized the defect. The stabilization was stable in all sheep, there were no adverse reactions, no loosening of screws or breakage of plates.

After 6 months, the sheep were sacrificed and samples were taken.

Samples were fixed in 4 % PFA and the following histological analyses were performed at the Julius-Wolf-Institue, Charité, Berlin. In an overview, the Van Kossa staining of the samples of all six sheep show mineralized tissue in black and connective tissue in red. A complete bridging is not visible in the samples.

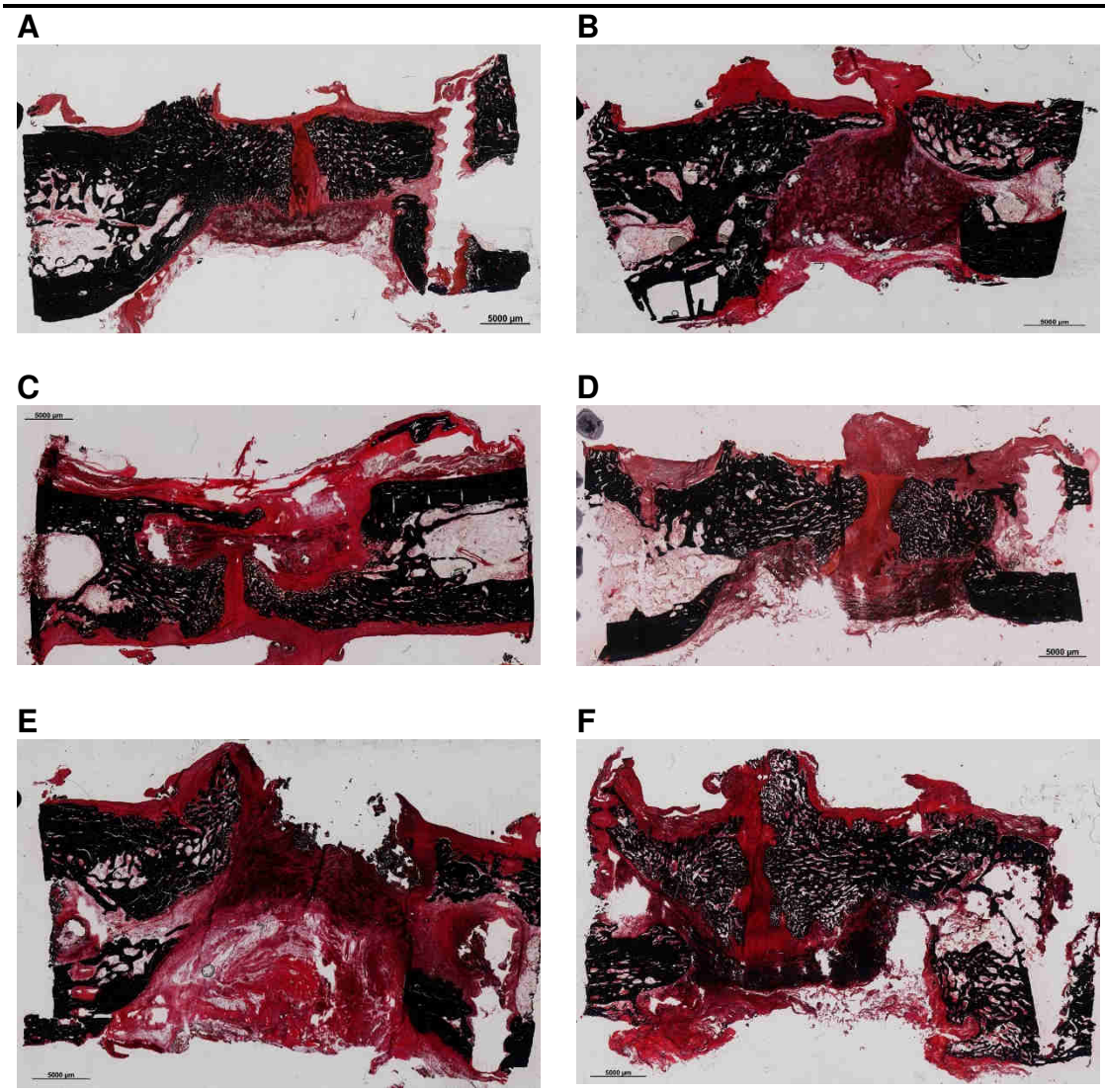

Figure 14: Histological staining of tibial samples of different donors.
Van Kossa staining of longitudinal sections of ovine tibia in the area of the defect site. Scale bar: 5 mm.

However, regeneration of the bony ends towards each other is apparent in all samples, especially in samples of sheep A and F. Progress of regeneration is advanced and only a connective tissue layer of about 1 mm separates the proximal and distal part of the tibia. The staining reveals amounts of connective tissue embedding the remaining ß-TCP that was brought into the defect during implantation, while the regenerated bone is in places where there is no ß-TCP

left, an indication for osteoclastic activity that resorbed parts of the synthetic material.

The immunohistochemical staining of α–smooth muscle actin in red color showed smooth muscle, which was an indication for vessels in the sample.

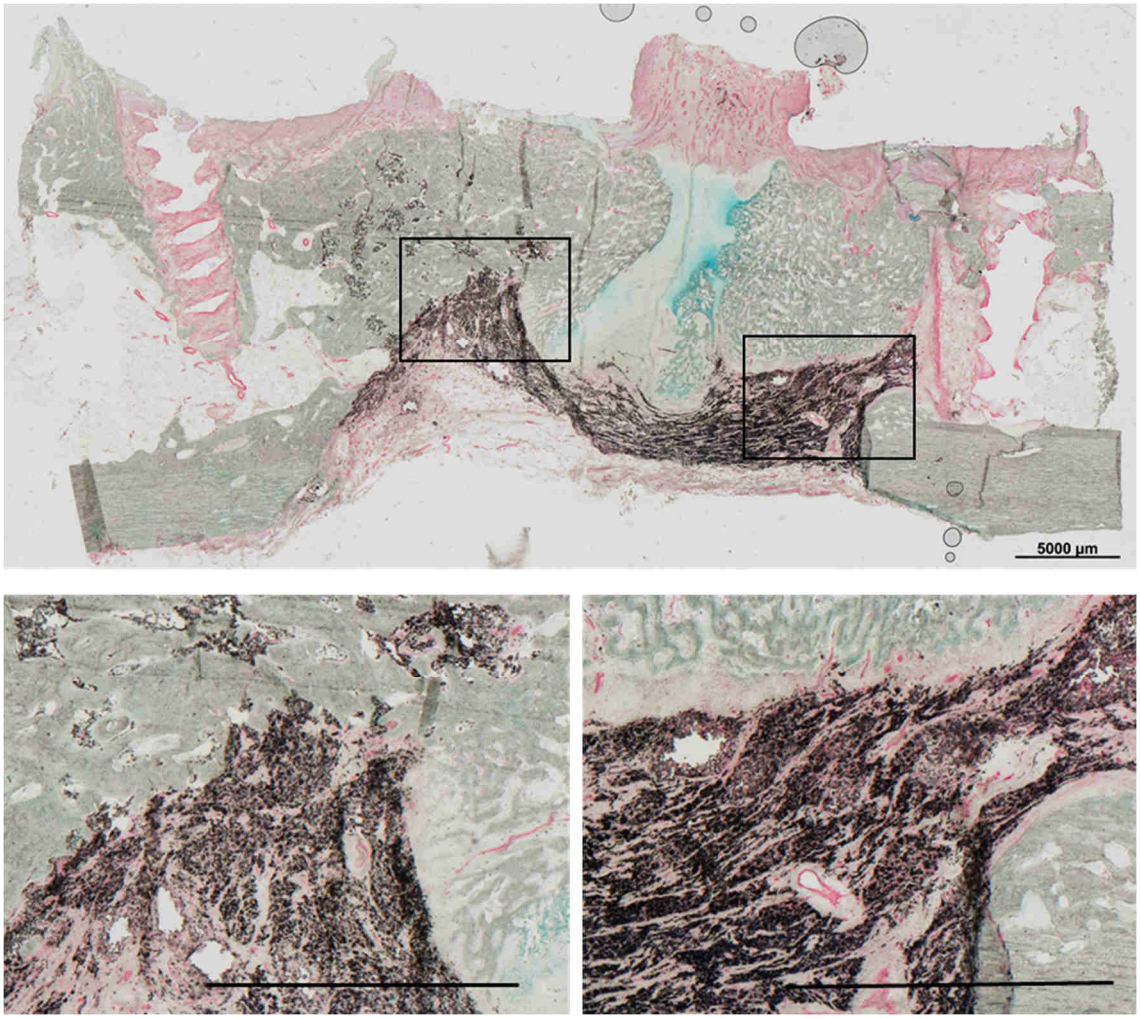

Figure 15: Immunohistochemical staining of tibial implant sample D.
α-smooth muscle staining of longitudinal section of ovine tibia in the area of the defect site. Scale bar: 5 mm.

Figure 12 shows an overview of sample D (Figure 14) and details indicated. The presence of red circular areas was detectable in the bright structures, representing regenerated bone, as well as in the black depicted synthetic material. The results are consistent over the samples of the different donors. The

blood vessels were distributed over the entirety of the defect site and consisted of various calibers.

µCT analysis of all samples are shown in Figure 16. Accordingly, to the histological results, there was no continuous union apparent and granules of the ß-TCP were identified.

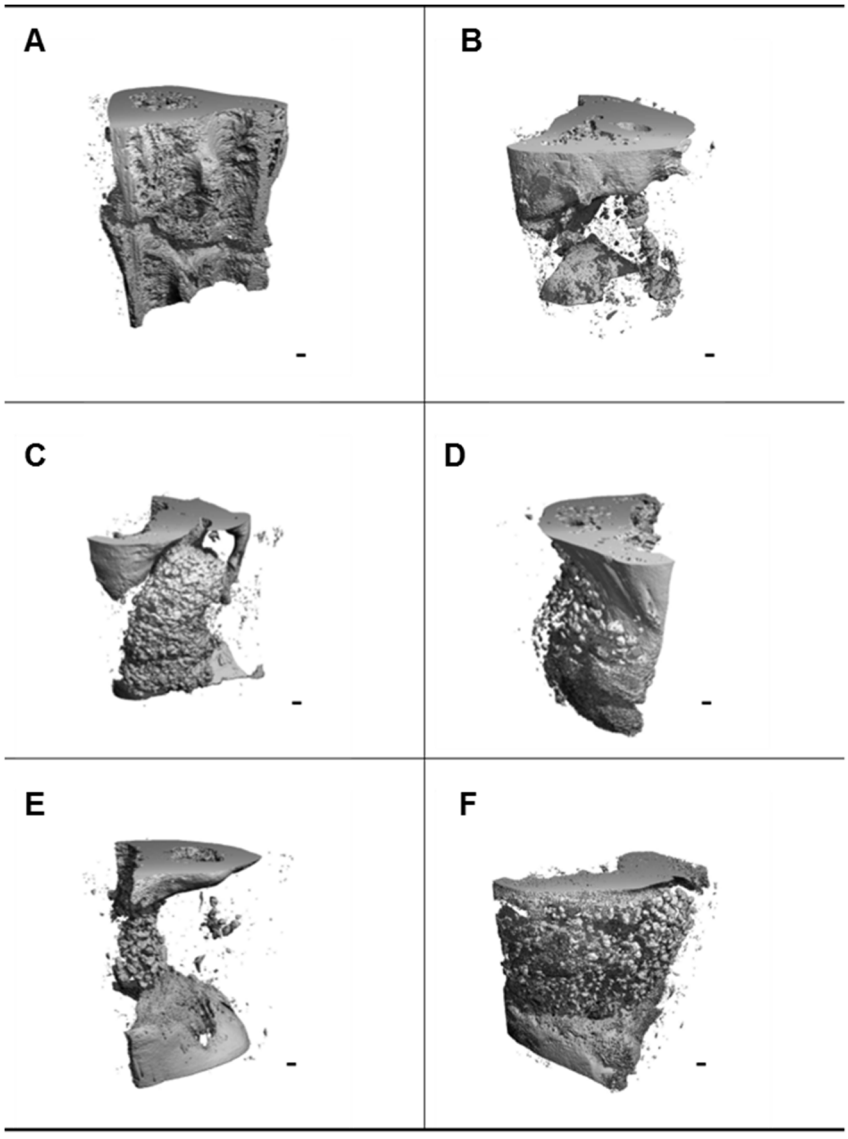

Figure 16: Bone regeneration after 6 months.
µCT analysis of the defect site in the tibia of 6 sheep. Scale bar: 1 mm.

The amount of dead space varied between samples. While sample A, D and F were filled out with dense material, bone or ß-TCP, samples B, D and E showed greater amounts of blank space in the µCT. This was an indication for soft material, e.g. soft tissue.

4.9 Animal experiment: Defect in the mandibular angle in sheep

In contrast to the experiments with the tibia defect, the bone graft filling a defect in the mandibular angle, were implanted with an anastomosis of the arterial and venous pedicles of the BioVaSc-TERM®. The implants were anastomosed to the facial artery and the accompanying vein in order to provide a connection to the blood circulatory system (Figure 17 C) and thus, nutritional supply to the cells inside. The site of implantation was the mandibular angle after the creation of a continuity defect. Stabilization was secured by two reconstruction plates fixed with osteosynthesis screws. The BioVaSc-TERM® itself was brought into the defect, the anastomosis was performed and the open ends of the lumen of the implant were pulled over the leading edges of the bony ends of the defect. Subsequently, the implant was covered by a titanium mesh that protected the implantation site and prevented a possible prolapse of the masticatory muscles. Anastomosis was performed and reperfusion of the vascular structures of the implant was observed for at least 15 minutes. During that time, the vasculature pulsated and no major leakage was apparent (Figure 14, D)

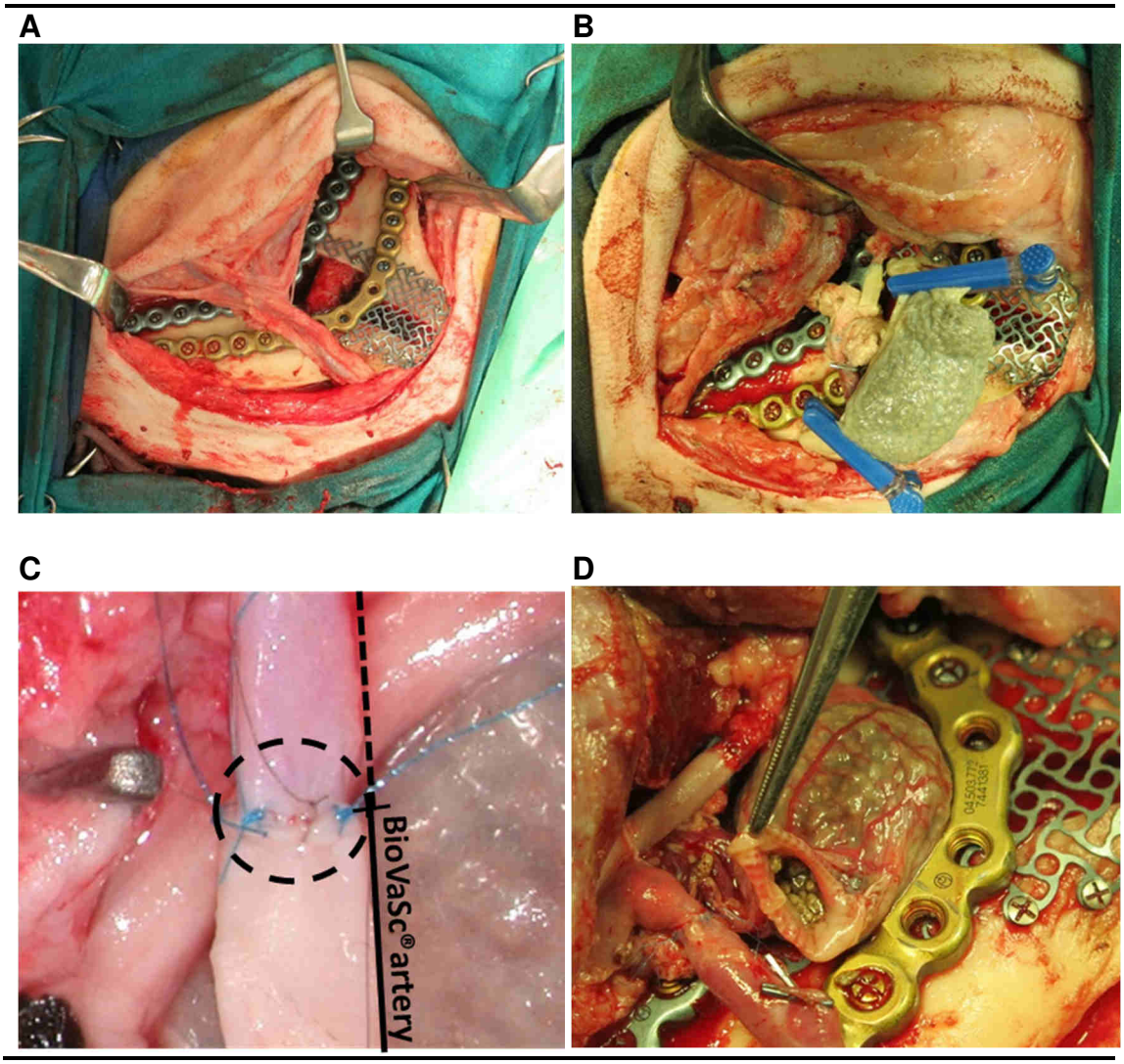

Figure 17: Mandible defect creation and bone graft implantation.
The defect was created in the mandibular angle and stabilized (A). Bone graft during implantation (B). Anastomosis of the graft with the host's vasculature (C). Arterial inlet was anastomosed to the facial artery (circle). Dotted line indicates native arterial vessel, solid line the arterial inlet of the implant. (D) Following the induction of the blood flow, the blood enters the vasculature of the BioVaSc-TERM® (D).

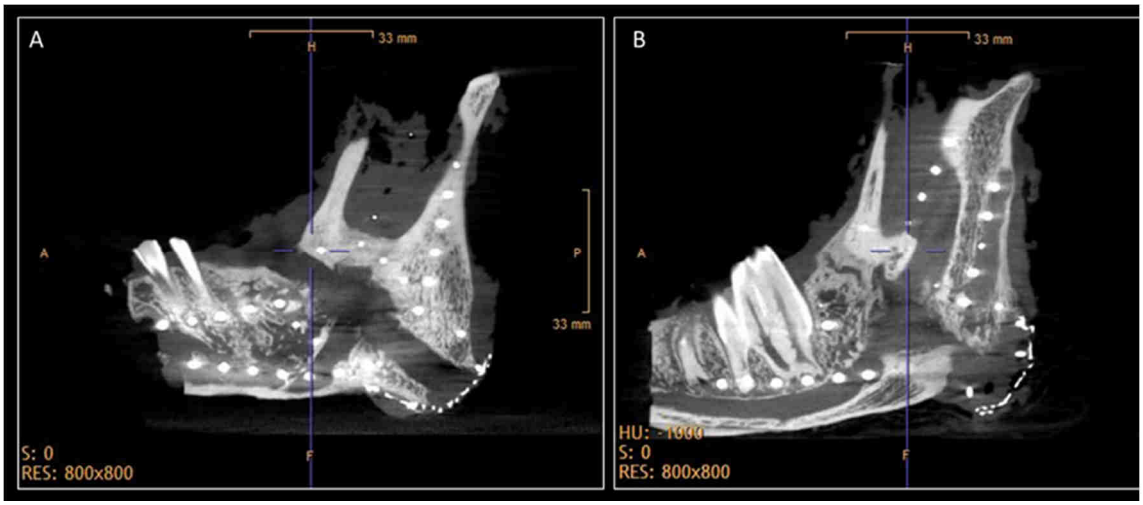

Figure 18: X-ray follow up after 6 months.
Defect site of the control animal (A) and the defect site of the implanted bone graft (B).

6 months after implantation, x-ray analysis showed the bridging of the defect in the sheep treated with the bone graft, while the defect in the control group was still present with no signs of bone regeneration. Figure 15 shows clear bone growth into the defect site with a completing union of the defect ends. However, signal intensity of the regenerated bone is lower than of the healthy native bone, indicating also a lower bone density. After sacrification, samples were plastic embedded and analyzed by toluidine-o staining. The treatment group of the implanted and anastomosed BioVaSc-TERM® showed signs of regeneration and remodeling. Bone formation occured adjacent to the cutting planes. The ingrowth of dense bone into the defect ended after ¼ of the original defect size and passed over to small bony island and ß-TCP bone replacement material. Although this was no large continuous bone area, the defect site was completely filled with small bone islands of 50 – 200 µm in dimension (Figure 19, A, C). They were evenly distributed over the whole defect site and were depicted as lightly brown stained areas. The dark black areas indicate remaining ß-TCP that was not yet resorbed

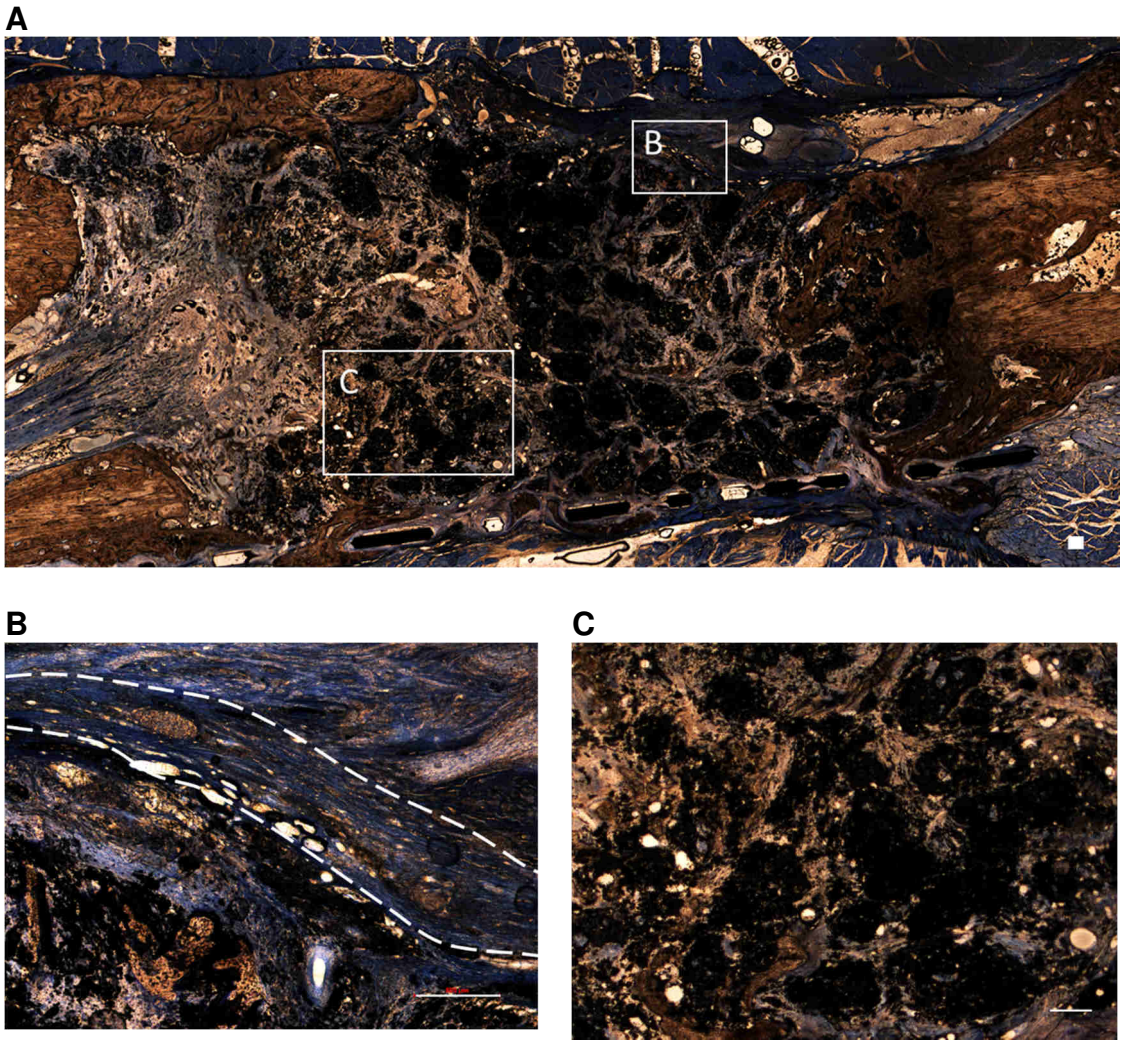

Figure 19: Transverse section of the mandibular angle defect treated with BoneVaSc® bone implant analyzed by toluidine-O staining, 6 months after implantation.
Overview of the defect bounded above and below by the collagenous structure of the BioVaSc-TERM® (A). Blue-stained laterally-oriented collagen fibers (white dotted lines) showed the course of the BioVaSc-TERM® preventing the ingrowth of connective tissue from outside the defect (B). Bright circular structures represent blood vessels of variable diameter within the formed tissue. Blood vessels and remaining ß-TCP material (black structures) embedded in newly formed bone tissue centrally in the defect (C). Scale bar: 500 µm.

The BioVaSc-TERM® was identifiable as a zone of parallel-oriented fibers at the outer rim of the ossifying area (Figure 19, B). This region contained many circular structures that were identified as blood vessels. The quantity of blood vessels

was highest in the BioVaSc-TERM® structure and evenly distributed over the whole defect site at a slightly lower concentration.

The detailed examination of a single bone island revealed the morphology of an osteon (Figure 20). The mineralized core is interspersed with osteocytes and spreading canaliculi. The outer rim of the osteon was densely seamed with bone lining cells (Figure 20, B). The osteon was centrally traversed by a prominent blood vessel (150 µm diameter) with erythrocytes visible inside the vessel (Figure 20, A).

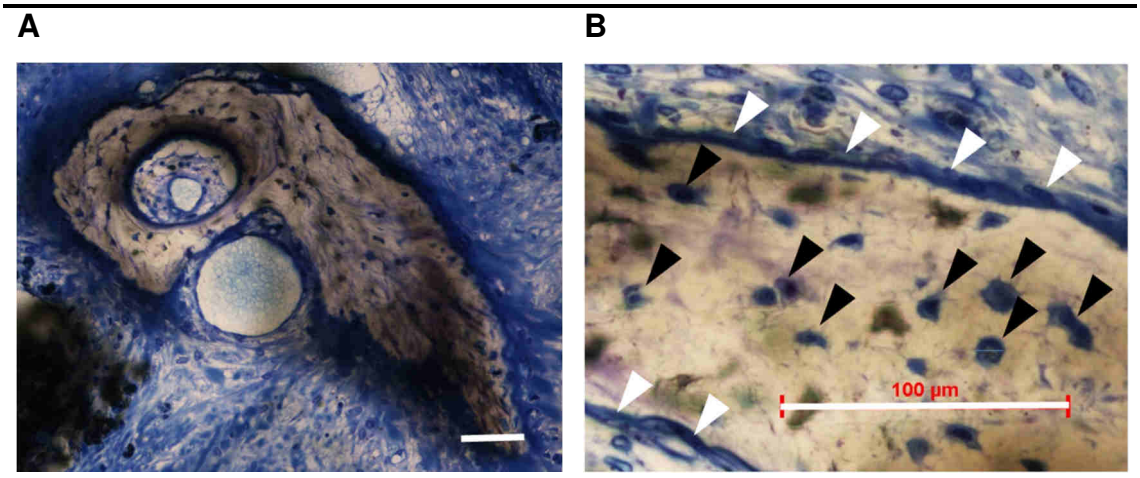

Figure 20: Transverse toluidine-O stained section of the mandibular defect treated with the bone implant after six months.
Osteon embedded in collagenous tissue with blood vessels passing through (A). Detail of an osteon (B) showing osteocytes with canaliculi (black arrows) and lining cells surrounding the osteon (white arrows). Scale bar: 100 µm

In contrast, the control sample showed light bone regeneration at the resection sides, the defect site was exclusively filled with soft tissue that is hardly cellularized. The presence of blood vessels was reduced in comparison to the treatment group.

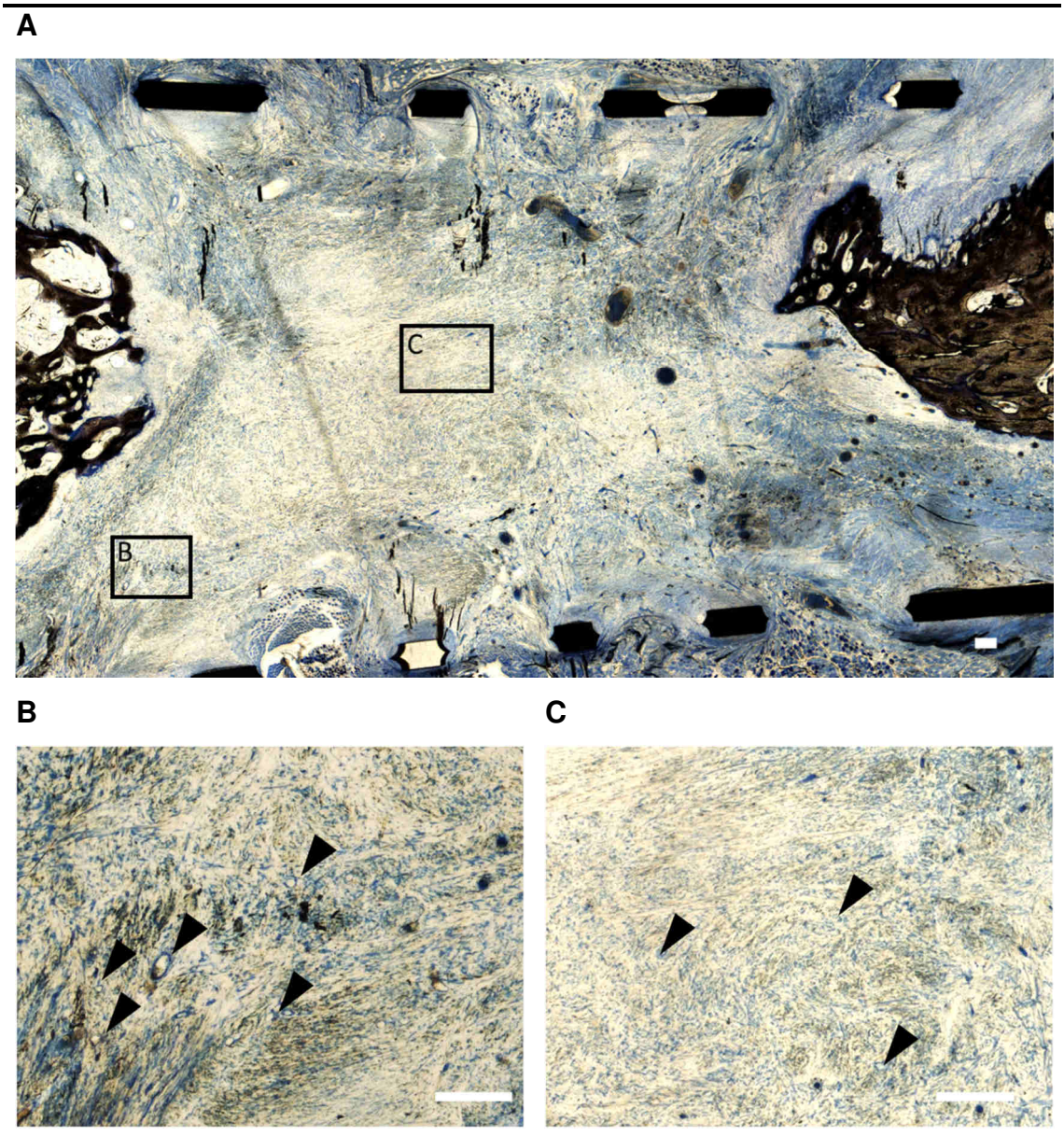

Figure 21: Transverse toluidine-o stained section of the mandibular defect control after six months.
Overview of the defect (A). Detail of the peripheral area (B) showed connective tissue with a decreasing number of blood vessels towards the central area (C).
Scale bar: 500 µm.

5 Discussion

The reconstruction of large and complex bone defects remains a challenge in reconstructive surgery despite bone's immense healing capacity. Ablative tumor resection, osteomyelitic bone removal, severe trauma or bone necrosis can result in defects exceeding the natural regenerative potential. The defect size as well as the quality of the surrounding tissue and the condition of the wound bed, the local vasculature and potential infections influence the healing perspective.

The aim of the thesis was the development of a prevascularized bone implant. Hence, a naturally derived scaffold of porcine origin (BioVaSc-TERM®) built the basis for vascularization and combined with synthetic material β-TCP, commonly used in bone reconstruction, resulted in the BoneVaSc-TERM®. Seeding of the BioVaSc-TERM® with EPCs restored its vascular functionality, while MSCs enhanced the osteogenic potential of the bone substitute material during implant maturation in in vitro culture.

Subsequently, the implantation into a large animal model allowed for investigation of the effect in a tibial and a mandibular defect in sheep, comparing the regenerative outcome in case of using or not using the implant's innate vasculature. The result in the tibial regeneration without blood vessel anastomosis showed a mainly supportive function in osteoconduction while the anastomosed implant in the mandible defect achieved the formation of numerous bony islands evenly distributed all over the defect site with extended vasculature.

An additional aim was the optimization of the manufacturing processes in order to bring such an implant as close to clinical supplication as possible. As a result the production of the BioVaSc-TERM® fulfills the necessary regulatory criteria by being GMP-conform, including the necessary documentations and quality controls.

5.1 Mobile incubator

The thesis included the design of a mobile incubator and bioreactor system for the long-distance transportation of the bone implant between the site of production and the site of clinical implantation. This scenario is of clinical

relevance since clinics might not have the capacity and necessary infrastructure for the local production of complex implants. Thus, a transportation over long distances becomes necessary. Since the implant at hand consists of several cell types, their requirements to their environment had to be fulfilled in order to secure the quality of the implant. Thermoregulation was implemented for optimal conditions as they are found in standard cell culture. The application of endothelial cells in the vascular structures of the implant necessitated the implementation of an option for perfusion of the vascular system. This was realized by the equipment of the mobile incubator with peristaltic pumps. The shear stress resulting from the perfusion of the vasculature is necessary for endothelial differentiation and endothelial cell maintenance. Shear stress for example regulates the expression of markers associated with cell adhesion and endothelial differentiation [149]. Additionally, this is important for vascular resilience by stabilizing cell-cell interactions and influencing endothelial cell proliferation, migration and survival [150]. A physiological pressure sensor integrated into the medium circulation via pressure dome performed the monitoring of the pressure inside the vasculature of the construct. The control integrated into the mobile incubator adjusted the pumping speed of the peristaltic pump in order to establish pressure conditions that are similar to the physiological situation, facilitating mechanical stimulation of the endothelial cells. A Peltier element that allowed heating of the incubation room to 37 °C as well as cooling down the system in case of direct sun exposure of the mobile incubator during summer achieved temperature control. The mobile incubator offered convenient digital monitoring of pressure regime and temperature progression of the implant, parameters relevant for assuring quality of the implant. Their recording is also required by GMP guidelines. Power supply via 220 V or 12 V power plug allowed for stationary as well as mobile operation in a car. Concluding, the mobile incubator system is a tool that covers all the necessary aspects for a secure transportation of an implant in a clinical context. The principle of the mobile incubator could easily be transferred to other complex implants or even organs for transporting organs of organ donors.

5.2 Animal models

There is a range of animal models available for bone regeneration and bone substitute material development [151–154]. Optimally, a suitable model should be reproducible, versatile regarding investigated materials or strategies and allow for several types of analysis. Influence of age and sex on bone regeneration through calciotrophic factors have to be considered [156]. The model should allow the generation of sufficient data, morbidity should be low and the costs reasonable [157].

The use of animals in experiments is discussed controversially and their value of predicting a human response is not self-evident. However, this transfer of observations is necessary for animal experiments to be valuable for medicinal progress. Principally, the correlation of in vitro and animal models with the human condition and the subsequent equalization of the in vitro and animal model response to certain conditions and the human response is an assumption. If this assumption is not critically challenged, the data gathered from in vitro or animal experiments may contribute to a vast amount of information that has little contact to the true medical demands [158].

Horrobin formulates examples that illustrate the lack of congruence of in vitro and in vivo models: The anatomical conditions and cell populations present in vitro and in vivo are different. The composition and availability of nutrition and oxygen supply, as well as carbon dioxide and metabolite removal are different. Conditions of cell multiplication are different. The quantity and participation of hormones together with their kinetic changes differ. The quaternary structure of proteins is dependent on the phospholipid composition of cells, which differs in cells in culture and cells in vivo. The membrane lipid microenvironment plays an important role in protein binding and thus, the function of proteins of cells in vitro and in vivo might differ [158, 159]. The critical discussion of the comparability of in vitro and in vivo experiments does not exist to a greater extend. This often results in the claim for abolishing animal experiments in favor of in vitro experiments, while the in vitro data cannot accurately reflect the human condition. An animal model can, under certain circumstances, deliver valuable insight into human disease. The prerequisites for a gain of knowledge are a comprehensive

understanding of the animal model and the same degree of understanding of the human disease as well as the examination of both conditions regarding congruence [158].

In the following, different animal models are presented for the investigation of bone regeneration and the similarities and differences to human bone structure and regeneration as already published in Current Molecular Biology Reports [160].

Depending on the aspect of investigation, different animal models can be taken into consideration. The most common species are rodents (mice and rats) that make up more than three-fourths, while pigs, rabbits, dogs, small ruminants and non-human primates represent the remaining model organism [161].

Rodents are easy in handling and they can be held in high numbers to generate statistically significant data. Mice are commonly used to conduct specific or conditional knockout studies. Athymic nude mice allow for the investigation of osteoconductive materials from allogenic or xenogeneic sources of which the immunogenicity is unclear [161].

Differences in general bone healing potential of animals as well as differences in the micro- and macrostructure in comparison to human bone regeneration are important to consider. The ratio of cortical and cancellous bone determine the biomechanical properties of the specific bone investigated [162]. Open growth plates in the epiphyses of mice and other rodents retain their longitudinal growth, which is not available for adult humans [163].

The Haversian system and closed growth plates in rabbits make them more suitable for a comparison to the human condition. Additionally, the bone density in both organisms is more similar, while shape and size of rabbit bones differ from the human anatomy, thus limiting the gain in knowledge regarding the investigation of mechanical properties [164]. Rabbit studies are commonly employed in cranial and mandible defects as well as age-related critical size defects using autologous cell-seeded or cell-free biomaterials, growth factors or the application of techniques as negative pressure [165, 166].

Canine models are used for periodontal and musculoskeletal research, the investigation of the regenerative potential of adipose-derived or bone marrow

stem cells and biomaterials. Dose-response studies of various growth factors were conducted [167, 168]. Structure, composition and remodeling rate of dogs and humans are similar which allows for the evaluation of implants that are suitable for human application regarding size. However, canine models are often critically viewed due to low social acceptance [169].

The regeneration process of pigs is similarly comparable to the one of humans as the one of dogs. Bone density of the trabecular network and increased bone strength in pigs differ from the human condition, while bone morphology, structure and composition closely resemble their counterparts. Common studies conducted with this model investigate fracture healing, femoral head necrosis or regulatory toxicity studies as well as testing of critical size bone substitutes, as the healing rate of pigs is similar to that of humans [170]. High growth rate, body weight and challenging handleability pose potential difficulties that were approached by the breeding of mini and micro pigs [171].

From the start, sheep and goats are more convenient in handling, animal cost and social acceptance [172]. Their comparable anatomy in long bones and their suitable dimensions make them a preferential choice for testing implants intended for human use [173, 174]. Humans and sheep share a similar bone macrostructure with a difference in the ratio of primary and secondary bone. This can be accounted for by using sheep of an age of 7 – 9 years, when secondary bone modeling begins. In spite of minor differences in the microstructure, the resemblance in bone metabolism, turnover and remodeling is significant [175]. Sheep have been used for segmental defect models [176], vertebral bone defect models including studies testing bone substitute materials [177], the effect of growth factors [178], and tissue engineering strategies [154]. While the use of small animals is convenient for many models, large animal studies are necessary to study the feasibility of methods or the sheer size to accommodate implants of a dimension that requires prevascularization and anastomosis when otherwise the survival of seeded cells would be affected. The data generated from large animals can be more comparable regarding biomechanical analysis and necessary surgical procedures can be evaluated for their suitability and redefined when appropriate. For this reason, the experiments of the thesis employed the

sheep model despite its increased complexity. The animal model was an ovine model for a segmental bone defect in the tibia [179] and a newly developed mandibular defect model by Rasse and Stigler (Clinical Department of Craniomaxillofacial and Oral Surgery, Medical University of Innsbruck). In both cases, the size of the implant was of clinically relevant dimensions. The tibia defect was easily accessible and offered a relatively simple possibility to suture the BioVaSc-TERM® to residual periosteum (Figure 13 C). Important in this scenario was the removal of the native periosteum over the defect itself so that the regeneration would be contributed to by the BioVaSc-TERM® alone. The mandibular defect model was chosen for relevance and challenge. Animals like sheep show a comparable operative situs, as in humans in respect of bone dimensions or vessel diameter. These aspects suggested a feasible transfer to the clinical situation in humans for the surgical techniques used in this study can be easily conveyed to the human anatomy due to the high degree of anatomical homology in the cranio-maxillofacial area.

In the mandibular model, the particular challenge lied in sheep being ruminants, so the mechanical requirements in this constellation exceed the human situation significantly. In sheep, the daily rumination is estimated with 600 min/day with 62 – 80 chews/min, resulting in 37,200 – 48,000 chews per day [180]. Two reconstruction plates fixed with osteosynthes screws were used to stabilize the defect. None of the sheep suffered from insufficient stabilization or breakage of the plates. Precedent biomechanical tests demonstrated the suitability of the method and ruled out the fixation with one plate only (experiments not shown, Medical University Innsbruck, Department of Cranio-Maxillofacial and Oral Surgery, Innsbruck, Austria).

The mandible defect is a clinically relevant scenario for ablative tumor resection or osteonecrosis caused by radiation or drugs as bisphosphonates in the maxillofacial context. The jaw angle below the musculus masseter was excised and stabilized with two titan plates and an additional titan cage. The prevascularized implant's arterial inlet and vein were anastomosed with the host's blood circulation via the facial transverse artery.

5.3 Bone graft implantation into critical size defects in sheep tibia and mandibale

Many strategies for bone tissue engineering that have been clinically approved are single component approaches while the incorporation of several if not all the current aspects of bone engineering might be necessary for successful bone regeneration in large defects [181]. In this approach, we employed and combined methods to address several clinically relevant aspects.

The thesis placed focus on minimally invasive methods for the design of an implantable bone graft. MSCs could be easily harvested from bone marrow aspiration while their enormous expansion potential and their similarity to periosteum stem cells make them a predestined choice [182]. They have a history of application in preclinical models and indicated therapeutic activity in musculoskeletal settings [183], as they play a major role in bone fracture repair and can secrete VEGF in hypoxic conditions [184]. Autologous MSCs were harvest from sheep and seeded on ß-TCP granules that might already have an osteogenic induction effect on the cells during in vitro culture [185]. The material additionally served as a guide rail for bone regeneration after implantation in vivo. Population of this substrate with MSCs could trigger attraction of EPCs by growth factor expression [186]. EPCs were the second cell type chosen for the implant as they are known for enhancement of neovascularization of ischemic tissues via participation in actual vessel formation [187, 188] and paracrine effects [189]. EPCs fulfilled the requirement of being accessible minimally invasively due to the isolation by density gradient centrifugation from peripheral blood. MSCs and EPCs have distinct positive attributes that make them suitable for the construction of a prevascularized bone implant by themselves but additionally synergize in bone regeneration by enhancement of early vascularization and thus, accelerating the healing process [190]. To make use of the advantageous attributes of the EPCs, the BioVaSc-TERM® was employed. The general clinical applicability of the scaffold was demonstrated in a two-year follow up of a tissue engineered airway patch [191]. The degree of standardization of the scaffold is illustrated by a current review by local authorities for the application of the scaffold

as tracheal implant. The analysis of the scaffold after decellularization showed low levels of residual DNA in the Feulgen staining and few cell remnants in the H&E staining; essential preconditions for the implantation of the xenogenic scaffold since otherwise an immune response upon implantation into the target organism must be expected. The BioVaSc-TERM® was the basis for in vitro prevasularization of the bone implants and has hypothetical potential for mimicking periosteal functions in the context of bone regeneration. Osteogenesis and cortical blood flow are influenced by the periosteum. Accordingly, studies showed the promotion of bone formation and neovascularization after injury when healthy periosteum covered the damaged bone [192]. The absence of periosteum due to injury results in delayed healing or non-unions [193, 194] and there have been approaches at tissue engineering periosteum human dermal matrices [195]. With this in mind, the use of the BioVaSc-TERM® seems suitable at providing vascularization of an ischemic site in a critically sized bone defect. While the vascularization aspect was covered by the aforementioned measures, promoting bone formation was aimed at by filling the lumen of the BioVaSc-TERM® with ß-TCP granules that were previously seeded with MSCs. Calcium phosphates are well-characterized materials that are commonly used in dental or craniofacial applications. In 1998, TCP has been approved for the repair of craniofacial defects by the Food and Drug Administration (FDA) [196]. It was used with good results for bone formation in sinus elevation [197, 198] and alveolar ridge preservation [199].

The treatment of the tibia defect with the BoneVaSc-TERM® was performed without the direct anastomosis of the vessel system but in close vicinity to the neurovascular bundle running down the tibia. The results of the histological and radiological analyses show an inhomogeneous appearance of the regeneration site. Defect bridging occurred in one single of the specimen. Generally, bony growth occurred at the defect ends towards each other; areas of remaining ß-TCP embedded in soft tissue as well as areas that predominantly contained connective tissue were detected. In all of the different compartments, blood vessels were identified by the α-SMA staining, suggesting the general accessibility of the defect site for angiogenesis. The aforementioned formation of

different tissue compartments appears to be unfavorable. While the bone regeneration seemed to take place only from the bony ends of the defect, the void space in the defect had been filled with connective tissue invading from the surrounding tissue. It might have been the case that the implants' effect mainly lay in the provision of the ß-TCP as osteoconductive material but no profound integration of the implant into the regeneration process. The results of a preclinical study by Kaempfen et al. investigating the effect of decellularized bone reseeded with bone marrow derived MSCs in a rabbit segmental defect model were similar. Prevascularization was achieved by ectopic implantation into a muscle flap close to the defect site. In a second procedure the whole flap, including bone graft, was transferred into the defect while keeping the vessels connected to allow sustained blood flow [200]. The defect did not consolidate or remodel to a greater extend. Callus formation occurred around the graft, not including it. The defect site hosted an increased amount of blood vessels, however, bone formation itself was limited. These findings were in line with those of the BoneVaSc-TERM®'s non-anastomosed study.

In contrast, the treatment of the defect in the mandible was performed including a direct anastomosis of the implant to the circulatory system of the experimental animals. The anastomosis of the BoneVaSc-TERM® scaffold to the facial vessels in the mandibular defect succeeded in all cases. Both the arterial inlet and the venous outlet of the BoneVaSc-TERM® were mechanically stable enough for the procedure. Observation of the implants for 15 minutes after reperfusion confirmed vessel patency. During that time, pulsating of the vasculature was detected in all implants with no leakage apparent. The successful anastomosis is an essential prerequisite making an implant more independent from the condition found inside the injury site. Analysis of sections from the defect site indicate a dense network of vessels of different caliber supplying the tissue, a relevant result since scaffolds often do not succeed in supporting viability on their inside [201].

In contrast to other studies [201, 202] the ß-TCP seemed not to be embedded in adjacent bone tissue, instead the granules appear to be resorbed by osteoclastic activity and at the same time replaced by newly formed osteons (Figure 20). Osteons are the basic functional unit of compact bone. The osteons found in the

defect exhibit an approximately cylindrical shape, which is their typical appearance [203]. Characteristic for an osteon is the centrally arranged Haversian canal containing a blood vessel, which supplies the osteon with essential nutrients. Figure 20 shows an osteon in detail with the blood vessel in the Haversian canal filled with tightly packed blood cells, identifiable by their discoid shape. The osteon was surrounded by bone lining cells with their generic flat shape. The presence of the bone lining cells might indicate a mature state of the osteon, as bone lining cells are one of three possible fates of osteoblasts upon the completion of forming bone matrix [204]. The other fates being the transformation into osteocytes and apoptosis [205]. As bone lining cells are considered quiescent cells “where neither bone resorption nor bone formation occurs” [5], the illustrated osteon might have reached its resting form, not contributing to any further bone formation. On the other hand, bone lining cells are associated with the initiation of resorption and bone formation, so that it is uncertain if the osteon would have grown in size with prolonged experiment duration or not [206]. The diameter of the Haversian canal diameter of about 160 µm appears to be almost double the size as compared to human dimensions [207]. It has to be noted that, in humans, there is already a significant intraspecific variability in Haversian canal diameter depending on their origin, for example from ribs or femurs [208].

Rather than osteoconduction, bone formation by osteoinduction seemed to have taken place in ß-TCP as substrate. The osteoclasts and osteoblasts that participated in the formation of the osteons could have derived from the MSCs originally seeded on the ß-TCP granules or the circulatory system. The MSCs might have taken part in the attraction of vessels into the inside of the implant. No adverse effects were detected due to the autologous cell sources and the immunological inert biological and synthetic scaffolds. The results show an extensive vascular network in the anastomosed implants as compared to the control defect. In the control, the encountered tissue was mainly soft tissue of a low organizational level and no signs of bone formation in the central defect area. Only in the area of the resection rim of the continuity defect, there were hints on bone formation.

The role of the EPC in the experiments appeared to contribute mainly to vascularization while other authors found results suggesting a possible role of EPC in bone regeneration itself: In a sheep model, a 3.2 cm defect in the tibia was created and treated with EPC transplantation [81]. The defect was stabilized with stainless steel plates and the wound was closed. EPC transplantation took place 2 weeks later by opening the wound and creating a v-wedge-shaped longitudinal canal in the regeneration scar tissue. 2 x 10^7 EPCs were applied to the canal; the wound was closed subsequently. Until sacrification 12 weeks later, x-ray images were taken every two weeks while µCT and histological analyses were performed after scarification. X-ray images revealed the beginning of bone regeneration 2 – 4 weeks after surgery in the treatment group while the control group exhibited no or minimal bone regeneration. X-rays indicated complete bridging 10 – 12 weeks later in the treatment group, minimal bone regeneration in the control group. Histological methods provided confirmation of the preceded analyses by showing woven bone structures in the regenerated defect site in the treatment group. The contribution of EPCs to an improved bone regeneration by accelerated vascularization immediately suggests itself. However, authors stated that the scar tissue after 2 weeks already showed a high degree of vascularization before the application of EPCs so that a positive effect due to any further increase in vascularization did not seem to be necessary. Alternatively, the authors consider a possible differentiation into the osteogenic linage. There are hints on the possibility of EPCs expressing an osteogenic phenotype under bone differentiation conditions in vitro [74, 81], but the true fate of the EPC in this experimentation remained speculative. The main difference between this investigation and work at hand regarding EPCs was their number and administration. The isolation method of the EPCs matched in both approaches but Rozen et al. placed a greater number of EPCs directly into the defect site straight after expansion when they possibly remained rather undifferentiated. The EPCs in the mandibular defect on the other hand were subject to differentiating cues in the vessel system of the BioVaSc-TERM® by the 3D structure itself and the pressure regime induced by the bioreactor, driving the EPCs into the

endothelial lineage. Thus, they most likely fulfil their role as endothelial cell as opposed to the comparative study in which they might form bone.

Furthermore, there have been reports on anastomosed implants following the in vivo bioreactor principle like free flap procedures or the utilization of AV loops with promising results [97, 107]. Such regeneration strategies are appropriate for the treatment of compromised transplant beds as they include a functional vascularization that makes them less dependent on the vasculature on-site. A dedicated implant vasculature provides the possibility of bringing the necessary requirements for successful healing as in endochondral ossification. The implant's innate blood supply allows for uninterrupted formation of cartilage hypertrophic chondrocytes and their progression into bone [209]. Drawbacks of the aforementioned in vivo bioreactor principle and free flaps are the two necessary operations; the first that brings in the desired implant or material into the flap, and the second operation for taking the implant out of the ectopic site for the actual treatment of the defect in another site. Depending on the site of harvesting, the donor site morbidities can range from discomfort and pain to limited mobility [210]. Additionally, every surgery bears the risk of surgical site infection accounting for 400,000 extra days spent at hospital in the USA alone. This equals a cost of US$ 10 billion per year [211]. Surgical site infections are defined as infections occurring up to 30 days after surgery, affecting the incision or the underlying tissue at the operation site and the incidence rate can be up to 20 % under unfavorable preconditions [212]. These steps were circumvented in the approach of the thesis by minimally invasive cell isolation from peripheral blood and bone marrow aspirate. The advantages of minimally invasive procedures over open procedures are a reduced incision area, earlier mobilization, and reductions in postoperative pain, better preservation of immune system function and decreased use of central venous catheters. The result is a significantly reduced risk for surgical site infections [213]. Following the same intention, Eweida et al. used a HA/β-TCP composite scaffold loaded with autogenous platelet-rich plasma BMP-2 in an attempt to induce bone formation in a defect in the mandibular angle of goats. After creating a defect without interrupting the mandible's continuity the bone graft was inserted and stabilized

with a titanium plate and screws [214]. The graft was anastomosed to facial vessels, creating an in situ AV loop already in the defect site. Investigations correlated bone growth with the central vascularization provided by the incorporated facial vessels. In contrast to the implants of this thesis, BMP-2, with its associated regulatory implications, was used and the defect created was marginal as opposed to the continuity defect in the sheep mandible.
Summarizing the presented results, the bone formation itself has to be improved further; the vascular basis for defect regeneration is promising and might facilitate the establishment of bone continuity if allowed to regenerate for a longer period than six months as it was the case in the study presented. This approach is a feasible alternative to free nonvascularized bone grafts from iliac crest, ribs, chin, fibula or tibia that successfully treat defects with good transplant bed conditions. Vascularized bone grafts, as the one presented in this study, are more resistant to poor transplant beds as found in medication-related osteonecrosis or radiotherapy. Additionally, second site surgeries could be avoided which reduces the associated risk for patients and increases acceptance of the procedure.

5.4 Consideration of the GMP principles

In order to get closer to the aim of clinical application of research in the field of regenerative medicine, the GMP principles were taken into account during the production of the implants used in this work and implemented in the case of the production of the BioVaSc-TERM®. The health condition of the donor animals as raw material for the production of the BioVaSc-TERM® was an essential criterion. Accordingly, all animals came from a combined, closed breeding establishment and fattening farm and were approved for food production according to Regulation (EC) 853/2004. A veterinarian performed herd health monitoring at least once a month. Livestock was vaccinated preemptively against swine influenza, erysipelas, smedi, rhinitis atrophicans, mycoplasma hyopneumoniae, porcine circovirus type 2, porcine circovirus associated disease and porcine intestinale adenomatose. Every four months samples (nasal swaps, blood and fecal samples) were taken randomly for bacterial, parasitical and virological for analysis by the Bavarian state office for health and food safety Erlangen

(Bayerisches Landesamt für Gesundheit und Lebensmittelsicherheit Erlangen). For the past two years, the livestock had to be free from notifiable diseases, from zoonosis or infectious diseases of the gastrointestinal tract as well as endo- and ectoparasites. The decellularization process as described in chapter 3.2 took place in a class D clean room and ensured inactivation of enveloped viruses within 5 minutes to a level below the detection limit of the test at 4.5-log reduction. The subsequently performed gamma irradiation should result in a log-reduction of 4 – 5 for small non-enveloped viruses. The dose of gamma irradiation will be elevated to 31 kGy in order to fulfill guideline EMA/CHMP/BWP/814397/2011 and the efficacy will be validated in a viral clearance study in the future. For quality control, bile acid concentration (< 50 µmol/l), endotoxin (≤ 1.0 EU/ml), DNA content (weak Feulgen staining), cell residue (weak H&E staining), mycoplasma (negative) and microbiological testing (negative) were determined after gamma irradiation and only samples that fulfilled the criteria were released for further processing. Accredited contract laboratories using validated test systems performed the testing of mycoplasma, endotoxin and microbiology.

The documentation of the process in manufacturing protocols allowed for complete trace- and replicability as required according to the GMP guidelines. The production of the BioVaSc-TERM® as basis for the prevascularized bone implants complied with regulatory requirements. The production, quality control and documentation met the requirements by local authorities and the Paul-Ehrlich-Institut during an audit for the obtainment of a manufacturing authorization. An additional study demonstrating the virus safety regarding small non-enveloped viruses of the produces matrices will be carried out in future.

The complete BoneVaSc-TERM® as a combination of the BioVaSc-TERM as medicinal product and cellular components (EPCs and MSC) make it a combined ATMP and subject matter of the *Guidelines on Good Manufacturing Practice specific to Advanced Therapy Medicinal Products*. The construction of the actual bone aspect considered the GMP standards in the choice of material and cell source, but it did not fulfill it in any aspect since in this part research was the focus, which does not allow for the rather inflexible GMP processing. From a regulatory point of view, this approach allowed the BioVaSc-TERM® to act as an

independent unit outfitted with manufacturing and documentation standards that can satisfy the strict demands necessary for a possible manufacturing authorization. As the BioVaSc-TERM® can be the basis for various prevascularized implants; a valuable foundation was created for the swift approval of such implants.

6 Outlook

The subpopulation of EPC used in this work was not determined. They fulfilled their function regarding repopulating the vascular structures and making them functional. It might be able to enhance the osteogenic potential by using EPC derived endothelial cells that are specifically useful in bone regeneration.

The maturation of the implant took place without the use of osteogenic culture medium, so initially the only impulse for the MSCs to commit themselves to the osteogenic lineage was the biomaterial. The main function and capability of the material lies in its osteoconductive properties and its task as guide rail; their osteoinductive impact, however, is low. The use of osteogenic differentiation medium during in vitro culture could bring the implant closer to its future area of application, the bone. This could potentially speed up the integration into and the regeneration of a defect. Another option to increase regeneration could be the incorporation of immobilized BMP into the biomaterial for example by covalent binding. This would allow for use of the protein at low dosages, which would circumvent the risks associated with the use of high dosages of BMP.

Furthermore, an advanced in vitro maturation of the implant could provide a bone regeneration model that allows testing of other one regeneration treatment strategies, including growth factors, biomaterials or therapeutic cells.

The results of the experiment of the anastomosed implant suggested a prolonged observation period of the experiments since there was substantial bone growth but no complete bridging with increased bone density. It would be of interest to investigate if the defect would heal completely after a longer experimental time or if the regeneration stopped at a certain point. Additionally, labeling techniques for cells populating the implant could deliver insight into the fate of the cells in vivo. Methods like cell labeling using iron oxides or perfluorcarbon are promising techniques as soon as their sensitivity can be increased to a level that allows for a non-invasive detection of a low number of cells in vivo. This could deliver more precise information on the function and fate of cells delivered.

7 References

1. Clarke B (2008) Normal bone anatomy and physiology. Clinical journal of the American Society of Nephrology 3(Supplement 3): S131-S139
2. Robling AG, Hinant FM, Burr DB et al. (2002) Improved bone structure and strength after long-term mechanical loading is greatest if loading is separated into short bouts. Journal of Bone and Mineral Research 17(8): 1545–1554
3. Weiner S, Wagner HD (1998) The material bone: structure-mechanical function relations. Annual Review of Materials Science 28(1): 271–298
4. Aszódi A, Bateman JF, Gustafsson E et al. (2000) Mammalian skeletogenesis and extracellular matrix: what can we learn from knockout mice? Cell structure and function 25(2): 73–84
5. Florencio-Silva R, Sasso, Gisela Rodrigues da Silva, Sasso-Cerri E et al. (2015) Biology of bone tissue: structure, function, and factors that influence bone cells. BioMed research international 2015
6. Pankovich AM, Simmons DJ, Kulkarni VV (1974) Zonal osteons in cortical bone. Clin Orthop Relat Res 100: 356–363
7. Arnett T (2003) Regulation of bone cell function by acid–base balance. Proceedings of the Nutrition Society 62(02): 511–520
8. Dobnig H, Turner RT (1995) Evidence that intermittent treatment with parathyroid hormone increases bone formation in adult rats by activation of bone lining cells. Endocrinology 136(8): 3632–3638
9. Franz-Odendaal TA, Hall BK, Witten PE (2006) Buried alive: how osteoblasts become osteocytes. Developmental Dynamics 235(1): 176–190
10. Bonewald LF (2011) The amazing osteocyte. Journal of Bone and Mineral Research 26(2): 229–238
11. Mullender MG, van der Meer DD, Huiskes R et al. (1996) Osteocyte density changes in aging and osteoporosis. Bone 18(2): 109–113
12. Rochefort GY, Pallu S, Benhamou C (2010) Osteocyte: the unrecognized side of bone tissue. Osteoporosis International 21(9): 1457–1469
13. Dallas SL, Prideaux M, Bonewald LF (2013) The osteocyte: an endocrine cell… and more. Endocrine reviews 34(5): 658–690
14. Bonewald LF (2007) Osteocytes as dynamic multifunctional cells. Annals of the New York Academy of Sciences 1116(1): 281–290
15. Cherian PP, Siller-Jackson AJ, Gu S et al. (2005) Mechanical strain opens connexin 43 hemichannels in osteocytes: a novel mechanism for the release of prostaglandin. Molecular biology of the cell 16(7): 3100–3106
16. Li X, Zhang Y, Kang H et al. (2005) Sclerostin binds to LRP5/6 and antagonizes canonical Wnt signaling. Journal of Biological Chemistry 280(20): 19883–19887
17. Cardoso L, Herman BC, Verborgt O et al. (2009) Osteocyte apoptosis controls activation of intracortical resorption in response to bone fatigue. Journal of Bone and Mineral Research 24(4): 597–605

18. Boyce BF, Xing L (2008) Functions of RANKL/RANK/OPG in bone modeling and remodeling. Archives of biochemistry and biophysics 473(2): 139–146
19. Goto T, Yamaza T, Tanaka T (2003) Cathepsins in the osteoclast. Journal of electron microscopy 52(6): 551–558
20. Teti A, Marchisio PC, Zallone AZ (1991) Clear zone in osteoclast function: role of podosomes in regulation of bone-resorbing activity. American Journal of Physiology-Cell Physiology 261(1): C1-C7
21. Ozaki A, Tsunoda M, Kinoshita S et al. (2000) Role of fracture hematoma and periosteum during fracture healing in rats: interaction of fracture hematoma and the periosteum in the initial step of the healing process. Journal of orthopaedic science 5(1): 64–70
22. Shapiro F (1988) Cortical bone repair. The relationship of the lacunar-canalicular system and intercellular gap junctions to the repair process. J Bone Joint Surg Am 70(7): 1067–1081
23. Kaderly RE (1991 Feb) Primary bone healing, vol 1, United States
24. Marsell R, Einhorn TA (2011) The biology of fracture healing. Injury 42(6): 551–555
25. Loi F, Córdova LA, Pajarinen J et al. (2016) Inflammation, Fracture and Bone Repair. Bone 86: 119–130. doi: 10.1016/j.bone.2016.02.020
26. Lafage-Proust M, Roche B, Langer M et al. (2015) Assessment of bone vascularization and its role in bone remodeling. BoneKEy Reports 4: 662. doi: 10.1038/bonekey.2015.29
27. Sivaraj KK, Adams RH (2016) Blood vessel formation and function in bone. Development 143(15): 2706–2715. doi: 10.1242/dev.136861
28. Murakami M, Simons M (2008) Fibroblast growth factor regulation of neovascularization. Curr Opin Hematol 15(3): 215–220. doi: 10.1097/MOH.0b013e3282f97d98
29. Adair TH, Montani J (2010) CIntegrated Systems Physiology: from Molecule to Function to Disease: BAngiogenesis. Angiogenesis. Integrated Systems Physiology: from Molecule to Function to Disease, San Rafael (CA)
30. Rafii S, Butler JM, Ding B (2016) Angiocrine functions of organ-specific endothelial cells. Nature 529(7586): 316–325. doi: 10.1038/nature17040
31. Kronenberg HM (2003) Developmental regulation of the growth plate. Nature 423: 332 EP -
32. Ramasamy SK (2017) Structure and Functions of Blood Vessels and Vascular Niches in Bone. Stem Cells International 2017: 5046953. doi: 10.1155/2017/5046953
33. Nagel A (1993) The clinical significance of the nutrient artery. Orthop Rev 22(5): 557–561
34. Wirth T, Syed Ali MM, Rauer C et al. (2002) The blood supply of the growth plate and the epiphysis: a comparative scanning electron microscopy and histological experimental study in growing sheep. Calcif Tissue Int 70(4): 312–319. doi: 10.1007/s00223-001-2006-x

35. Hunter WL, Arsenault AL (1990) Vascular invasion of the epiphyseal growth plate: analysis of metaphyseal capillary ultrastructure and growth dynamics. Anat Rec 227(2): 223–231. doi: 10.1002/ar.1092270211
36. Kim J, Lee J, Shin K et al. (2015) Haversian system of compact bone and comparison between endosteal and periosteal sides using three-dimensional reconstruction in rat. Anatomy & Cell Biology 48(4): 258–261. doi: 10.5115/acb.2015.48.4.258
37. Cicconetti A, Sacchetti B, Bartoli A et al. (2007) Human maxillary tuberosity and jaw periosteum as sources of osteoprogenitor cells for tissue engineering. Oral Surg Oral Med Oral Pathol Oral Radiol Endod 104(5): 618.e1-12. doi: 10.1016/j.tripleo.2007.02.022
38. Fujita J, Itabashi Y, Seki T et al. (2012) Myocardial cell sheet therapy and cardiac function. American Journal of Physiology-Heart and Circulatory Physiology 303(10): H1169-H1182
39. Johner R, Wruhs O (1983) Classification of tibial shaft fractures and correlation with results after rigid internal fixation. Clin Orthop Relat Res 178: 7–25
40. Langer R, Vacanti JP (1993) Tissue engineering. Science 260(5110): 920–926
41. Ikada Y (2006) Challenges in tissue engineering. J R Soc Interface 3(10): 589–601. doi: 10.1098/rsif.2006.0124
42. Hansmann J, Groeber F, Kahlig A et al. (2013) Bioreactors in tissue engineering - principles, applications and commercial constraints. Biotechnol J 8(3): 298–307. doi: 10.1002/biot.201200162
43. McFetridge PS, Abe K, Horrocks M et al. (2007) Vascular tissue engineering: bioreactor design considerations for extended culture of primary human vascular smooth muscle cells. ASAIO J 53(5): 623–630. doi: 10.1097/MAT.0b013e31812f3b7e
44. Yeatts AB, Fisher JP (2011) Bone tissue engineering bioreactors: dynamic culture and the influence of shear stress. Bone 48(2): 171–181. doi: 10.1016/j.bone.2010.09.138
45. Jensen G, Morrill C, Huang Y (2018) 3D tissue engineering, an emerging technique for pharmaceutical research. Acta Pharmaceutica Sinica B. doi: 10.1016/j.apsb.2018.03.006
46. Mafi R, Hindocha S, Mafi P et al. (2011) Sources of adult mesenchymal stem cells applicable for musculoskeletal applications - a systematic review of the literature. Open Orthop J 5 Suppl 2: 242–248. doi: 10.2174/1874325001105010242
47. Ullah I, Subbarao RB, Rho GJ (2015) Human mesenchymal stem cells - current trends and future prospective. Bioscience Reports 35(2): e00191. doi: 10.1042/BSR20150025
48. Hass R, Kasper C, Böhm S et al. (2011) Different populations and sources of human mesenchymal stem cells (MSC): A comparison of adult and neonatal tissue-derived MSC. Cell Commun Signal 9: 12. doi: 10.1186/1478-811X-9-12

49. Lanza RP, Klimanskaya I (2009) Essential stem cell methods. Reliable lab solutions. Academic Press, London
50. Dominici M, Le Blanc K, Mueller I et al. (2006) Minimal criteria for defining multipotent mesenchymal stromal cells. The International Society for Cellular Therapy position statement. Cytotherapy 8(4): 315–317. doi: 10.1080/14653240600855905
51. Madonna R, Montero-Menei C, Karam J et al. (2014) Induction of angiogenesis and prevention of apoptosis by implantation of adipose tissue-derived mesenchymal stromal cells on VEGF-releasing PLGA microspheres: A combined growth factor therapy cell transplantation approach. European Heart Journal 34(suppl 1)
52. Hatzistergos KE, Quevedo H, Oskouei BN et al. (2010) Bone marrow mesenchymal stem cells stimulate cardiac stem cell proliferation and differentiation. Circ Res 107(7): 913–922. doi: 10.1161/CIRCRESAHA.110.222703
53. Korr H (1980) Proliferation of different cell types in the brain. Adv Anat Embryol Cell Biol 61: 1–72
54. Johnson KE, Wilgus TA (2014) Vascular Endothelial Growth Factor and Angiogenesis in the Regulation of Cutaneous Wound Repair. Advances in wound care 3(10): 647–661. doi: 10.1089/wound.2013.0517
55. Alberts B (2002) Molecular biology of the cell, 4. ed. Garland, New York
56. Dixelius J, Jakobsson L, Genersch E et al. (2004) Laminin-1 promotes angiogenesis in synergy with fibroblast growth factor by distinct regulation of the gene and protein expression profile in endothelial cells. J Biol Chem 279(22): 23766–23772. doi: 10.1074/jbc.M311675200
57. Peiró C, Redondo J, Rodríguez-Martínez MA et al. (1995) Influence of endothelium on cultured vascular smooth muscle cell proliferation. Hypertension 25(4): 748–751
58. Kader KN, Akella R, Ziats NP et al. (2000) eNOS-overexpressing endothelial cells inhibit platelet aggregation and smooth muscle cell proliferation in vitro. Tissue engineering 6(3): 241–251
59. Koch AE, Distler O (2007) Vasculopathy and disordered angiogenesis in selected rheumatic diseases: rheumatoid arthritis and systemic sclerosis. Arthritis Res Ther 9 Suppl 2: S3. doi: 10.1186/ar2187
60. Patan S (2004) Vasculogenesis and angiogenesis. Cancer Treat Res 117: 3–32
61. Yoder MC, Ingram DA (2009) Endothelial progenitor cell: ongoing controversy for defining these cells and their role in neoangiogenesis in the murine system. Curr Opin Hematol 16(4): 269–273. doi: 10.1097/MOH.0b013e32832bbcab
62. Purhonen S, Palm J, Rossi D et al. (2008) Bone marrow-derived circulating endothelial precursors do not contribute to vascular endothelium and are not needed for tumor growth. Proc Natl Acad Sci U S A 105(18): 6620–6625. doi: 10.1073/pnas.0710516105

63. Salven P, Purhonen S, Rossi D et al. (2008) Reply to Kerbel et al.: EPCs are again claimed to be essential in yet other models despite the irreproducibility of the original experiments introducing them. Proceedings of the National Academy of Sciences 105(34): E55. doi: 10.1073/pnas.0805971105
64. Chong, Mark Seow Khoon, Ng WK, Chan, Jerry Kok Yen (2016) Concise Review: Endothelial Progenitor Cells in Regenerative Medicine: Applications and Challenges. Stem Cells Transl Med 5(4): 530–538. doi: 10.5966/sctm.2015-0227
65. Asahara T, Murohara T, Sullivan A et al. (1997) Isolation of putative progenitor endothelial cells for angiogenesis. Science 275(5302): 964–967
66. Bongiovanni D, Bassetti B, Gambini E et al. (2014) The CD133+ cell as advanced medicinal product for myocardial and limb ischemia. Stem Cells Dev 23(20): 2403–2421. doi: 10.1089/scd.2014.0111
67. Shantsila E, Watson T, Lip, Gregory Y H (2007) Endothelial progenitor cells in cardiovascular disorders. J Am Coll Cardiol 49(7): 741–752. doi: 10.1016/j.jacc.2006.09.050
68. Taylor RG, Lewis JC (1986) Endothelial cell proliferation and monocyte adhesion to atherosclerotic lesions of white carneau pigeons. Am J Pathol 125(1): 152–160
69. Fang S, Wei J, Pentinmikko N et al. (2012) Generation of functional blood vessels from a single c-kit+ adult vascular endothelial stem cell. PLoS Biol 10(10): e1001407. doi: 10.1371/journal.pbio.1001407
70. Ingram DA, Mead LE, Tanaka H et al. (2004) Identification of a novel hierarchy of endothelial progenitor cells using human peripheral and umbilical cord blood. Blood 104(9): 2752–2760. doi: 10.1182/blood-2004-04-1396
71. Yoder MC, Mead LE, Prater D et al. (2007) Redefining endothelial progenitor cells via clonal analysis and hematopoietic stem/progenitor cell principals. Blood 109(5): 1801–1809. doi: 10.1182/blood-2006-08-043471
72. Bou Khzam L, Bouchereau O, Boulahya R et al. (2015) Early outgrowth cells versus endothelial colony forming cells functions in platelet aggregation. J Transl Med 13: 353. doi: 10.1186/s12967-015-0723-6
73. Yoon C, Hur J, Park K et al. (2005) Synergistic neovascularization by mixed transplantation of early endothelial progenitor cells and late outgrowth endothelial cells: the role of angiogenic cytokines and matrix metalloproteinases. Circulation 112(11): 1618–1627. doi: 10.1161/CIRCULATIONAHA.104.503433
74. Han Y, Hsieh FH (2014) Osteogenic differentiation of late-outgrowth CD45-negative endothelial progenitor cells. J Vasc Res 51(5): 369–375. doi: 10.1159/000368929
75. Kuroda R, Matsumoto T, Miwa M et al. (2011) Local transplantation of G-CSF-mobilized CD34(+) cells in a patient with tibial nonunion: a case report. Cell Transplant 20(9): 1491–1496. doi: 10.3727/096368910X550189

76. Zigdon-Giladi H, Bick T, Lewinson D et al. (2014) Mesenchymal stem cells and endothelial progenitor cells stimulate bone regeneration and mineral density. J Periodontol 85(7): 984–990. doi: 10.1902/jop.2013.130475
77. Zigdon-Giladi H, Bick T, Lewinson D et al. (2015) Co-transplantation of endothelial progenitor cells and mesenchymal stem cells promote neovascularization and bone regeneration. Clin Implant Dent Relat Res 17(2): 353–359. doi: 10.1111/cid.12104
78. Pang H, Wu X, Fu S et al. (2013) Prevascularisation with endothelial progenitor cells improved restoration of the architectural and functional properties of newly formed bone for bone reconstruction. Int Orthop 37(4): 753–759. doi: 10.1007/s00264-012-1751-y
79. Seebach C, Henrich D, Wilhelm K et al. (2012) Endothelial progenitor cells improve directly and indirectly early vascularization of mesenchymal stem cell-driven bone regeneration in a critical bone defect in rats. Cell Transplant 21(8): 1667–1677. doi: 10.3727/096368912X638937
80. Matsumoto T, Kawamoto A, Kuroda R et al. (2006) Therapeutic potential of vasculogenesis and osteogenesis promoted by peripheral blood CD34-positive cells for functional bone healing. Am J Pathol 169(4): 1440–1457. doi: 10.2353/ajpath.2006.060064
81. Rozen N, Bick T, Bajayo A et al. (2009) Transplanted blood-derived endothelial progenitor cells (EPC) enhance bridging of sheep tibia critical size defects. Bone 45(5): 918–924. doi: 10.1016/j.bone.2009.07.085
82. Nikolaos C. Keramaris, Sarandos Kaptanis, Helen Lucy Moss et al. (2012) Endothelial Progenitor Cells (EPCs) and Mesenchymal Stem Cells (MSCs) in Bone Healing. Curr Stem Cell Res Ther 7(4): 293–301. doi: 10.2174/157488812800793081
83. Koob S, Torio-Padron N, Stark GB et al. (2011) Bone formation and neovascularization mediated by mesenchymal stem cells and endothelial cells in critical-sized calvarial defects. Tissue Eng Part A 17(3-4): 311–321. doi: 10.1089/ten.TEA.2010.0338
84. Gómez-Barrena E, Rosset P, Müller I et al. (2011) Bone regeneration: stem cell therapies and clinical studies in orthopaedics and traumatology. Journal of cellular and molecular medicine 15(6): 1266–1286. doi: 10.1111/j.1582-4934.2011.01265.x
85. Bohner M (2010) Resorbable biomaterials as bone graft substitutes. Materials Today 13(1): 24–30. doi: 10.1016/S1369-7021(10)70014-6
86. Yang S, Leong KF, Du Z et al. (2001) The design of scaffolds for use in tissue engineering. Part I. Traditional factors. Tissue engineering 7(6): 679–689. doi: 10.1089/107632701753337645
87. Gerhardt L, Boccaccini AR (2010) Bioactive Glass and Glass-Ceramic Scaffolds for Bone Tissue Engineering. Materials 3(7): 3867–3910. doi: 10.3390/ma3073867
88. Hammouche S, Hammouche D, McNicholas M (2012) Biodegradable bone regeneration synthetic scaffolds: in tissue engineering. Curr Stem Cell Res Ther 7(2): 134–142

89. Walsh, W, Bruce et al. IN VIVO MECHANISM FOR CALCIUM SULFATE BONE GRAFT SUSBTITUTE
90. Kumar C Y, K B N, Menon J et al. (2013) Calcium Sulfate as Bone Graft Substitute in the Treatment of Osseous Bone Defects, A Prospective Study. Journal of Clinical and Diagnostic Research : JCDR 7(12): 2926–2928. doi: 10.7860/JCDR/2013/6404.3791
91. Yuan H, Fernandes H, Habibovic P et al. (2010) Osteoinductive ceramics as a synthetic alternative to autologous bone grafting. Proc Natl Acad Sci U S A 107(31): 13614–13619. doi: 10.1073/pnas.1003600107
92. Somrani S, Rey C, Jemal M (2003) Thermal evolution of amorphous tricalcium phosphate. J. Mater. Chem. 13(4): 888–892. doi: 10.1039/b210900j
93. Dobelin N, Luginbuhl R, Bohner M (2010) Synthetic calcium phosphate ceramics for treatment of bone fractures. Chimia (Aarau) 64(10): 723–729
94. Thompson ID, Hench LL (1998) Mechanical properties of bioactive glasses, glass-ceramics and composites. Proc Inst Mech Eng H 212(2): 127–136. doi: 10.1243/0954411981533908
95. Hench LL (1998) Bioceramics. Journal of the American Ceramic Society 81(7): 1705–1728. doi: 10.1111/j.1151-2916.1998.tb02540.x
96. Hench LL (2004) Stimulation of Bone Repair by Gene Activating Glasses. Key Engineering Materials 254-256: 3–6. doi: 10.4028/www.scientific.net/KEM.254-256.3
97. Huang R, Kobayashi E, Liu K et al. (2016) Bone Graft Prefabrication Following the In Vivo Bioreactor Principle. EBioMedicine 12: 43–54
98. Henrotin Y (2011) Muscle: a source of progenitor cells for bone fracture healing. BMC medicine 9(1): 136
99. Liu R, Schindeler A, Little DG (2010) The potential role of muscle in bone repair. J Musculoskelet Neuronal Interact 10(1): 71–76
100. Abou-Khalil R, Yang F, Lieu S et al. (2015) Role of muscle stem cells during skeletal regeneration. Stem cells 33(5): 1501–1511
101. Khouri RK, Koudsi B, Reddi H (1991) Tissue transformation into bone in vivo: a potential practical application. Jama 266(14): 1953–1955
102. Kusumoto K, Bessho K, Fujimura K et al. (1998) Prefabricated muscle flap including bone induced by recombinant human bone morphogenetic protein-2: an experimental study of ectopic osteoinduction in a rat latissimus dorsi muscle flap. British journal of plastic surgery 51(4): 275–280
103. Carrel A (1937) The culture of whole organs: I. technique of the culture of the thyroid gland. The Journal of experimental medicine 65(4): 515
104. Williams DF (1999) The Williams dictionary of biomaterials. Liverpool University Press
105. Cuthbert RJ, Churchman SM, Tan HB et al. (2013) Induced periosteum a complex cellular scaffold for the treatment of large bone defects. Bone 57(2): 484–492

106. Beier JP, Hess A, Löw J et al. (2011) De novo generation of an axially vascularized processed bovine cancellous-bone substitute in the sheep arteriovenous-loop model. European Surgical Research 46(3): 148–155
107. Warnke PH, Springer IN, Wiltfang J et al. (2004) Growth and transplantation of a custom vascularised bone graft in a man. The Lancet 364(9436): 766–770
108. Horch RE, Beier JP, Kneser U et al. (2014) Successful human long-term application of in situ bone tissue engineering. Journal of cellular and molecular medicine 18(7): 1478–1485
109. Wilkinson A, Hewitt RN, McNamara LE et al. (2011) Biomimetic microtopography to enhance osteogenesis in vitro. Acta Biomaterialia 7(7): 2919–2925
110. Zimmermann G, Moghaddam A (2011) Allograft bone matrix versus synthetic bone graft substitutes. Injury 42: S16-S21
111. Stephen F Badylak (2002) The extracellular matrix as a scaffold for tissue reconstruction 5
112. Linke K, Schanz J, Hansmann J et al. (2007) Engineered liver-like tissue on a capillarized matrix for applied research. Tissue engineering 13(11): 2699–2707
113. Walles T, Puschmann C, Haverich A et al. (2003) Acellular scaffold implantation--no alternative to tissue engineering. The International journal of artificial organs 26(3): 225–234
114. Mertsching H, Hansmann J (2008) Bioreactor technology in cardiovascular tissue engineering
115. Schanz J, Pusch J, Hansmann J et al. (2010) Vascularised human tissue models: a new approach for the refinement of biomedical research. Journal of biotechnology 148(1): 56–63
116. Glynn JJ, Hinds MT (2014) Endothelial outgrowth cells: function and performance in vascular grafts. Tissue Eng Part B Rev 20(4): 294–303. doi: 10.1089/ten.teb.2013.0285
117. Obi S, Yamamoto K, Ando J (2014) Effects of shear stress on endothelial progenitor cells. J Biomed Nanotechnol 10(10): 2586–2597
118. Schanz JE (2007) Etablierung einer biologischen vaskularisierten Matrix als Grundlage für ein in-vitro-Lebertestsystem. Universität Stuttgart
119. Cheng CW, Solorio LD, Alsberg E (2014) Decellularized tissue and cell-derived extracellular matrices as scaffolds for orthopaedic tissue engineering. Biotechnol Adv 32(2): 462–484. doi: 10.1016/j.biotechadv.2013.12.012
120. Gruskin E, Doll BA, Futrell FW et al. (2012) Demineralized bone matrix in bone repair: history and use. Adv Drug Deliv Rev 64(12): 1063–1077. doi: 10.1016/j.addr.2012.06.008
121. Wang EA (1993) Bone morphogenetic proteins (BMPs): therapeutic potential in healing bony defects. Trends Biotechnol 11(9): 379–383. doi: 10.1016/0167-7799(93)90096-R

122. Abula K, Muneta T, Miyatake K et al. (2015) Elimination of BMP7 from the developing limb mesenchyme leads to articular cartilage degeneration and synovial inflammation with increased age. FEBS Lett 589(11): 1240–1248. doi: 10.1016/j.febslet.2015.04.004
123. Luu HH, Song W, Luo X et al. (2007) Distinct roles of bone morphogenetic proteins in osteogenic differentiation of mesenchymal stem cells. J Orthop Res 25(5): 665–677. doi: 10.1002/jor.20359
124. Kanakaris NK, Giannoudis PV (2008) Clinical applications of bone morphogenetic proteins: current evidence. J Surg Orthop Adv 17(3): 133–146
125. Hustedt JW, Blizzard DJ (2014) The Controversy Surrounding Bone Morphogenetic Proteins in the Spine: A Review of Current Research. Yale J Biol Med 87(4): 549–561
126. Burkus JK, Gornet MF, Dickman CA et al. (2002) Anterior lumbar interbody fusion using rhBMP-2 with tapered interbody cages. J Spinal Disord Tech 15(5): 337–349
127. Stafford RS (2008) Regulating off-label drug use--rethinking the role of the FDA. N Engl J Med 358(14): 1427–1429. doi: 10.1056/NEJMp0802107
128. Liu J, Chen L, zhou Y et al. (2014) Insulin-like growth factor-1 and bone morphogenetic protein-2 jointly mediate prostaglandin E2-induced adipogenic differentiation of rat tendon stem cells. PLoS ONE 9(1): e85469. doi: 10.1371/journal.pone.0085469
129. James AW, LaChaud G, Shen J et al. (2016) A Review of the Clinical Side Effects of Bone Morphogenetic Protein-2. Tissue Eng Part B Rev 22(4): 284–297. doi: 10.1089/ten.TEB.2015.0357
130. Ishihara A, Weisbrode SE, Bertone AL (2015) Autologous implantation of BMP2-expressing dermal fibroblasts to improve bone mineral density and architecture in rabbit long bones. J Orthop Res 33(10): 1455–1465. doi: 10.1002/jor.22791
131. Caron, M. M. J., Emans PJ, Cremers A et al. (2013) Hypertrophic differentiation during chondrogenic differentiation of progenitor cells is stimulated by BMP-2 but suppressed by BMP-7. Osteoarthritis and Cartilage 21(4): 604–613. doi: 10.1016/j.joca.2013.01.009
132. Fraser JK, Wulur I, Alfonso Z et al. (2006) Fat tissue: an underappreciated source of stem cells for biotechnology. Trends Biotechnol 24(4): 150–154. doi: 10.1016/j.tibtech.2006.01.010
133. Chen D, Ji X, Harris MA et al. (1998) Differential Roles for Bone Morphogenetic Protein (BMP) Receptor Type IB and IA in Differentiation and Specification of Mesenchymal Precursor Cells to Osteoblast and Adipocyte Lineages. J Cell Biol 142(1): 295. doi: 10.1083/jcb.142.1.295
134. Carragee EJ, Hurwitz EL, Weiner BK (2011) A critical review of recombinant human bone morphogenetic protein-2 trials in spinal surgery: emerging safety concerns and lessons learned. Spine J 11(6): 471–491. doi: 10.1016/j.spinee.2011.04.023

135. Benglis D, Wang MY, Levi AD (2008) A comprehensive review of the safety profile of bone morphogenetic protein in spine surgery. Neurosurgery 62(5 Suppl 2): ONS423-31; discussion ONS431. doi: 10.1227/01.neu.0000326030.24220.d8
136. Burkus JK, Sandhu HS, Gornet MF (2006) Influence of rhBMP-2 on the Healing Patterns Associated With Allograft Interbody Constructs in Comparison With Autograft. Spine (Phila Pa 1976) 31(7): 775–781. doi: 10.1097/01.brs.0000206357.88287.5a
137. McClellan JW, Mulconrey DS, Forbes RJ et al. (2006) Vertebral Bone Resorption After Transforaminal Lumbar Interbody Fusion With Bone Morphogenetic Protein (rhBMP-2). J Spinal Disord Tech 19(7): 483–486. doi: 10.1097/01.bsd.0000211231.83716.4b
138. Vaidya R, Sethi A, Bartol S et al. (2008) Complications in the use of rhBMP-2 in PEEK cages for interbody spinal fusions. J Spinal Disord Tech 21(8): 557–562. doi: 10.1097/BSD.0b013e31815ea897
139. Williams BJ, Smith JS, Fu KG et al. (2011) Does bone morphogenetic protein increase the incidence of perioperative complications in spinal fusion? A comparison of 55,862 cases of spinal fusion with and without bone morphogenetic protein. Spine (Phila Pa 1976) 36(20): 1685–1691. doi: 10.1097/BRS.0b013e318216d825
140. Chan DS, Garland J, Infante A et al. (2014) Wound complications associated with bone morphogenetic protein-2 in orthopaedic trauma surgery. J Orthop Trauma 28(10): 599–604. doi: 10.1097/BOT.0000000000000117
141. Spicer PP, Kretlow JD, Young S et al. (2012) Evaluation of bone regeneration using the rat critical size calvarial defect. Nat Protoc 7(10): 1918–1929
142. Paul-Ehrlich-Institut, Bundesinstitut für Impfstoffe biomedizinische Arzneimittel (2012) Arzneimittel für neuartige Therapien: Regulatorische Anforderungen und praktische Hinweise
143. (2007) Verordnung (EG) Nr 1394/2007 des Europäischen Parlaments und des Rates
144. Bundesministeriums für Gesundheit (2006) Leitfaden der Guten Herstellungspraxis Teil I. Banz. S. 6887
145. Mosmann T (1983) Rapid colorimetric assay for cellular growth and survival: Application to proliferation and cytotoxicity assays. Journal of Immunological Methods 65(1-2): 55–63. doi: 10.1016/0022-1759(83)90303-4
146. (1986) Fluorescent carbocyanine dyes allow living neurons of identified origin to be studied in long-term cultures. J Cell Biol 103(1): 171–187
147. Honig MG, Hume RI (1989) DiI and diO: versatile fluorescent dyes for neuronal labelling and pathway tracing. Trends Neurosci 12(9): 333-5, 340-1

148. Voyta JC, Via DP, Butterfield CE et al. (1984) Identification and isolation of endothelial cells based on their increased uptake of acetylated-low density lipoprotein. J Cell Biol 99(6): 2034–2040
149. Ballermann BJ, Ott MJ (1995) Adhesion and differentiation of endothelial cells by exposure to chronic shear stress: a vascular graft model. Blood Purif 13(3-4): 125–134
150. Murohara T, Witzenbichler B, Spyridopoulos I et al. (1999) Role of endothelial nitric oxide synthase in endothelial cell migration. Arteriosclerosis, thrombosis, and vascular biology 19(5): 1156–1161
151. Cooper GM, Mooney MP, Gosain AK et al. (2010) Testing the critical size in calvarial bone defects: revisiting the concept of a critical-size defect. Plast Reconstr Surg 125(6): 1685–1692. doi: 10.1097/PRS.0b013e3181cb63a3
152. Schmitz JP, Hollinger JO (1986) The critical size defect as an experimental model for craniomandibulofacial nonunions. Clin Orthop Relat Res(205): 299–308
153. Spicer PP, Kretlow JD, Young S et al. (2012) Evaluation of bone regeneration using the rat critical size calvarial defect. Nat Protoc 7(10): 1918–1929. doi: 10.1038/nprot.2012.113
154. Reichert JC, Epari DR, Wullschleger ME et al. (2010) Establishment of a preclinical ovine model for tibial segmental bone defect repair by applying bone tissue engineering strategies. Tissue Eng Part B Rev 16(1): 93–104. doi: 10.1089/ten.TEB.2009.0455
155. Bergman RJ, Gazit D, Kahn AJ et al. (1996) Age-related changes in osteogenic stem cells in mice. J Bone Miner Res 11(5): 568–577. doi: 10.1002/jbmr.5650110504
156. Pashuck TD, Franz SE, Altman MK et al. (2009) Murine model for cystic fibrosis bone disease demonstrates osteopenia and sex-related differences in bone formation. Pediatr Res 65(3): 311–316. doi: 10.1203/PDR.0b013e3181961e80
157. Einhorn TA (1999) Clinically applied models of bone regeneration in tissue engineering research. Clin Orthop Relat Res(367 Suppl): S59-67
158. Horrobin DF (2003) Modern biomedical research: an internally self-consistent universe with little contact with medical reality? Nature Reviews Drug Discovery 2: 151 EP -
159. Witt MR, Nielsen M (1994) Characterization of the influence of unsaturated free fatty acids on brain GABA/benzodiazepine receptor binding in vitro. J Neurochem 62(4): 1432–1439
160. Rücker C, Kirch H, Pullig O et al. (2016) Strategies and First Advances in the Development of Prevascularized Bone Implants. Curr Mol Biol Rep 2(3): 149–157. doi: 10.1007/s40610-016-0046-2
161. O'Loughlin PF, Morr S, Bogunovic L et al. (2008) Selection and development of preclinical models in fracture-healing research. J Bone Joint Surg Am 90 Suppl 1: 79–84. doi: 10.2106/JBJS.G.01585

162. Brandi ML (2009) Microarchitecture, the key to bone quality. Rheumatology (Oxford) 48 Suppl 4: iv3-8. doi: 10.1093/rheumatology/kep273
163. Lelovas PP, Xanthos TT, Thoma SE et al. (2008) The Laboratory Rat as an Animal Model for Osteoporosis Research. Comp Med 58(5): 424–430
164. Bagi CM, Berryman E, Moalli MR (2011) Comparative bone anatomy of commonly used laboratory animals: implications for drug discovery. Comp Med 61(1): 76–85
165. Zhang Y, Yang Z, Zhang H et al. (2013) Negative pressure technology enhances bone regeneration in rabbit skull defects. BMC Musculoskelet Disord 14: 76. doi: 10.1186/1471-2474-14-76
166. Hassanein AH, Couto RA, Nedder A et al. (2011) Critical-size defect ossification: effect of leporid age in a cranioplasty model. J Craniofac Surg 22(6): 2341–2343. doi: 10.1097/SCS.0b013e318232a71d
167. Xu L, Zhang W, Lv K et al. (2016) Peri-Implant Bone Regeneration Using rhPDGF-BB, BMSCs, and beta-TCP in a Canine Model. Clin Implant Dent Relat Res 18(2): 241–252. doi: 10.1111/cid.12259
168. Tatakis DN, Koh A, Jin L et al. (2002) Peri-implant bone regeneration using recombinant human bone morphogenetic protein-2 in a canine model: a dose-response study. J Periodontal Res 37(2): 93–100
169. Hasiwa N, Bailey J, Clausing P et al. (2011) Critical evaluation of the use of dogs in biomedical research and testing in Europe. ALTEX 28(4): 326–340
170. Li Y, Chen S, Li L et al. (2015) Bone defect animal models for testing efficacy of bone substitute biomaterials. Journal of Orthopaedic Translation 3(3): 95–104. doi: 10.1016/j.jot.2015.05.002
171. Schwarz F, Sculean A, Engebretson SP et al. (2015) Animal models for peri-implant mucositis and peri-implantitis. Periodontol 2000 68(1): 168–181. doi: 10.1111/prd.12064
172. Turner AS (2007) Experiences with sheep as an animal model for shoulder surgery: strengths and shortcomings. J Shoulder Elbow Surg 16(5 Suppl): S158-63. doi: 10.1016/j.jse.2007.03.002
173. Newman E, Turner AS, Wark JD (1995) The potential of sheep for the study of osteopenia: current status and comparison with other animal models. Bone 16(4 Suppl): 277S-284S
174. Reichert JC, Cipitria A, Epari DR et al. (2012) A tissue engineering solution for segmental defect regeneration in load-bearing long bones. Sci Transl Med 4(141): 141ra93. doi: 10.1126/scitranslmed.3003720
175. Reichert JC, Saifzadeh S, Wullschleger ME et al. (2009) The challenge of establishing preclinical models for segmental bone defect research. Biomaterials 30(12): 2149–2163. doi: 10.1016/j.biomaterials.2008.12.050
176. Nair MB, Varma HK, Menon KV et al. (2009) Tissue regeneration and repair of goat segmental femur defect with bioactive triphasic ceramic-coated hydroxyapatite scaffold. J Biomed Mater Res A 91(3): 855–865. doi: 10.1002/jbm.a.32239

177. Yang HL, Zhu XS, Chen L et al. (2012) Bone healing response to a synthetic calcium sulfate/beta-tricalcium phosphate graft material in a sheep vertebral body defect model. J Biomed Mater Res B Appl Biomater 100(7): 1911–1921. doi: 10.1002/jbm.b.32758
178. Maissen O, Eckhardt C, Gogolewski S et al. (2006) Mechanical and radiological assessment of the influence of rhTGFbeta-3 on bone regeneration in a segmental defect in the ovine tibia: pilot study. J Orthop Res 24(8): 1670–1678. doi: 10.1002/jor.20231
179. Reichert JC, Epari DR, Wullschleger ME et al. (2010) Establishment of a preclinical ovine model for tibial segmental bone defect repair by applying bone tissue engineering strategies. Tissue Engineering Part B: Reviews 16(1): 93–104
180. Welch JG (1982) Rumination, Particle Size and Passage from the Rumen. Journal of Animal Science 54(4): 885–894. doi: 10.2527/jas1982.544885x
181. Drosse I, Volkmer E, Capanna R et al. (2008) Tissue engineering for bone defect healing: An update on a multi-component approach. Injury 39: S9-S20. doi: 10.1016/S0020-1383(08)70011-1
182. Mara CSd, Sartori AR, Duarte AS et al. (2011) Periosteum as a source of mesenchymal stem cells: the effects of TGF-β3 on chondrogenesis. Clinics 66(3): 487–492
183. Yamada Y, Ueda M, Hibi H et al. (2006) A novel approach to periodontal tissue regeneration with mesenchymal stem cells and platelet-rich plasma using tissue engineering technology: A clinical case report. International Journal of Periodontics & Restorative Dentistry 26(4)
184. Ejtehadifar M, Shamsasenjan K, Movassaghpour A et al. (2015) The effect of hypoxia on mesenchymal stem cell biology. Advanced pharmaceutical bulletin 5(2): 141
185. Barradas A, Yuan H, Blitterswijk CA et al. (2011) Osteoinductive biomaterials: current knowledge of properties, experimental models and biological mechanisms. Eur Cell Mater 21: 407–429
186. Seebach E, Freischmidt H, Holschbach J et al. (2014) Mesenchymal stroma cells trigger early attraction of M1 macrophages and endothelial cells into fibrin hydrogels, stimulating long bone healing without long-term engraftment. Acta Biomaterialia 10(11): 4730–4741
187. Balaji S, King A, Crombleholme TM et al. (2013) The role of endothelial progenitor cells in postnatal vasculogenesis: implications for therapeutic neovascularization and wound healing. Advances in wound care 2(6): 283–295
188. Li B, Sharpe EE, Maupin AB et al. (2006) VEGF and PlGF promote adult vasculogenesis by enhancing EPC recruitment and vessel formation at the site of tumor neovascularization. The FASEB Journal 20(9): 1495–1497
189. Palma M de, Venneri MA, Roca C et al. (2003) Targeting exogenous genes to tumor angiogenesis by transplantation of genetically modified hematopoietic stem cells. Nature medicine 9(6): 789–795

190. Seebach C, Henrich D, Kähling C et al. (2010) Endothelial progenitor cells and mesenchymal stem cells seeded onto β-TCP granules enhance early vascularization and bone healing in a critical-sized bone defect in rats. Tissue Engineering Part A 16(6): 1961–1970
191. Steinke M, Dally I, Friedel G et al. (2014) Host-integration of a tissue-engineered airway patch: two-year follow-up in a single patient. Tissue Engineering Part A 21(3-4): 573–579
192. Lin Z, Fateh A, Salem DM et al. (2014) Periosteum Biology and Applications in Craniofacial Bone Regeneration. Journal of dental research 93(2): 109–116
193. Zhang X, Xie C, Lin ASP et al. (2005) Periosteal progenitor cell fate in segmental cortical bone graft transplantations: implications for functional tissue engineering. Journal of Bone and Mineral Research 20(12): 2124–2137
194. Xie C, Reynolds D, Awad H et al. (2007) Structural bone allograft combined with genetically engineered mesenchymal stem cells as a novel platform for bone tissue engineering. Tissue engineering 13(3): 435–445
195. Schönmeyr B, Clavin N, Avraham T et al. (2009) Synthesis of a tissue-engineered periosteum with acellular dermal matrix and cultured mesenchymal stem cells. Tissue Engineering Part A 15(7): 1833–1841
196. Friedman CD, Costantino PD, Takagi S et al. (1998) BoneSource™ hydroxyapatite cement: a novel biomaterial for craniofacial skeletal tissue engineering and reconstruction. Journal of biomedical materials research 43(4): 428–432
197. Schulze-Späte U, Dietrich T, Kayal RA et al. (2012) Analysis of bone formation after sinus augmentation using β-tricalcium phosphate. Compendium of continuing education in dentistry (Jamesburg, NJ: 1995) 33(5): 364–368
198. Szabó G, Huys L, Coulthard P et al. (2005) A Prospective Multicenter Randomized Clinical Trial of Autogenous Bone Versus β-Tricalcium Phosphate Graft Alone for Bilateral Sinus Elevation: Histologic and Histomorphometric Evaluation. International Journal of Oral & Maxillofacial Implants 20(3)
199. Horowitz RA, Mazor Z, Miller RJ et al. (2009) Clinical evaluation alveolar ridge preservation with a beta-tricalcium phosphate socket graft. Compend Contin Educ Dent 30(9): 588–590
200. Kaempfen A, Todorov A, Güven S et al. (2015) Engraftment of Prevascularized, Tissue Engineered Constructs in a Novel Rabbit Segmental Bone Defect Model. Int J Mol Sci 16(6): 12616–12630. doi: 10.3390/ijms160612616
201. Karande TS, Ong JL, Agrawal CM (2004) Diffusion in musculoskeletal tissue engineering scaffolds: design issues related to porosity, permeability, architecture, and nutrient mixing. Annals of biomedical engineering 32(12): 1728–1743

202. Jelusic D, Zirk ML, Fienitz T et al. (2016) Monophasic ß-TCP vs. biphasic HA/ß-TCP in two-stage sinus floor augmentation procedures–a prospective randomized clinical trial. Clinical oral implants research
203. Hennig C, Thomas CDL, Clement JG et al. (2015) Does 3D orientation account for variation in osteon morphology assessed by 2D histology? J Anat 227(4): 497–505. doi: 10.1111/joa.12357
204. Matic I, Matthews BG, Wang X et al. (2016) Quiescent Bone Lining Cells Are a Major Source of Osteoblasts During Adulthood. Stem Cells 34(12): 2930–2942. doi: 10.1002/stem.2474
205. Hock JM, Krishnan V, Onyia JE et al. (2001) Osteoblast apoptosis and bone turnover. J Bone Miner Res 16(6): 975–984. doi: 10.1359/jbmr.2001.16.6.975
206. Everts V, Delaissé JM, Korper W et al. (2002) The bone lining cell: its role in cleaning Howship's lacunae and initiating bone formation. J Bone Miner Res 17(1): 77–90. doi: 10.1359/jbmr.2002.17.1.77
207. Skedros JG, Clark GC, Sorenson SM et al. (2011) Analysis of the effect of osteon diameter on the potential relationship of osteocyte lacuna density and osteon wall thickness. Anat Rec (Hoboken) 294(9): 1472–1485. doi: 10.1002/ar.21452
208. Pfeiffer S (1998) Variability in osteon size in recent human populations. Am J Phys Anthropol 106(2): 219–227. doi: 10.1002/(SICI)1096-8644(199806)106:2<219:AID-AJPA8>3.0.CO;2-K
209. Mackie EJ, Ahmed YA, Tatarczuch L et al. (2008) Endochondral ossification: How cartilage is converted into bone in the developing skeleton. The International Journal of Biochemistry & Cell Biology 40(1): 46–62. doi: 10.1016/j.biocel.2007.06.009
210. Kartus J, Movin T, Karlsson J (2001) Donor-site morbidity and anterior knee problems after anterior cruciate ligament reconstruction using autografts. Arthroscopy 17(9): 971–980. doi: 10.1053/jars.2001.28979
211. (2017) Global Guidelines for the Prevention of Surgical Site Infection. World Health Organization
212. Leaper DJ, van Goor H, Reilly J et al. (2004) Surgical site infection - a European perspective of incidence and economic burden. Int Wound J 1(4): 247–273. doi: 10.1111/j.1742-4801.2004.00067.x
213. Boni L, Benevento A, Rovera F et al. (2006) Infective complications in laparoscopic surgery. Surg Infect (Larchmt) 7 Suppl 2: S109-11. doi: 10.1089/sur.2006.7.s2-109
214. Eweida AM, Nabawi AS, Abouarab M et al. (2014) Enhancing mandibular bone regeneration and perfusion via axial vascularization of scaffolds. Clin Oral Investig 18(6): 1671–1678. doi: 10.1007/s00784-013-1143-8

8 Appendix

8.1 Affidavit

I hereby confirm that the thesis entitled “Development of a prevascularized bone implant” is the result of my own work. I did not receive any help or support from commercial consultants. All sources and/or materials applied are listed and specified in the thesis.

Furthermore, I confirm that this thesis has not yet been submitted as part of another examination process neither in identical nor in similar form.

…… ……

Place, Date Signature

8.2 Acknowledgement

First of all, I want to thank Prof. Dr. Heike Walles for the opportunity to write my doctoral thesis at the Chair Tissue Engineering & Regenerative Medicine. Thank you for your continuous support and guidance over the years, the corrections and conversations that enriched the presented work and the possibility to visit many conferences and symposia in countries all over the world.

Thank you, PD Dr. Alois Palmetshofer, for your second opinion on the thesis as reviewer.

I want to thank Prof. Dr. Dietmar Hutmacher, Dr. Dr. Jan Henkel, Prof. Dr. Dr. Michael Rasse and especially Dr. Dr. Robert Stigler for the cooperation; otherwise, the complex experiments would not have been possible.

My thanks regarding everything touching the GMP topic go to the group of PD Dr. Oliver Pullig together with Barbara Bayer, Heidi Linß, Kirsten Langenbrink, Dr. Meike Haddad-Weber, Tanja Kraus and Sarah Frosch.

Thanks to the Werkstatt, especially Steffan Krziminski and Thomas Schwarz for their help regarding technical topics.

I thank all PhD, master and bachelor students, colleagues and friends of the department for the great working atmosphere, conversations and activities outside the institute.

Last but not least I thank my family who supported and motivated me throughout the years.

This research has received funding from the European Union's Seventh Framework Programme for research, technological development and demonstration under grant agreement n°242175.